

University of Alberta

**Epigenetic Regulation of Centromere Formation and
Kinetochore Function**

By

Ryan John Heit

A thesis submitted to the Faculty of Graduate Studies and Research
in partial fulfillment of the requirements for the degree of

Master of Science
in
Experimental Oncology

Department of Oncology

©Ryan John Heit
Fall, 2009
Edmonton, Alberta

Permission is hereby granted to the University of Alberta Libraries to reproduce single copies of this thesis and to lend or sell such copies for private, scholarly or scientific research purposes only. Where the thesis is converted to, or otherwise made available in digital form, the University of Alberta will advise potential users of the thesis of these terms.

The author reserves all other publication and other rights in association with the copyright in the thesis and, except as herein before provided, neither the thesis nor any substantial portion thereof may be printed or otherwise reproduced in any material form whatsoever without the author's prior written permission.

Examining Committee

Michael Hendzel, Oncology

Gordon Chan, Oncology

Alan Underhill, Oncology

Robert Campbell, Chemistry

Abstract

One form of protein regulation is accomplished by post-translational modification (PTM). In order to test the importance one type of PTM, methylation, in chromosome segregation, we inhibited protein methylation for brief periods in G2 using the general methylation inhibitor adenosine dialdehyde (AdOx). Inhibiting methylation solely in late G2 leads to mitotic defects. We observed that several methylated histone residues; H3K9me3, H4K20me3 and H4K20me1, are predominantly affected by AdOx in G2. We show both that the kinetochore proteins are not affected and that the mitotic checkpoint is intact. Further, we observed structural defects and chromosome misalignment in mitotic cells. These results indicate that methylation events during late G2 operate to maintain and ensure the structural integrity of pericentromeric heterochromatin prior to mitosis. These results suggest that pericentromeric heterochromatin is required for the proper sensing of kinetochore tension and inactivation of the mitotic checkpoint.

Table of Contents

Section 1 – Introduction	1
1.1 Chromatin Structure – Histones and the Nucleosome	1
1.1.1 Histones	1
1.1.2 The nucleosome	4
1.1.3 Histone modifications	7
1.1.4 Diverse Roles of Lysine Methylation	10
1.2 Regulation of Higher-Order Compaction of Chromatin	12
1.2.1 Organization of Chromatin in vivo	12
1.2.2 Bivalent Model of Effector-Mediated Events	18
1.3 The Centromere, Kinetochore and Mitosis	22
1.3.1 Epigenetic Determination of Centromeres	22
1.3.2 Specification of the Centromere	26
1.3.3 Kinetochore Formation and Chromosome Segregation	29
1.4 H3K9 Methylation and Pericentromeric Heterochromatin	
1.4.1 H3K9 Methylation	34
1.4.2 Additional regulation of pericentromeric heterochromatin	35
1.4.3 Dynamics of Histone Modifications During Mitosis	42
1.5 Hypothesis	46
Section 2 – Materials and Methods	47
Section 3 – Results	56
3.1 Mitotic defects found in HeLa cells treated with Adenosine Dialdehyde	56

3.2 AdOx treatment decreases the apparent abundance of H3K9me3 and H4K20me3	60
3.3 The loss of H3K9me3 does not account for the full severity of the defect seen by inhibiting global methylation	66
3.4 Methylation is most critical for chromosome segregation 1-3 hours prior to mitosis	72
3.5 Mitotic checkpoint activated with AdOx treatment	74
3.6 Kinetochore proteins affected by loss of methylation	78
3.7 Interkinetochore distance in AdOx treated cells: Changes in Tension or Structural abnormalities	87
3.8 Transmission electron microscopy shows structural defects in AdOx-treated mitotic cells	90
Section 4 – General Discussion	92
4.1 Discussion	92
4.2 Future Directions	101
Section 5 – Bibliography	104

List of Figures and Tables

Figure 1: Sequence Alignment of Histone H4 Across Various Species	3
Figure 2: The Nucleosome Structure and Histone Modifications	6
Figure 3: The Structure of the Centromere	33
Figure 4: A simplified model of heterochromatin maintenance	40
Figure 5: High resolution image of DNA stain in mitotic HeLa cells	57
Figure 6: Adenosine Dialdehyde defects in mitosis	59
Figure 7: High resolution images of the range of severity of AdOx mediated defects	59
Figure 8: Altered methylation levels in AdOx treated HeLa cells	62
Figure 9: H3K4me3 unaffected in mitotic AdOx treated cells	63
Figure 10: Peptide competition assay	64
Figure 11: Flow cytometry DNA profiles of <i>SUV39h1/h2</i> ^{-/-} and parental mouse epithelial fibroblast (WT) cells.	68
Figure 12: H3K9me3, H4K20me3 and DNA methylation do not account for the full severity of the mitotic defect seen with AdOx treatment	69
Figure 13: SUV420h1 and SUV420h2 knockdown in MEF cells.	70
Figure 14: Methylation occurs in both S phase and G2 with an important window occurring 1-3 hours prior to mitosis	72
Figure 15: Metaphase-Anaphase Checkpoint is active but checkpoint failure does occur in some cells.	74
Figure 16: Time lapse microscopy of stably transfected Histone H2B-GFP HeLa cells shows tetraploidy	76

Figure 17: CENH3, CENP-B and CENP-C localize properly in AdOx treated cells, microtubules fail to stably attach to kinetochores.	78
Figure 18: CENP-F localization remains unchanged with AdOx treatment	81
Figure 19: Aim-1 localization in control and AdOx treated cells	82
Figure 20: Kinetochores proteins accumulate on misaligned chromosomes with AdOx treatment	85
Figure 21: Interkinetochore distance of four groups	88
Figure 22: TEM emphasizes structural defects in the centromere/kinetochore of the AdOx exposed cells.	90
Table 1: Histone modifications affected by methylation inhibition	65

List of Abbreviations

ACA	anti-centromeric antigen
AdOx	adenosine dialdehyde
AOD	amine oxidase domain
AUT	acid-urea triton
BSA	bovine serum albumin
Bub1	budding uninhibited by benzimidazoles 1
BubR1	budding uninhibited by benzimidazoles related 1
CEN chromatin	centromeric chromatin
CENP	centromere protein
CHD1	Chromodomain helicase DNA binding protein 1
ChIP	chromatin immunoprecipitation
CID	<i>Drosophila</i> CENP-A homolog
CIN	chromosomal instability
CoREST	RE-1 silencing transcription factor corepressor
CpG	cytosine and guanine separated by a phosphate
DAPI	4',6-diamidino-2-phenylindole
DBC1	deleted in breast cancer 1
DMEM	Dulbecco's modified Eagle's medium
DNMT	DNA methyltransferase
EDTA	ethylenediaminetetraacetic acid
EGTA	ethylene glycol tetraacetic acid
GFP	green fluorescent protein

HDAC	histone deacetylase
HJURP	Holliday junction recognition protein
HP1	heterochromatin protein 1
hSMC1	human structural maintenance of chromosomes protein
hZW10	human Zeste White 10
IIF	indirect immunofluorescence
INCENP	inner centromeric protein
JMJD	Jumonji domain-containing protein
LSD	lysine specific demethylase
MBT	malignant brain tumour
MCAK	mitotic centromere-associated kinesin
MEF	mouse embryonic fibroblasts
MSL3	male-specific lethal 3
NEAA	non-essential amino acids
NURF	nucleosome remodeling factor
PBS	phosphate-buffered saline
PHD	plant homeodomain finger
Pic/NuA4	Piccolo/nucleosome acetyltransferase of H4 complex
Plk1	polo-like kinase 1
PTM	post-translational modification
RNAi	RNA interference
SANT	SWI-SNF, ADA, N-CoR, and TFIIB

SET	Suppressor of variegation 3-9, the polycomb group protein Enhancer of zeste, and the trithorax-group protein Trithorax
SirT1	Sirtuin1
Sgo2	shugoshin 2
SUV39	suppressor of variegation 3-9
SWIRM	Swi3p, Rsc8p, and Moira
TBS	tris-buffered saline
TEM	transmission electron microscopy

Section 1

Introduction

1.1 Chromatin Structure – Histones and the Nucleosome

1.1.1. Histones

Histone proteins are the most abundant proteins in the nucleus. They are small (11-22 kDa) and are rich in lysine and arginine, giving them a high net positive charge. There are five histone proteins: four core histones, histones that form an octameric protein scaffold for wrapping and binding DNA and forming the nucleosome, H2A, H2B, H3, and H4. The fifth histone, histone H1, binds the DNA strand as it enters and exits the nucleosome. Alterations of the nucleosome affect the structure of chromatin which, in turn, influences transcription. This includes the incorporation of histone variants that diverge in amino acid sequence and expression profiles from the major isoforms. Histone H3 variants include H3.3, associated with transcriptional activity, and centromere protein A (CENP-A also known as CENH3), a centromere specific variant. Histone H2A variants include H2AX, which plays a role in DNA double strand break repair, H2AZ, which is associated with gene activation in yeast and silencing in mammals, macroH2A, which is enriched in the inactive X chromosome and H2A.Bbd, which is excluded from the inactive X chromosome and associated with less stable nucleosomes (for review see (Sarma and Reinberg, 2005)). Histones H2B and H4, conversely contain few examples of variant forms.

The major forms of the histones are highly conserved between species, an example is shown for histone H4 (Figure 1). The numerous histone variants differ in this respect as only histone H3.3 and histone H2AZ seem to be conserved (Jackson et al., 1996; Kamakaka and Biggins, 2005) while others are restricted to vertebrates or mammals. The core domain of CENH3 is conserved, however, the N-terminal tail is highly divergent (Malik and Henikoff, 2003). The deposition of the major forms of histones are coupled to DNA replication, exclusively for histone H3 and H4 and predominantly (>50%) for H2A and H2B (Kimura and Cook, 2001). Conversely, histone H3.3 deposition occurs both during replication and during active transcription (Ahmad and Henikoff, 2002) whereas CENH3 deposition occurs in telophase/early G1 (Dunleavy et al., 2009; Foltz et al., 2009; Pidoux et al., 2009; Williams et al., 2009). Finally, the transcription of the major histones are cell cycle-regulated whereas variant transcription is not similarly restricted (reviewed in (Sarma and Reinberg, 2005)). The various histone forms and their incorporation into the nucleosome affect the identity of the cell through the roles they play in determining chromatin structure and, consequently, transcription.

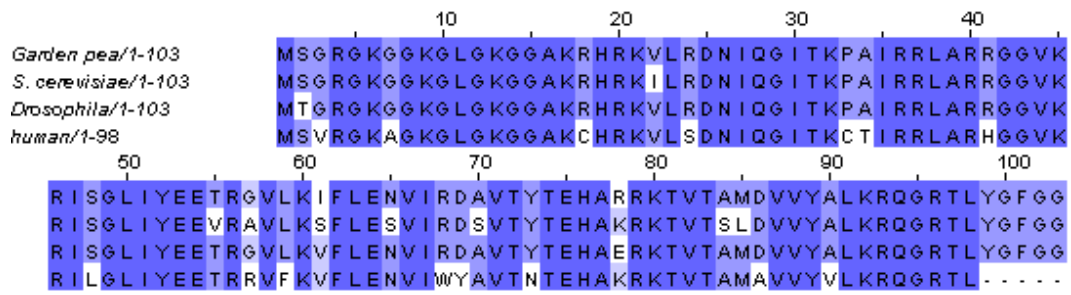


Figure 1 Sequence Alignment of Histone H4 Across Various Species

The high degree of sequence conservation of histone proteins is shown in the sequence alignment of histone H4. The degree of amino acid conservation is shown as shades of blue: the lighter shades correspond to sequence divergence.

1.1.2 The nucleosome

The basic unit of chromatin structure, the nucleosome, partitions the DNA into units of approximately 200 base pairs in length. At the molecular level, each chromosome is a repeat of nucleosomes and linking DNA (Kornberg, 1974). The nucleosome core particle is comprised of 147 base pairs of DNA that makes 1.75 turns around the outer surface of a histone octamer. The histone octamer is assembled from a tetramer of the histones H3 and H4 and two dimers of the histones H2A and H2B (Luger et al., 1997) (Figure 2A and B). The linking DNA is associated with histone H1 which binds DNA as it enters and exits the nucleosome to stabilize two complete turns of the DNA around the histone octamer (Thomas, 1999). The assembly of the nucleosome, linking DNA and histone H1 is sometimes referred to as the chromatosome.

Histone proteins play a crucial role in regulating the structure and function of chromatin. This regulation is due to the nature of the core histone proteins. The four core histones each contain a structured globular domain and unstructured amino- (N-) terminal and carboxy- (C-) terminal tails. The globular domains of the histones form a structured core of the nucleosome and are responsible for the binding and wrapping of DNA around the outer surface. The N-terminal and C-terminal unstructured histone tails are not incorporated into the core of the nucleosome, but rather emanate from the core. It is believed that the histone tails are intrinsically disordered: that is,

they are predominantly unstructured and only adopt a particular conformation upon interaction with a substrate (Hansen et al., 2006). The histone tails are also the target of a large number of post-translational modifications (Figure 2C and described in the next section) that are implicated in a variety of cellular processes which include: chromatin structure, regulation of gene expression (Rea et al., 2000), X-inactivation (Rougeulle and Avner, 2003), cell differentiation (Kubicek et al., 2006) and DNA repair (Rogakou et al., 1998; Schotta et al., 2008). It is these post-translational modifications, largely located in the N-termini of the histone proteins, which encode most of the epigenetic information specifying chromatin structure and function (Bradbury, 1992; Davie, 1996; Shilatifard, 2006). For example, reduced acetylation of the N-terminal lysines of histone H4 (Braunstein et al., 1993; Kristjuhan et al., 2003; Richards and Elgin, 2002), trimethylation of lysine 20 on histone H4 (Biron et al., 2004; Kourmouli et al., 2004; Schotta et al., 2004), trimethylation of lysine 9 on histone H3 (Fischle et al., 2003; Gonzalo et al., 2005; Peters et al., 2001; Rice et al., 2003), and trimethylation of lysine 27 of histone H3 (Chadwick and Willard, 2004) have all been correlated with heterochromatin structures.

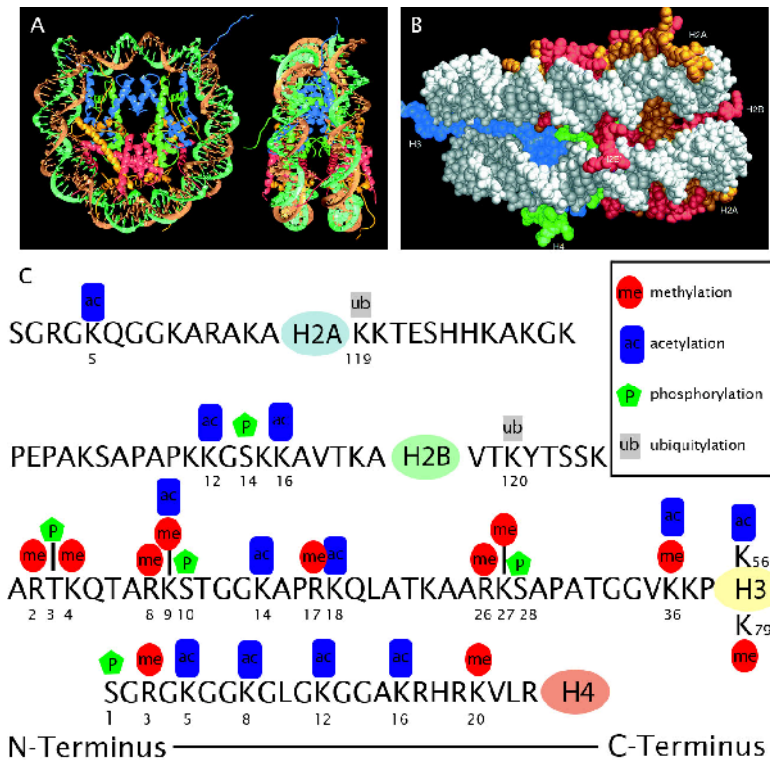


Figure 2 The Nucleosome Structure and Histone Modifications

Atomic detail of the X-ray crystal structure of the nucleosome is shown as a ribbon model (A) and a space-filling model (B). A: The X-ray structure allows us to view the organization of the histone proteins (blue: H3, green: H4, red, H2B, orange, H2A) within the nucleosome. Little detail is afforded to the histone tails as they are not present in the high resolution structure and are believed to be intrinsically disordered. B: The space filling model shows the arrangement of the histone tails as they protrude from the nucleosome core. H3 and H2B tails pass through the channels formed from the alignment of minor grooves of the two DNA coils within the nucleosome. H2A and H4 tails protrude from the lateral surface of the nucleosome and do not pass between the two DNA coils. C: The linear sequence of the histone tails is shown to illustrate a list of identified *in vivo* histone modifications. The sequence is read from N-terminal to C-terminal. The globular domains of each histone are represented by a coloured circle. Each amino acid residue shown to contain a modification is identified by a number corresponding to its position in relation to the N-terminus as well as by the modification that occurs. The majority of histone modifications occur within the tails, however K56 acetylation and K79 methylation of histone H3 are contained within the globular domain.

1A and 1B Reprinted with permission from Luger, K., et al., 1997.

1.1.3 Histone Modifications

Histone modifications play many roles affecting chromatin properties and are an ongoing area of intensive investigation. The histone proteins can be covalently modified by the addition of numerous chemical moieties which include methylation, acetylation, phosphorylation, ubiquitylation, sumoylation, and ADP-ribosylation, or altered by proline isomerisation or deimination (Kouzarides, 2007). As mentioned, the majority of these modifications occur predominantly on the N-termini of the histones that protrude from the core of the nucleosome. Some modifications, however, occur both on the C-termini and within the globular domain. A list of these modifications that have been confirmed to occur *in vivo* is shown in Figure 2C. Histone tails are involved in internucleosomal interactions, comprise between 25-30% of the histone protein mass and play a large role in histone-DNA and histone-histone interactions (Wolffe and Hayes, 1999). These roles in chromatin folding will regulate the accessibility of chromatin to nuclear factors. As an example of this, we will briefly discuss histone acetylation. Histone acetylation seems to cause both an opening of the nucleosome structure as well a decondensation of the higher order folding of chromatin (Bartsch et al., 1996; Grunstein, 1997; Shogren-Knaak et al., 2006; Walia et al., 1998). Histone acetylation-mediated decondensation also results in transcriptional activation in previously silenced genes and therefore plays a role in the transition between heterochromatin and euchromatin (Garcia-Ramirez et al., 1995; Grunstein, 1997), a topic that will be discussed below.

The mechanism of acetylation-mediated decondensation of chromatin is in two parts. First, the neutralization of a positive charge on the lysine residues by the addition of an acetyl groups disrupts DNA-histone contacts and leads to enhanced nucleosome mobility (Shahbazian and Grunstein, 2007). Second, internucleosomal interactions between the acidic patch on histone H2A and the N-terminal tail of histone H4 are disrupted (Annunziato et al., 1988; Garcia-Ramirez et al., 1995; Govin et al., 2006; Luger et al., 1997; Robinson et al., 2008; Shahbazian and Grunstein, 2007; Toth et al., 2006). It is interesting to note that reconstituted nucleosome octamers lacking their N-terminal tails fail to condense, supporting the role of histone tails in chromatin compaction, while the nucleosome assembly is not altered (Garcia-Ramirez et al., 1992; Hayes et al., 1991).

In addition to direct effects an additional mechanism whereby histone tails mediate chromatin structure is through effector-mediated events. Histone tail modifications are binding sites for many characterized effector proteins. It is through these two mechanisms, direct effects and effector-mediated, that histone modifications play a role in chromatin structure. Returning to histone acetylation, the earliest example of a modified histone binding domain is the bromodomain which binds acetylated lysines of histones (Dhalluin et al., 1999). With this finding it seems that histone acetylation mediates its effects through both mechanisms. The specific role of histone acetylation involves transcriptional regulation as it is shown that coactivator complexes required for transcription contain histone

acetyltransferases (Brownell et al., 1996; Kuo and Allis, 1998; Kuo et al., 1998; Ogryzko et al., 1996) while corepressor complexes containing histone deacetylases silence the underlying genes (Alland et al., 1997; Taunton et al., 1996; Utley et al., 1998). This modification occurs on several residues on the histone tails including lysines 9, 14, 18, 23 and 36 on histone H3 and lysines 5, 8, 12, 16 on histone H4 (reviewed in (Strahl and Allis, 2000)).

Histone phosphorylation is less well understood. Phosphorylated histone residues include serine 1 of histone H4 (H4Ser1), H2BSer14, H3Ser10 and H3Ser28 as well as a reported threonine phosphorylation on H3Thr3. Considering only electrostatic potential of the phosphorylation, this modification should lead to chromatin decondensation similar to that of acetylation. However, the established roles of histone phosphorylation seem to be effector-mediated as opposed to being mediated by alterations in histone/histone or histone/DNA interactions. Some specific roles include the phosphorylation of serine 10 on histone H3 which occurs coincidentally with chromosome condensation in late G2 (Hendzel et al., 1997) and the phosphorylation of serine 139 of the H2A variant, H2AX, which is hyperphosphorylated in response to and localized at double strand breaks (Paull et al., 2000; Rogakou et al., 1998).

The effects of methylation of histone proteins are not as straightforward as those of acetylation or phosphorylation. Histone acetylation is transcriptionally-activating and chromatin-disrupting and

seems to contain a level of redundancy. Mutation of a single lysine to arginine on histone H4, thereby eliminating an acetylation site while retaining a positive charge, causes a slight decrease in transcriptional activity (Dion et al., 2005). The level of transcriptional repression is positively correlated to the number of lysines mutated regardless of the position mutated, save for lysine 16 which had specific transcriptional roles at certain loci. This provides evidence that the majority of histone acetylation effects are similar and cumulative. Conversely, the effects of histone methylation are dependent on the specific residue methylated as well as the degree of methylation present. Each lysine can be mono-, di- or trimethylated. Arginine can also be methylated where it may be found in mono-, disymmetrically or diasymmetrically methylated forms.

1.1.4 Diverse Roles of Lysine Methylation

Lysine methylation has been extensively studied and it has been shown that there are antagonistic downstream effects dependent upon the residue. For example, methylation of H3K4, H3K36 and H3K79 is enriched in active euchromatin, whereas methylation of H3K9, H3K27 and H4K20 is enriched in heterochromatin or silent regions (Klose and Zhang, 2007). Further, the extent of methylation of a given residue may impart a different function. For example, mono- and dimethylated lysine 9 of histone H3(H3K9me1/2) are enriched in silent domains within euchromatin whereas H3K9me3 is enriched in pericentromeric and telomeric heterochromatin

(Peters et al., 2001; Rice et al., 2003), H4K20me3 is also enriched in pericentromeric and telomeric heterochromatin while H4K20me2 is near ubiquitous and has been linked with DNA damage response (Botuyan et al., 2006; Sanders et al., 2004; Schotta et al., 2004; Yang et al., 2008). The effects of the various histone methylation residues are believed to be carried out primarily through effector-mediated events.

Methyl binding domains have been studied extensively and include, among others, chromodomains, which bind to H3K4me2/3, H3K9me2/3 and H3K27me2/3, tudor domains, which bind to H3K4me3 and H4K20me2, MBT (malignant brain tumour) domains, which bind to H3K4me1 and H4K20me1/2 and PHD (plant homeodomain finger) domains, which bind to H3K4me3, H3K9me3 and H3K36me3 (reviewed in (Ruthenburg et al., 2007) and (Taverna et al., 2007)). It is perhaps due to these specific protein binding domains that the various histone methylation states have such diverse characteristics.

The identification of the roles of histone methylation was initially characterized through studies of single marks at discrete loci. From these initial studies, a pattern of typical roles was established for a given methylation. For example, H3K4me3 was found to be enriched at the promoter regions of actively transcribed genes and so is believed to play a role in transcription initiation (Schneider et al., 2004). This is shown to be mediated by both the PHD binding domain of NURF (nucleosome

remodeling factor) (Wysocka et al., 2006) as well as the double chromodomain of CHD1 (chromodomain helicase DNA binding protein 1) (Pray-Grant et al., 2005; Sims et al., 2005). Alternatively, H3K9me3 was found to be required for the formation and maintenance of heterochromatin and transcriptional repression (Gonzalo et al., 2005; Schotta et al., 2004; Zinner et al., 2005). This is also due to effector-mediated binding as the chromodomain of heterochromatin protein 1 (HP1) binds to H3K9me3 (Bannister et al., 2001; Lachner et al., 2001; Nakayama et al., 2001) and allows for chromatin folding. However, recently developed techniques have shown that these earlier characterizations of histone methylation not true in all cases. Recent advances in mass spectrometry and chromatin immunoprecipitation (ChIP) analysis have led to the detection of multiple modified residues on a single nucleosome as well as enabled the study of histone signatures on a genome-wide level. These recent findings have shown that H3K4me3 is present on untranscribed promoters in stem cells (Mikkelsen et al., 2007) and that H3K9me3 and HP1 can be associated with transcriptional elongation (Vakoc et al., 2005). So it seems that the roles of methylation marks can be context dependent.

1.2 Regulation of Higher-Order Compaction of Chromatin

1.2.1 Organization of Chromatin in vivo

The regulation of the chromatin is carried out in large part by the nucleosome and post-translational modifications of histones. We will now discuss the structure of chromatin in order to understand the mechanism by

which histone modifications accomplish this regulation. The relationship has been evident since the earliest light microscopy studies on chromosomes and nuclei. The DNA present in the eukaryotic cell has been characterized by early light microscopists as being comprised of both euchromatin and heterochromatin. Heterochromatin was defined as the chromatin that remained densely packed throughout the cell cycle and is the more abundant class of chromatin. In contrast, euchromatin decondenses to a point where it is no longer visible during interphase and is the minor class. Heterochromatin can be further distinguished as constitutive or facultative based upon whether there is a consistent relationship between the DNA sequence involved and its presence as heterochromatin across cell types and differentiation state. The former is exemplified by centromeric and pericentromeric heterochromatin, which are virtually always highly condensed, while the latter contains sequences that are either heterochromatic or euchromatic, depending on the cell type and state of differentiation. The inactivation of 1 of the 2 human X chromosomes in females is an example of facultative heterochromatin.

Beginning in the 1980's, biochemical properties that distinguish these different morphological classes of interphase chromatin have been identified and their mechanistic bases are increasingly understood. In this regard, DNase I digestion kinetics have proven to be one of the most revealing features of chromatin and reflects the close relationship between structure and function, where differences are reflected in the accessibility of the underlying DNA sequence to the nuclease probe. At the coarsest level,

sequences that are transcribed or in a chromatin conformation compatible with transcription in a given cell are digested about 3-times more rapidly than sequences that are never transcribed in the same cell (Weintraub and Groudine, 1976). Increased rates of digestion at this level have been correlated with increased histone acetylation and reduced histone H1 content (Iovcheva et al., 1984; Krajewski and Becker, 1998; Perry and Annunziato, 1989; Ridsdale et al., 1988). At higher resolution, small regions of sequences involved in transcriptional regulation are digested at rates at least ten times faster than the surrounding sequences. These sites are consistently associated with the binding of proteins directly involved in the regulation of transcriptional activation (Keene et al., 1981; Lu and Richardson, 2004).

This higher level of compaction seen in heterochromatin as opposed to euchromatin is a function of the level of folding of the chromatin strands. The formation of mitotic chromosomes is an example of folding and compaction of chromatin to the densest biologically relevant form. The mechanism of chromatin folding and compaction is not well described, however, much work has focused on the 30nm chromatin fiber. The 30nm fiber represents the first order of folding of a nucleosome array and is believed to be transcriptionally silent (reviewed in (Staynov, 2008)). Doubts exist, however, as to whether the 30nm fiber exists *in vivo* or is an artifact of chromatin isolation. Despite these doubts, much *in vitro* evidence has led to a broad outline of the 30 nm fiber suggesting that the basic architecture is a helical arrangement of nucleosomes with a diameter of ~33nm and a pitch of

~11nm (McGhee et al., 1983; Widom and Klug, 1985). The nucleosome packing density is more variable as it is commonly shown to contain 6-7 nucleosomes/11nm (Gerchman and Ramakrishnan, 1987; Ghirlando and Felsenfeld, 2008; Widom and Klug, 1985) but has been found to be as dense as 14-15 nucleosomes/11nm (Robinson et al., 2006). It may be the case that the packing density of fibers is variable and dependent upon the region of chromatin studied (Bassett et al., 2009; Gilbert and Allan, 2001). The 30nm fiber is also characterized both by the linker DNA length, which is found to range between 20 and 90bp but are usually found in increments of 10bp (a distance corresponding approximately to one helical turn of DNA) (Strauss and Prunell, 1983; Widom, 1992), and the suggested organization of the nucleosomal helix as a two-start coil (Dorigo et al., 2004; Schalch et al., 2005).

The ability of chromatin to assemble into higher level folding such as the 30nm fiber seems to be dependent on the ability of nucleosomes to interact and stack (Mangenot et al., 2003). These nucleosomal interactions are required to overcome the destabilization due to entropy in the 30nm fiber and are a result of contacts on the nucleosome surface. The regular pattern of the 30nm fiber dictates that the nucleosomes must be stacked so that they have similar orientation in relation to each other. This may explain the finding that the DNA linker length is found in increments of 10bp as this would allow a regular positioning of the nucleosomes. This regular orientation allows for internucleosomal interactions throughout the length of

the fiber which seem to be mediated by specific contact between H4K16 and an acidic patch on H2A (Luger et al., 1997; Robinson et al., 2008; Shogren-Knaak et al., 2006; Zhou et al., 2007) as well as a lesser described interaction between H2B- 3 and H2B- C helices (Bassett et al., 2009; Luger et al., 1997)). The chromatin fiber is also stabilized *in vivo* by chromatin binding proteins, such as HP1, which may be able to join neighbouring nucleosomes through dimerizing and binding to adjacent H3K9me3 sites (Bannister et al., 2001; Cowieson et al., 2000).

Chromatin folding of higher order than the 30nm fiber is more controversial. Several models exist which attempt to describe this organization. Early studies proposed the existence of a radial-loop model where loops of 30nm fibers are anchored to a protein scaffold running axial to the condensed structure (Marsden and Laemmli, 1979). In support of this model, many non-histone proteins are required for chromatin condensation. These proteins that drive condensation include topoisomerase II and condensins (Earnshaw et al., 1985; Hudson et al., 2003; Maeshima and Laemmli, 2003). However, certain findings seem to dispute this model. A brief nuclease treatment leads to a loss of chromatin elasticity, a finding that would not occur if a protein scaffold was responsible for retaining a condensed chromatin state (Poirier and Marko, 2002). Additionally, the rapid recovery of topoisomerase II after photobleaching is not indicative of a stable scaffold for chromatin attachment (Christensen et al., 2002; Tavormina et al., 2002). Various other models have also been proposed such as the helical

coiling of the 30nm fiber into progressively larger forms until maximum compaction is reached (Belmont et al., 1987; Kireeva et al., 2004), or the random loop polymer model characterized by loops of random size with scaffold proteins present at the loop attachment points (Mateos-Langerak et al., 2009).

Most models of chromatin folding are built upon the idea that the 30nm fiber is the starting point for higher order folding, however a more recent model has been proposed suggesting that the 30nm fiber is not involved in the most densely compacted form of chromatin, the mitotic chromosome. Cryo-electron microscopy, electron microscopy that ensures images of near-native states of the cell and involves no chemical treatment, of mitotic chromosomes shows a uniform chromatin mass with no evidence of a 30nm fiber (Eltsov et al., 2008). The authors put forth the dynamic melt model. This model postulates that a higher packing density of nucleosomes will lead to internucleosomal interactions from neighbouring 30nm fibres. This will lead to interfiber binding competing with intrafiber binding until a homogeneous “melt” occurs. This model explains the absence of evidence of the 30nm fiber in mitotic cells as well as the finding that the folding of the mitotic chromosome is not regular and reproducible (Strukov and Belmont, 2009). This model also provides a mechanism to form a condensed chromosome structure without the need of stable topoisomerase II or other scaffold proteins. To date, no further testing of this model exists.

Regardless of whether the 30nm fiber exists *in vivo* or which model of higher order folding and mitotic condensation is shown to be correct, one crucial player in chromatin compaction is the internucleosomal interaction mediated by exposed histone surfaces and N-terminal “tails”. It is this contact between the exposed histone surfaces of the nucleosomes that allows the folding of chromatin. As discussed above, this is carried out by direct and effector-mediated interactions with the histone tails. However, we have also seen the discrepancies in the established characteristics of certain post-translational modifications. Recent findings have led to the proposal of bivalent interactions in order to explain certain discrepancies.

1.2.2 Bivalent Model of Effector-Mediated Events

The recent advances in ChIP techniques, namely ChIP-Seq (Barski et al., 2007; Mikkelsen et al., 2007), allow for the identification of the DNA to which a given histone modification will bind on a genome-wide level, while recent advances in mass spectrometry, namely top-down mass spectrometry (Han et al., 2006; Pesavento et al., 2008a), allow for the identification of all possible modifications and combinations of modifications on a given histone. The potential of these techniques to further our understanding of epigenetic marks is revolutionary; however, both techniques are averaging the content of a particular cell population. This will lead to the underrepresentation of histone marks that may be specific to a subpopulation of cells or cell cycle-dependent changes if heterogeneity of these characteristics exists.

It is now evident that multiple modified residues can coexist on the same nucleosome, which may lead to some of the conflicting results in the literature. The presence of one histone mark may either be “overridden” by a neighbouring mark or perhaps histone modifications function in combination with neighbouring marks. An early theory regarding effector-mediated chromatin effects, termed “the histone code hypothesis” states: “that multiple histone modifications, acting in a combinatorial or sequential fashion on one or multiple histone tails, specify unique downstream functions” (Strahl and Allis, 2000). This hypothesis led to the postulation that a given histone signature will result in a given downstream effect. However, as we have seen, there seem to be redundant marks within the histone signature, inconsistencies as to the effects of certain histone marks, as well as multiple binding partners for a particular post-translational modification (PTM). These inconsistencies require that revisions be made to the histone code hypothesis.

Recently, discussion is taking place that focuses on the effector-mediated roles of physical proximity of the myriad of possible histone modifications. It is now postulated that multivalent interactions of histone binding domains contained within a single protein or protein complex will greatly alter the specificity, binding affinity and dissociation rates of the complex (reviewed in (Ruthenburg et al., 2007)). Early experiments in the chromatin modification field focused on correlating histone modifications with gene activation and binding domains. Frequently, data on dissociation

rates, binding affinities, and specificity were not measured or taken into account. What resulted was development of a canon of interactions between a given histone modification, the modified-histone binding domains and presumed function based on correlative evidence. We have seen, however, that recent techniques show conflicting modification marks present on the same nucleosome. The presence of multivalent interactions may account for these inconsistencies.

For example, complexes that contain multivalent interactions exponentially increase binding affinities when the associated histone modifications are in close proximity and in the proper conformation. Conversely, binding affinities of a multivalent complex may not be sufficient to form a stable interaction when only one binding site is present. This may account for the observed inconsistencies. Evidence exists that supports this theory. Several proteins and protein complexes contain bivalent domains: the lysine demethylase jumonji domain-containing protein 2A (JMJD2A) contains two tudor domains (Klose et al., 2006; Whetstone et al., 2006), the Piccolo/nucleosome acetyltransferase of H4 (PicNuA4) complex contains both a PhD and a bromo domain (Berndsen et al., 2007), the LSD-CoREST demethylase complex (lysine specific demethylases-RE-1 silencing transcription factor corepressor) contains a DNA binding SANT domain (SWI-SNF, ADA, N-CoR, and TFIIB) and the methylated-lysine binding amine oxidase domain (AOD) and SWIRM (Swi3p, Rsc8p, and Moira) domains (Yang et al., 2006) as well as many others. Critical information

regarding binding of these multivalent complexes is lacking to support or refute this theory.

Of interest to the regulation of chromatin folding and compaction, if the conformation is not optimized for a multivalent complex then strain is introduced and binding affinities are decreased. Interestingly, the precise positioning of the nucleosomes provided by linker DNA consistently found in 10bp increments may play a role in reducing strain in multivalent interactions in addition to the hypothesized nucleosome-nucleosome interactions. The variation of nucleosome spacing between euchromatin and heterochromatin would also play a role in the positioning of histone tail binding sites and the binding of multivalent complexes. It is now clear that the study of histone modifications has led to an abundance of data, yet the complexity of its regulation has prevented our full understanding of the process.

Despite the ambiguity in both the roles of histone modifications as well as the mechanisms by which downstream effects are accomplished, many functional studies have detailed the protein components and outlined potential pathways of regulation of histone modifications. The requirements of heterochromatin formation and maintenance of pericentromeric regions in particular is well studied and central to the interests of the research described in this thesis. Pericentromeric heterochromatin contains a well-documented epigenetic signature, the disruption of which leads to loss of chromatin

compaction. This results in defects when the cells undergo mitosis. However, prior to discussing the maintenance of pericentromeric heterochromatin, we must discuss the centromere in order to understand what roles the heterochromatin may play in mitotic defects.

1.3 The Centromere, Kinetochore and Mitosis

1.3.1 Epigenetic Determination of Centromeres

The centromere is essential for the correct segregation of sister chromatids during cell division. During entry into mitosis, the centromeric chromatin specifies the initiation of kinetochore assembly (Chan et al., 2005), which is a massive multi-protein assembly occupying a surface area of approximately $0.2\mu\text{m}^2$ /kinetochore (Cherry et al., 1989). The kinetochore mediates microtubule attachment at the centromere during mitosis. Remarkably, as centromeric sequences were defined across species, the centromere was found to be one of the fastest evolving regions of the genome (Malik et al., 2002). Although this may account for the lack of primary sequence conservation of the centromere, certain elements, such as alphoid satellite DNA and GGAAT repeats, are common (Grady et al., 1992; Nakano et al., 2003) and are known to contribute to the assembly of the human centromere. Alphoid DNA is not sufficient for the recruitment of many essential kinetochore proteins such as CENH3, CENP-C and CENP-E (Nakano et al., 2003; Sullivan and Schwartz, 1995; Warburton, 2001; Warburton et al., 1997). The migration of centromeres within otherwise

conserved arrangements of genes and the existence of neocentromeres in humans provide convincing evidence for an epigenetic basis to centromere specification (Warburton, 2001).

In order to describe the requirements of centromere establishment, Warburton et al. (2001) comprehensively catalogued protein recruitment to normal, neo and inactive centromeres. Neocentromeres refer to fully functioning centromeres that have no α -satellite DNA while inactive centromeres refer to the inactive centromere in a dicentric chromosome. Certain characteristics such as intense DAPI (4',6-diamidino-2-phenylindole) staining (denoting highly condensed AT-rich DNA) and, by definition, α -satellite DNA, were shared among the normal and inactive centromeres but were absent from neocentromeres. From this, it can be concluded that these sequences are neither sufficient nor required for the formation of a centromere. This result was mirrored independently when it was demonstrated that CENH3 containing chromatin is able to spread over non α -satellite DNA when non α -satellite DNA is added to α -satellite centromeric DNA (Lam et al., 2006). This divergence from a strict sequence-dependence of the centromere has led to the conclusion that the centromere is specified epigenetically in higher eukaryotes.

Chromatin in the centromere differs biochemically from the remainder of the genome in some very fundamental ways. Early studies indicated that three proteins, CENH3, CENP-B and CENP-C, were found to be specific to

functional centromeres (Earnshaw and Migeon, 1985). Following this discovery, the study of CENH3 revealed it to be a homolog of histone H3 that is specific for centromeric regions (Palmer et al., 1989; Palmer et al., 1991; Palmer et al., 1987). These results are corroborated by the finding that CENH3 substitutes for H3 in active centromeric and neocentromeric nucleosomes, but is not present at inactive centromeres (Warburton, 2001; Warburton et al., 1997).

By stretching chromatin on glass slides, Sullivan and Karpen (2004) mapped the histone H3 and CENH3 distribution in HeLa and *Drosophila* centromeric chromatin (CEN chromatin). This study determined that the *Drosophila* CENH3 homologue, CID, is incorporated as clusters of nucleosomes 10-40 kbps in length that are interspersed with histone H3-containing nucleosomes. However, 3-D analysis of chromatin in *Drosophila* cells shows that CID-containing nucleosomes localize immediately underneath the kinetochore protein CENP-E, implying localization to the centromere (Blower et al., 2002; Schueler and Sullivan, 2006; Sullivan and Karpen, 2004). Thus, while the linear DNA sequence contains interspersed clusters of CENH3 and histone H3-containing nucleosomes, within the 3-dimensional organization CENH3 and histone H3 nucleosomes segregate into independent regions of the centromere.

This same paper by Sullivan and Karpen (2004) also showed in human cells that the H3-containing nucleosomes within CEN chromatin were

found to be hypoacetylated, typical of heterochromatin, and enriched in H3K4me2, typically associated with potentiated regions of chromatin. A subsequent study by Lam et al. (2006) has helped to elucidate a role for the dimethylation of lysine 4 on histone H3 in CEN chromatin. This study provides evidence that this modification is present in varying amounts interspersed with CEN chromatin and separating the CEN chromatin from the flanking pericentromeric heterochromatin (Lam et al., 2006). Chromatin immunoprecipitation studies of *S. pombe* confirmed that the centromere is enriched in dimethylated lysine 4 and depleted in trimethylated lysine 9 on histone H3 (Cam et al., 2005). Regarding whether this unique modification signature is transcriptionally active or silencer, in *S. Pombe*, it has been found that the CENH3 chromatin is less effective at repressing the expression of a reporter gene than the surrounding pericentromeric heterochromatin (Allshire et al., 1994; Lam et al., 2006; Pidoux and Allshire, 2004).

Experiments mis-expressing CENH3 that lead to its incorporation into regions of the genome other than centromeres have demonstrated that its presence is not sufficient to generate a functional centromere (Van Hooser et al., 2001). Nonetheless, it is equally clear that CENH3 incorporation is a feature of all functional centromeres. As stated above, CENH3 is a histone H3 homolog. An important distinction between H3 and CENH3 is found in its N-terminal sequence, which is required for proper centromeric function. The N-terminal sequence is required for the assembly of at least one protein

complex at the yeast centromere (Chen et al., 2000) and is able to recruit CENP-C, hSMC1 (human structural maintenance of chromosomes protein), and hZW10 (human Zeste White 10) in human cells (Van Hooser et al., 2001). Conversely, it is the globular domain of CENH3 which dictates incorporation specifically into the centromere. Divergence from histone H3 in the L1 loop and the 2-helix are necessary and sufficient to target CENH3 to the centromere (Black et al., 2004). When this domain is placed into the histone H3 sequence, the synthetic histone H3 targets to the centromere (Black et al., 2004).

1.3.2 Specification of the Centromere

In addition to CENH3, other proteins have been found to localize to the centromere throughout the cell cycle. Since most kinetochore proteins are recruited to the centromere only at mitosis, proteins that are constitutively present may play an important role in the specification of the centromere. To date, it is evident that at least six proteins are constitutively centromeric, CENH3, CENP-B, CENP-C, CENP-H, CENP-I (hMis6) and hMis12 (Chan et al., 2005) and thus, each should be looked at more closely in order to determine their respective roles. It is known that CENP-B is not required for a functional centromere (Perez-Castro et al., 1998; Warburton, 2001) and so must not be a crucial protein for centromere specification. Recruitment of each of CENP-C, CENP-H and CENP-I appear to be downstream of CENH3 localization. Centromeric localization of CENP-C requires both CENP-H and

CENP-I, while CENP-H and CENP-I are dependent on each other for proper localization (Fukagawa et al., 2001; Nishihashi et al., 2002). Additionally, although CENH3 and hMis12 are both needed for CENP-I localization, the knockdown of any one of CENP-C, CENP-H or CENP-I has no effect on CENH3 localization (Fukagawa et al., 2001; Goshima et al., 2003; Liu et al., 2003; Nishihashi et al., 2002). This contradicts the expectation, based on *S. pombe* experiments, that CENP-I, the human Mis6 homologue, is required for replication independent assembly of CENH3 into centromeric nucleosomes (Hayashi et al., 2004). In all cases, however, these studies demonstrate that CENH3 incorporation is central to the assembly of a functional centromere.

As CENH3 is a structural variant of histone H3, its incorporation into the nucleosome at the centromere will play a large role in centromere positioning. In *S. pombe*, the genetics of CENH3 incorporation are relatively well defined. In *S. pombe*, there are two separate pathways for CENH3 incorporation and the protein is incorporated in both S-phase and in G2. S-phase incorporation requires a GATA family member, Ams2 (Takahashi et al., 2005). The G2 pathway, however, is of particular relevance to the replication-independent assembly that appears to operate in mammalian cells. This pathway is dependent upon the *S. pombe* homologue of RbAp46 and RbAp48, Mis16, and Mis18 (Hayashi et al., 2004; Takahashi et al., 2005). These proteins have a number of functions in chromatin and are associated with chromatin remodeling complexes, chromatin modifying enzymes, and

histone chaperones (Loyola and Almouzni, 2004; Zhang et al., 1999). In *S. pombe*, these proteins are responsible for recruiting a complex of Mis6, Mis15, Mis17 (Hayashi et al., 2004) and, more recently, Scm3 (Pidoux et al., 2009; Williams et al., 2009), which seem to be responsible for CENH3 deposition. Seemingly homologous with the Mis16-Scm3 pathway in *S. pombe*, recent findings indicate that RbAp46/RbAp48 is required for the stabilization of HJURP (Holliday junction recognition protein) localization to centromeres in telophase/early G1 (Dunleavy et al., 2009; Foltz et al., 2009). This complex is proposed to carry out the centromeric nucleosome remodeling and CENH3 incorporation. Contrary to earlier findings, it now seems that CENH3 incorporation occurs in telophase/early G1 in both *S. pombe* and mammalian cells (Dunleavy et al., 2009; Foltz et al., 2009; Pidoux et al., 2009; Williams et al., 2009).

Recent findings using atomic force microscopy in *Drosophila melanogaster* have shown that the centromeric nucleosomes differ greatly from the canonical nucleosome in that it is a tetramer of H2A, H2B, CENH3 homolog and H4 (Dalal et al., 2007a; Dalal et al., 2007b). This unique nucleosome structure, termed “hemisome”, contains longer linker DNA and seems to account for the altered micrococcal nuclease digestion pattern that has been observed at centromeres (Takahashi et al., 2000). As mentioned, the centromere serves as the kinetochore assembly site, which then allows for microtubule binding and chromosome segregation. The unique qualities of the hemisome have led to a revised model of the centromere whereby the

interspersed heterochromatin sections in the linear sequence of chromatin (described in (Lam et al., 2006)) packs tightly leading into mitosis. In this proposed model, the hemisome, which is smaller in size, long linker DNA and asymmetry, is not able to incorporate into the compacted centromeric chromatin. As such, it is extruded from the packing and is exposed as the periphery of the centromere. Kinetochore proteins are then able to bind to the exposed hemisomes (Dalal et al., 2007a) and allow for chromosome segregation.

1.3.3 Kinetochore Formation and Chromosome Segregation

The centromere is crucial for cell cycle progression because it is the specialized chromatin region that allows for the assembly of the kinetochore. The kinetochore, in turn, is needed because it is both the regulator of the mitotic checkpoint and the point of attachment for microtubules in mitosis. The mitotic checkpoint is a cellular mechanism that prevents chromosome segregation until all chromosomes are under bi-polar tension. Tension is created by proper microtubule attachment to kinetochores on either side of each chromosome (Chan et al., 2005). We will briefly discuss the formation of kinetochores and the mechanism of chromosome segregation.

As the cell enters mitosis in prophase, replicated chromosomes are compacted while, concomitantly, kinetochores begin to assemble at the centromeres of sister chromatids. Following the breakdown of the nuclear envelope in prophase, microtubules originating from the paired spindle poles

are then able to interact with the assembled kinetochores to ultimately attain bipolar attachment on each chromosome. Once bipolar attachment is achieved on a chromosome, it is able to align along the metaphase plate. Upon alignment of all chromosomes in metaphase, the sister chromatids are then separated and migrate to the opposing poles. The cell is prevented from separating prematurely, prior to the bipolar attachment and alignment of the chromosomes, by the mitotic checkpoint (also referred to as the spindle-assembly checkpoint). The checkpoint is able to be maintained by the presence of a single unattached or improperly attached kinetochores (for review see (Cheeseman and Desai, 2008)).

The greater than 80 different kinetochore proteins identified thus far are found in subcomplexes in and around the centromere and carry out several crucial functions. There are constitutive kinetochore proteins that are found on the centromere and seem to play roles in centromere specification as discussed in the previous section. Other kinetochore proteins are required for assembly of the kinetochore complex, microtubule binding, stabilization of kinetochore-microtubule attachment and monitoring kinetochore-microtubule attachment in order to maintain the mitotic checkpoint.

Microtubules emanate from the spindle poles in and are able to polymerize towards kinetochores by responding to a Ran-GTP gradient that exists near kinetochores. The interaction of microtubules with the outer kinetochore then allows for microtubule binding. This microtubule-

kinetochore interaction is stabilized by CENP-E binding and the tension generated by the pulling force of the kinesin molecules associated with the microtubules, dynein-dynactin (Dewar et al., 2004; McEwen et al., 2001). In the absence of adequate tension, the microtubule-kinetochore interaction is destabilized. This allows the destabilization of microtubules that are improperly bound, such as a syntelic attachment (both kinetochores bound to microtubules emanating from the same pole) or a merotelic attachment (a single kinetochore bound to microtubules emanating from both poles). Data exists that demonstrate that the stabilization of microtubule attachment is carried out by the tension-mediated hyperphosphorylation of BubR1 (budding uninhibited by benzimidazoles related 1) by Plk1 (polo-like kinase 1) (Elowe et al., 2007). Additionally, tension leads to the physical separation of the kinase Aurora B (Aim-1 in mammalian cells) from its substrate, mitotic centromere-associated kinesin (MCAK). This separation prevents further MCAK phosphorylation, the loss of which destabilizes microtubules (Cheeseman and Desai, 2008; Liu et al., 2009).

Cohesin is critical to maintain cohesion between sister chromatids and seems to be present along the chromosome arms. Recent evidence in yeast shows that it may be deficient at the centromere in mitosis (Sakuno et al., 2009). The HP1 yeast homolog, swi6, recruited by H3K9me3, has been shown to be directly involved in the recruitment of the cohesin complex in yeast cells (Bernard and Allshire, 2002; Bernard et al., 2001; Nonaka et al., 2002). This function appears not to be conserved in mammalian cells

because HP1 and cohesin are found to be independent (Koch et al., 2008; Serrano et al., 2009). Upon satisfaction of the mitotic checkpoint, the cohesin is cleaved by separase. The checkpoint is believed to be satisfied when tension arising from proper bipolar microtubule attachment is present along all chromosomes. Although the exact mechanism of tension mediated mitotic checkpoint remains unclear, several recent studies show possible mechanisms. Shugoshin (Sgo2) is tightly bound to cohesin at the inner centromere prior to microtubule-mediated generation of tension and then rapidly relocalizes to the kinetochore in the presence of tension (Lee et al., 2008a). While bound, Sgo2 plays a role in inhibiting separase in yeast (Clift et al., 2009).

As we have seen, the centromere is necessary for chromosome segregation. It not only allows for the formation of the kinetochore but also is required to transmit tension in order to satisfy the mitotic checkpoint. The 3-dimensional organization of the centromere is believed to contain the centromeric chromatin at the exposed surface and the pericentromeric heterochromatin forming the inner layer of the primary constriction (Dalal et al., 2007a; Marshall et al., 2008; Sakuno et al., 2009; Sullivan and Karpen, 2004) (Figure 3). With this arrangement, the potential importance of pericentromeric heterochromatin in chromosome segregation becomes clear. This compacted chromatin is contained within the inner centromere region, the region housing tension-sensing kinetochore proteins crucial for the mitotic checkpoint.

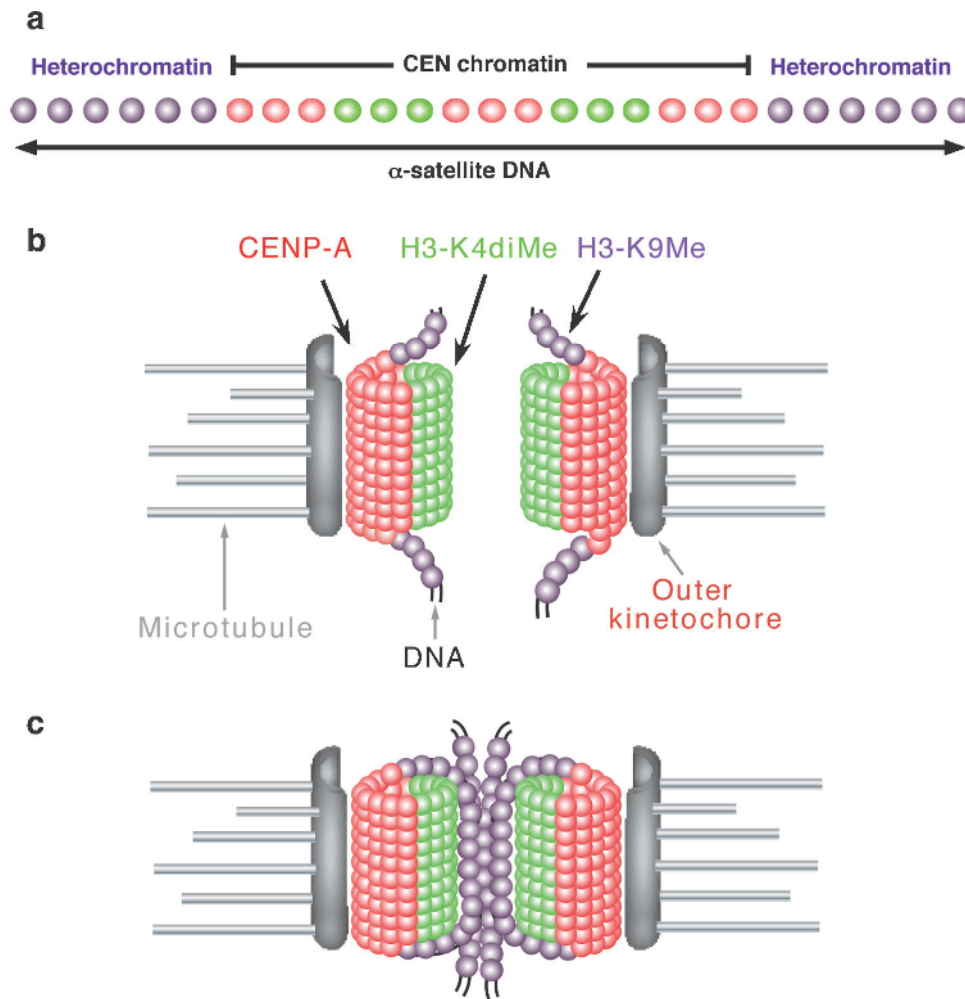


Figure 3 The Structure of the Centromere

A: The two dimensional organization of human centromeric chromatin shows a unique organization of subdomains of nucleosomes containing CENH3 (in red) interspersed with subdomains of H3K4me2 within the centromere. This arrangement of centromeric chromatin is flanked by heterochromatin containing H3K9me3 and is contained within the megabase regions of α -satellite DNA present at active centromeres. B: Upon chromatin condensation in mitosis the subdomains coil to allow the CENH3 containing nucleosomes to form the outer layer of the primary constriction, while the H3K4me2 subdomains form the underlying region. This conformation allows for the accessibility of CENH3 containing nucleosomes to other kinetochore proteins. C: The final conformation of the primary constriction in mitosis includes pericentromeric heterochromatin forming a distinct domain at the inner centromere.

Reprinted with permission from Schueler, M.G. and B.A. Sullivan, 2006.

1.4 H3K9 Methylation and Pericentromeric Heterochromatin

1.4.1 H3K9 Methylation

H3K9me3 has been briefly mentioned as being both present at and required for pericentromeric heterochromatin and will be described further. The trimethylation of H3K9 is catalyzed by SUV39h1 and SUV39h2 (suppressor of variegation 3-9) (Bannister et al., 2001; Fischle et al., 2005; Lachner et al., 2001; Nakayama et al., 2001). The SUV39h1 gene is located on the X-chromosome and encodes a 47 kDa protein containing both a chromo- and a SET (Suppressor of variegation 3-9, Enhancer of zeste, and Trithorax) domain. The localization of SUV39h1 is dependent upon the chromodomain and an adjacent HP1 interaction domain (Lachner et al., 2001; Melcher et al., 2000). The SET domain is the catalytic subunit responsible for trimethylating H3K9 (Rea et al., 2000) and requires phosphorylation for its proper localization and activation (Firestein et al., 2000). It has also been shown that SUV39h1 is preferentially phosphorylated within mitosis (Aagaard et al., 2000). Additionally, the SET domain of SUV39h1 can be acetylated on lysine 266 and needs to be deacetylated by Sirtuin1 (SirT1) for its activity (Vaquero et al., 2007). DBC1 (deleted in breast cancer 1) inhibits the interaction of SirT1 with the SET domain of SUV39h1 by competitively inhibiting both proteins, thereby inactivating SUV39h1 activity (Li et al., 2009). The HP1 interaction domain enhances SUV39h1 binding but is not required for the stability of this binding

(Krouwels et al., 2005). Surprisingly, the catalytic SET domain and adjacent regions play a large role in the stabilization of SUV39h1 binding to heterochromatin (Krouwels et al., 2005). SUV39h1/h2, as well as the majority of methylation events within the cell, obtain the methyl group from the global methyl donor, s-adenosylmethionine (Loenen, 2006).

This stable binding to heterochromatin allows for the maintenance of H3K9me3 as well as the maintenance of additional heterochromatin marks, among them HP1 (Stewart et al., 2005). Knock-out studies of the SUV39h1 and SUV39h2 homologs in mice results in widespread genomic instability and increased incidence of lymphomas (Peters et al., 2001). More recently, we characterized chromosome segregation defects in immortalized mouse embryonic fibroblasts isolated from SUV39h1/h2 double null mice. We found an approximately 4-fold increase in the number of chromosome alignment and chromosome segregation defects (McManus et al., 2006). Conversely, the overexpression of SUV39h1 alters cell proliferation and causes growth retardation in mice (Czvitkovich et al., 2001). The intricate regulation of SUV39h1 activity and the defects associated with its misregulation suggest an important role for H3K9me3 in pericentromeric heterochromatin.

1.4.2 Additional regulation of pericentromeric heterochromatin

The DNA within pericentromeric heterochromatin in mammalian cells consists mainly of α -satellite DNA (Maison and Almouzni, 2004). This α -

satellite DNA makes up the entire centromeric and pericentromeric regions on each chromosome (Schueler and Sullivan, 2006), however the sequence of the α -satellite DNA is specific to each. Pericentromeric heterochromatin flanks the centromere in the linear structure of chromatin and, as mentioned above, forms the innermost layers of the centromere in mitosis when folded *in vivo* (Gieni et al., 2008a; Schueler and Sullivan, 2006). The chromosomal site for the centromere and the pericentromeric heterochromatin, when properly formed *in vivo*, is referred to as the primary constriction.

Pericentromeric heterochromatin is characteristically enriched in HP1 (Minc et al., 1999), H3K9me3 (Peters et al., 2003), H4K20me3 (Biron et al., 2004; Schotta et al., 2004), H3K27me1 (Rice et al., 2003), hypoacetylated histones H3 and H4 (Johnson et al., 1998), and the methylation of cytosine within the DNA (5-meC) (Henikoff, 2000). The maintenance of histone modifications in pericentromeric heterochromatin involves many proteins and the loss of any of a number of these proteins leads to mitotic defects. The pathway involved in heterochromatin maintenance involves a cyclical pathway where positive feedback loops seem to be established. As mentioned above, lysine residues can be both methylated and acetylated (e.g. H3K9). The presence of an acetyl group on H3K9 interferes with both heterochromatin structure and the addition of methyl groups. The removal of acetyl groups is accomplished by histone deacetylase (HDAC) complexes (Xin et al., 2004). H3K9 methylation is dependent upon both this removal of an acetyl group and the presence of DNA methylation which is catalyzed by

DNA methyltransferases (DNMT) (Xin et al., 2004). The H3K9me3 provides a binding site for HP1 which, in turn, enables the recruitment of numerous heterochromatin forming proteins, including SUV39h1/h2, DNMT1 and HDACs (Lechner et al., 2005; Lehnertz et al., 2003; Smallwood et al., 2007; Smothers and Henikoff, 2000; Yamada et al., 2005; Zhang et al., 2002) (Figure 4 and reviewed in (Grewal and Jia, 2007)). Additionally, H3K9me3-dependent localization of HP1 is required for the localization of SUV420h1/h2 and subsequent trimethylation of H4K20 (Schotta et al., 2004). Knock-out studies of SUV420h1/h2 in mice yielded similar findings in that both genomic instability and cell cycle delay results (Schotta et al., 2008). Findings in SUV420h1/h2 mice did not extend, however, into mitosis so no further evidence of its role in mitosis is described. Inhibiting DNMT1, HDACs or HP1 results in mitotic defects similar to those seen with the loss of H3K9me3 (Chen et al., 2007; Cheutin et al., 2003; Cimini et al., 2003; Inoue et al., 2008; Robbins et al., 2005; Stevens et al., 2008; Taddei et al., 2001; Tryndyak et al., 2006).

In addition to this cyclical dependence, the enzymatic machinery that carry out the modifications at the pericentromeric heterochromatin are also regulated by both the Rb family of proteins (Brehm et al., 1998; Luo et al., 1998; Magnaghi-Jaulin et al., 1998; Pradhan and Kim, 2002; Robertson et al., 2000; Vaute et al., 2002; Zhang et al., 2000) and short non-coding RNA transcripts derived from pericentromeric DNA (Maison et al., 2002; Muchardt et al., 2002). Regarding Rb involvement, the study of mouse

embryonic fibroblasts (MEFs) from triple null mice for the three Rb family member genes revealed that the trimethylation of lysine 20 on histone H4, but not lysine 9 on histone H3, was lost (Gonzalo et al., 2005) indicating that Rb functions downstream of H3K9me3. The karyotypes of these cells show the prevalence of mitotic defects. The phenotype of these cells includes elongated telomeres and an apparent defect in the release of cohesin near the centromeres, as well as genomic instability with a tendency to increase chromosome number with increased passage (Gonzalo et al., 2005). This phenotype parallels what has been reported for the SUV39 double null mice (Peters et al., 2001).

Further, heterochromatin maintenance unexpectedly also requires short RNA transcripts. With respect to this RNA dependence of heterochromatin, chromodomains are capable of binding to RNA transcripts (Akhtar et al., 2000). Since this discovery, HP1, which contains a chromodomain (Jacobs and Khorasanizadeh, 2002), has specifically been shown to require both H3K9me3 and an RNA component in order to bind to pericentromeric heterochromatin (Maison et al., 2002; Muchardt et al., 2002). An RNA binding component is not unique to HP1 as some centromeric proteins also require RNA. Both the centromeric protein CENPC1 and inner centromeric protein (INCENP), are dependent on RNA transcripts, specifically α -satellite RNA transcripts, for localization (Wong et al., 2007). Additionally, RNA transcripts may play a role via RNA interference (RNAi). In addition to the roles in post-translational silencing

via the degradation of mRNA, RNAi also induces silencing at a transcriptional level in certain organisms. The RNAi pathway is required for heterochromatin maintenance, best described in *S. pombe* and *Drosophila* (Pal-Bhadra et al., 2004; Verdel et al., 2004; Volpe et al., 2002). In these organisms, the loss of RNAi machinery leads to the loss of H3K9 methylation, HP1 localization, and heterochromatin silencing. This RNAi-dependent heterochromatin maintenance is also shown to be important in the proper establishment of centromeric chromatin and centromere formation (Folco et al., 2008). This process may be conserved in some vertebrates as chicken cell heterochromatin is shown to be dependent on Dicer function (Fukagawa et al., 2004). RNAi-mediated heterochromatin formation/maintenance is more controversial in mammals with some groups finding that the RNAi pathway is needed to maintain chromatin silencing and DNA CpG (cytosine and guanine separated by a phosphate) methylation (Kanellopoulou et al., 2005; Ting et al., 2008) while others show that it is not necessary (Wang et al., 2006).

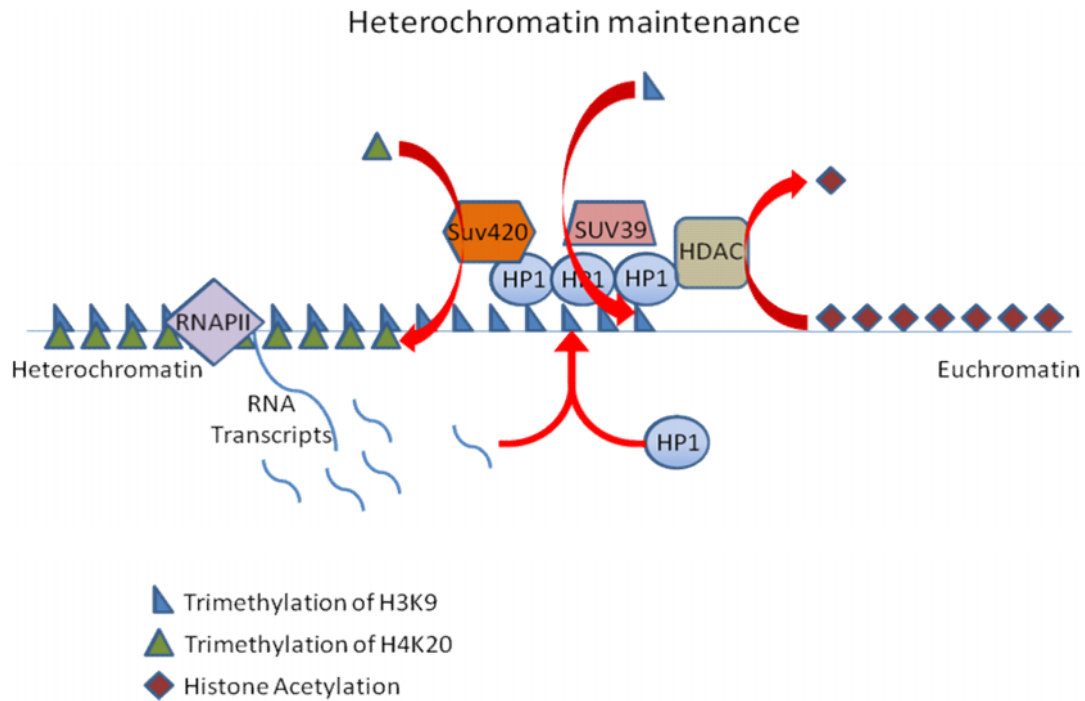


Figure 4 – A simplified model of heterochromatin maintenance

The various players implicated in heterochromatin maintenance are shown with the specific roles each plays. Histone acetylation must be removed in order for methylation to occur. This is accomplished by histone deacetylases (HDACs). Once deacetylation has occurred, trimethylation of H3K9 is catalyzed by SUV39h1/2. This methylation is both required for and dependent upon HP1 localization in a cyclical manner. HP1 also requires heterochromatin RNA transcripts in order to bind. Once HP1 and H3K9me3 is established, SUV420 then binds and trimethylates H4K20. The presence of each of these proteins and modifications are required for heterochromatin maintenance.

Although not functionally implicated in pericentromeric heterochromatin maintenance, additional potential players include the rapidly growing group of identified histone demethylases (Cloos et al., 2006; Fodor et al., 2006; Klose et al., 2006; Klose and Zhang, 2007; Lee et al., 2008b; Shi et al., 2004; Tsukada et al., 2006). It seems that most of these demethylases are specific to a single, or small number of, methylated state(s), with Jmjd2b specific to H3K9me3 with very slight activity on H3K9me2 and Jmjd2a specific to H4K20me3 and H3K4me3 (Fodor et al., 2006; Lee et al., 2008b). To date, the characterization of demethylases is mostly limited to identification and determining their specificity. Therefore, very little data exists regarding their expression profiles, regulation or activity *in vivo*. For these reasons, the effect that histone demethylases have on methylation levels *in vivo* is largely unknown. However, their existence does imply the presence of a dynamic equilibrium in methylation states.

The cyclical nature of the pericentromeric heterochromatin maintenance pathway and the presence of a dynamic epigenetic signature imply that a particular epigenetic signature may be able to spread laterally across the chromatin. Several findings support this mode of chromatin maintenance. First, we have already seen the H3K9me3/HP1 pathway, which allows for further trimethylation in a *cis* manner (Lachner et al., 2001). Second, with an overexpression of CENH3 and concomitant decrease of H3K9me2 within the centromeric chromatin, there is evidence that the pericentromeric heterochromatin, as denoted by H3K9me3, can expand (Lam

et al., 2006). This suggests that H3K9me2 acts to maintain a boundary between chromatin domains. Third, the finding that JMJD2A is able to demethylate H3K9me3 (Klose et al., 2006), a heterochromatin marker, and is recruited to H3K4me3 (Huang et al., 2006), a euchromatin marker, implies that there is active maintenance of chromatin at boundary regions and that the euchromatin mark may be able to spread laterally. Finally, MSL3 (male-specific lethal 3), a H4K16 acetyltransferase, contains a chromodomain and is known to be involved in transcriptional activation. MSL3 containing a mutated chromodomain is shown to lack the ability to spread laterally across the chromatin due to an inability to bind to H3K36me3 (Sural et al., 2008). These results clearly demonstrate the dynamic nature of heterochromatin domains and imply an ability of chromatin marks to spread if the equilibrium is altered in some manner.

1.4.3 Dynamics of Histone Modifications During Mitosis

In early G2, the pericentromeric heterochromatin is phosphorylated by the Aurora B kinase (Adams et al., 2001b; Fischle et al., 2005; Zeitlin et al., 2001). This targeting occurs as part of the INCENP-survivin-Aurora B complex (Adams et al., 2001a). The resulting phosphorylation of serine 10 on histone H3 correlates with the displacement of HP1 α , β , and γ , both reaching a maximum in metaphase, although a small amount of HP1 α is retained near the centromeres (Bartova et al., 2005; Fischle et al., 2005; Hirota et al., 2005). The purpose or function of HP1 displacement during mitosis is not known. Site-directed mutagenesis of lysine 9 and serine 10

revealed that each of these amino acids were important in recruiting HP1 to pericentromeric heterochromatin in *S. pombe* (Mellone et al., 2003). Moreover, mutations at each of these sites lead to chromosome segregation defects.

A possible explanation for these observations is the behavior of the Aurora B/Aim-1 kinase in the absence of lysine 9 trimethylation. Specifically, Aurora B/Aim-1 is not properly targeted to pericentromeric heterochromatin during G2 and the initiation of serine 10 phosphorylation is spatially and temporally altered relative to wild type cells (Heit et al., 2006). This raises the possibility that some of the mitotic defects observed in the absence of histone lysine 9 trimethylation are a result of a reduction in Aurora B/Aim-1 kinase activity in this domain. In the absence of Aurora B/Aim-1 kinase activity in *Drosophila*, histone H3 is not phosphorylated during mitosis (Adams et al., 2001b) and this correlates with an increase in the number of lagging chromosomes observed in anaphase figures (Adams et al., 2001b; Giet and Glover, 2001). It also correlates with an inability to recruit condensin, which compacts the metaphase chromosome (Giet and Glover, 2001). Together, this raises the possibility that some of the mitotic defects observed in the absence of histone H3 lysine 9 trimethylation may be a result of a reduction in Aurora B/Aim-1 kinase activity in this domain.

In addition to serine 10 phosphorylation, several methylated amino acid residues increase in mitosis. Early findings regarding histone

methylation indicated that the extent of methylation dynamics must be low because studies examining the turnover of radiolabel on histone proteins showed that the lifetime of the methylation paralleled the lifetime of the histone and was greater than the time required to complete a cell cycle (Annunziato et al., 1995; Borun et al., 1972). However, dynamic methylation that is restricted to either brief periods of the cell cycle or restricted to a small subset of residues (either site-specific or reflecting the dynamics of specific small pools of histones) may not be adequately labeled to be detected in a pulse-chase experiment.

Previous experiments in our laboratory have established that H3K9me3 increases beginning in late G2 and peaking in metaphase before decreasing in anaphase to reach a basal level in G1 (McManus et al., 2006). As mentioned above, the global loss of this methylation leads to chromosome segregation defects. Due to the dependence of the trimethylation of H4K20 on H3K9me3, there is also a possibility that H4K20me3 is affected by the increase in H3K9me3. This, however, is unconfirmed in the literature. H4K20me1 increases upon entry into mitosis (Houston et al., 2008; Rice et al., 2002). The global loss of this modification leads to global chromosome condensation errors and G2 arrest, a marked difference compared to the chromosome segregation defects associated with H3K9me3 and H4K20me3. This difference leads us to believe that H4K20me1 plays a separate role from H3K9me3 and H4K20me3. The experimental protocols of the studies describing the defects resulting from the loss of the above modifications

involved time periods of several cell cycles. However the demonstration that histone methylation increases in mitosis indicates that maintenance of heterochromatin may be dependent on active late G2 methylation that is required every cell cycle.

Section 1.5 Hypothesis

To date, established roles of histone methylation, such as the regulation of gene expression (Rea et al., 2000), X-inactivation (Rougeulle et al., 2003), and cell differentiation (Kubicek et al., 2006), suggest stability in the methylated residue. These roles require a methylation mark that is stable over successive cell cycles. The more recent findings described above imply that methylation may have an additional role that acts on a much shorter time scale. Specifically, H3K9 methylation is cell cycle-dependent (McManus et al., 2006) and must be very tightly regulated because both the over-expression (Melcher et al., 2000) and the loss (Peters et al., 2001) of SUV39h1 results in mitotic defects. These findings lead us to hypothesize that late G2 methylation is important for mitotic progression and chromosome segregation. Further, due to the roles of H3K9me3 in pericentromeric heterochromatin maintenance, the localization of pericentromeric heterochromatin in the centromere and the importance of tension in chromosome segregation, we hypothesize that the roles of late G2 methylation in mitosis will be mediated through kinetochore assembly and through structural roles of heterochromatin.

Section 2

Materials and Methods

Cell Culture

HeLa cell lines: HeLa (human epithelial cervical adenocarcinoma) cells were cultured in Dulbecco's modified Eagle's medium (DMEM) plus 10% fetal bovine serum in a 37 °C incubator with 5% CO₂. HeLa S3 cells, although typically grown in suspension, were used here as adherent cells. Culture was similar to HeLa cells. Immortalized embryonic fibroblast cell lines from SUV39h1 and SUV39h2 double null embryos were provided by Dr. Thomas Jenuwein (Peters et al., 2001). Cells were cultured in Dulbecco's modified Eagle's medium plus β -mercaptoethanol and non-essential amino acids (NEAA) in a 37 °C incubator with 5% CO₂.

Generation of HeLa Cells Stably Expressing green fluorescent protein (GFP) constructs

Three stably transfected HeLa cell lines (H2B-GFP, ZW10-GFP, and BubR1-GFP) were kindly provided by the Dr. Gordon Chan laboratory. These were cultured in the same manner as the parent HeLa cells with the addition of G418 (Invitrogen) to a final concentration of 50 μ g/mL in order to maintain the vector.

Drug Treatments

Adenosine Dialdehyde (AdOx): Cells were treated with 250 μ M adenosine dialdehyde (Sigma) for varying lengths of time. Cells were subsequently fixed, permeabilized, and counterstained with 4,6-diamidino-2-phenylindole (DAPI), and phenotypic abnormalities were manually scored.

5-Azacytidine: Cells treated with 5-azacytidine were first synchronized at the G1-S boundary using a double thymidine block. Cells were plated at 5×10^4 cells/mL into a 10cm dish. 24 hours later media was replaced with fresh media and 2mM final concentration thymidine was added. Fifteen hours later, media was removed and cells were rinsed twice with 1X phosphate-buffered saline (PBS). 9 hours later media was replaced once again with fresh media containing 2mM final concentration thymidine. After a second 15 hour-long thymidine treatment, media was removed and cells were rinsed twice with 1X PBS. Fresh media was added and a synchronized cell population was allowed to progress. Immediately following release 5-azacytidine was added to a final concentration of 3 μ M.

Nocodazole: Cells were treated with nocodazole at a final concentration of 15 μ M for 1-2 hours.

Immunofluorescent Labeling

Asynchronous cells were plated onto sterilized glass coverslips 1 day prior to immunostaining such that they were 50–80% confluent on the

following day. Cells were fixed, permeabilized, immunofluorescently labeled, and mounted as detailed elsewhere (McManus and Hendzel, 2003). The following primary antibodies were used at the dilutions indicated: anti-dMeK9 (1:200; Abcam ab7312), anti-tMeK9 (1:200; Abcam ab6001), anti-tMeLys4 (1:200; Abcam ab1012), anti-tMeK20 (1:200; Abcam ab9053) anti-centromeric antigen (1:1000; Dr. G. Chan), anti-CENP-E (1:1500; Dr. G. Chan), anti-CENP-F (1:1500; Dr. G. Chan), anti-tubulin (1:2000; Dr. G. Chan) and anti-phosphohistone H3 (Ser10) (1:400; Upstate Biotechnology, Inc., Lake Placid, NY 05-806). Appropriate secondary antibodies (*e.g.* goat anti-mouse IgG (H+L) or goat anti-rabbit IgG (H+L)) conjugated to fluorophores (*e.g.* Alexa Fluor 488 or Cy-3) were used for visualization of primary antibodies and were purchased from Molecular Probes, Inc. (Eugene, OR) or Jackson ImmunoResearch Laboratories, Inc. and used at a dilution of 1:200.

Cold Destabilization of Microtubules

Cells were grown on glass coverslips. Prior to fixation, media was replaced with ice-cold media and incubated for 10 minutes on ice. Cells were then fixed by adding 2 mL of 3.5% paraformaldehyde in 100 mM PIPES (piperazine-N,N-bis(2-ethanesulfonic acid)) at pH 6.8, 10 mM EGTA (ethylene glycol tetraacetic acid), 1 mM MgCl₂ and 0.2% Triton X-100. Cells were then washed in buffer A (10 mM Tris pH 7.5, 150mM NaCl and 0.1% BSA) plus 0.2% Triton X-100 for 5 minutes followed by a 5 minute wash in

buffer A. Antibody staining proceeded as above. The buffer A recipe is as follows: 10 mM Tris pH 7.5, 150mM NaCl and 0.1% bovine serum albumin (BSA).

Indirect Immunofluorescence Microscopy

Images were collected using MetaMorph (Universal Imaging Corp.) to control an Axiovert 200 M (Carl Zeiss MicroImaging, Inc.) equipped and acquired with a 12-bit charge-coupled device camera (Sensicam; Cooke Corp.) or a 14-bit charge-coupled device camera (Cascade; Photometrics). GFP was excited using a Xenon or Argon lamp. For images acquired on fields of cells, either a 0.75 NA Fluor 20x objective or a 1.3 NA Plan Fluor 40x objective (Carl Zeiss MicroImaging, Inc.) was used. For higher resolution images, either a 1.4 NA Plan Apo 63x objective or a 1.4 NA Plan Apo 100x objective (Carl Zeiss MicroImaging, Inc.) was used. Three channels, DAPI, FITC/Alexa 488 and Cy3 were used to obtain images of the various secondary antibodies. Time-lapse experiments were acquired at 37°C in standard DMEM with 10% fetal calf serum and a continuous CO₂ supply. Images were collected using Ultraview ERS (Perkin Elmer) coupled to an Axiovert 200 M (Carl Zeiss MicroImaging, Inc.) equipped and acquired with the Ultraview ERS Rapid Confocal Imager. GFP was excited using a 488 nm laser line and images were obtained with a FITC/Alexa 488 filter set.

Image Processing and Figure Construction

Images were directly exported as 16-bit TIFF files and rescaled over an 8-bit data range. In most cases, the background fluorescence of the medium and the base signal from the detector were subtracted to better represent the dynamic range of the data content in the image. In some instances, three-dimensional image sets were imported into Imaris 5.7 (BitPlane) and three-dimensional image sets were generated. In this instance, the image was scaled to map the data over the range of the display and the screen capture function in Imaris 5.7 was used to capture the image used in the figure. Figures were prepared in Photoshop CS2 (Adobe) for Windows. In general, images were scaled to span the 8-bit range after subtraction of background in the process, and then pasted into a composite canvas that was either 8-bit grayscale or 24-bit RGB color. If necessary, images were interpolated to 300 dpi using Photoshop.

Immunoblot Analysis

To confirm the availability and accessibility of all methylation epitopes and show their temporal regulation throughout the cell cycle, immunoblot analysis was conducted on protein extracts isolated from asynchronously growing cells and compared with extracts isolated from mitotic cells. HeLa cells were arrested at the G1/S-phase boundary by standard double thymidine block, washed extensively with PBS, media was added back to the cells, and they were permitted to progress for varying times. Asynchronous and subconfluent cells were harvested using 0.53 mM EDTA

(ethylenediaminetetraacetic acid). Cells were pelleted by centrifugation at 500 x g for 5 min at 4 °C and resuspended in PBS. Following the final PBS wash, cells were lysed in Nuclear Isolation Buffer (250 mM sucrose, 150 mM NaCl, 20 mM Tris-HCl (pH 8.0), 2 mM MgCl₂, 1 mM CaCl₂, 1% Triton X-100, and 1 mM phenylmethanesulfonyl fluoride). Nuclei were pelleted by centrifugation for 10 minutes at 3200xg and resuspended in 0.4N H₂SO₄ and placed on ice for 30 min. Nuclear debris was cleared by centrifugation at 25,000x g for 10 min. Supernatants were collected and added to 60 µl of 1 M Tris (pH 8.0) and 40 µl of 10 N NaOH.

The acid-extracted proteins from 2.0×10^5 asynchronously growing and mitotic-arrested cells were resolved on an 18% Sodium Dodecyl Sulfate (SDS)-polyacrylamide gel. The gel was run at a constant 80V for 20 minutes before being run at 155V for 140 minutes. Proteins were transferred to 0.2 µm nitrocellulose membranes at a constant 110V for 60 minutes and protein loading was confirmed by SYPRO® Ruby protein blot stain (Molecular Probes, Inc.) and visualized on the Typhoon Imager 8600 (Amersham Biosciences) using a 532nm excitation laser and a 610nm emission filter. Blots were then blocked with 5% BSA in Tris-buffered saline (TBS) for one hour, and incubated with the appropriate antibody in 5% BSA in TBS plus 0.05% Tween, with shaking for one hour. Immunoblots were then incubated with IR800-conjugated secondary antibodies in the dark (1:12,000; Rockland Immunochemicals). Fluorescence imaging of the immunoblots was

performed on the Odyssey Imaging System (Li-Cor Biosciences) in the IR800 channel as described by the manufacturer.

Electron Microscopy

Cells were grown on 35 mm cell culture dishes with or without the addition of AdOx as described above. The samples were fixed in Karrovsky's buffer composed of 2% glutaraldehyde and 2.5% paraformaldehyde in PBS. The samples were washed in buffer and post-fixed in 2% OsO₄ for 20 minutes. The samples were then passed through a graded ethanol series and subsequently infiltrated with Polybed 812 resin. Polymerization was performed at 60°C for 24 hours. Portions of the embedded cell monolayer containing cells of interest were selected by light microscopy and cut from the epon disc and mounted on epon blanks. Silver-gray sections were cut with a ultramicrotome (Leica) equipped with a Dumont (Hatfield PA) diamond knife and sections were stained with uranyl acetate and lead citrate and examined in a Hitachi H-7000 electron microscope.

Flow Cytometry

Cells were grown on 10 cm cell culture dishes with and without the addition of AdOx as described above. The cells were then removed from the plate with the addition of trypsin for 5 minutes, centrifuged at 500 x g for 10 minutes and resuspended in 0.5mL PBS. The resuspended cells were added to 70% ethanol for fixation and left at -20°C overnight. Cells were then collected by centrifugation, resuspended and rinsed in PBS and recollected

by centrifugation at 500 x g for 5 minutes. Pelleted cells were then resuspended in 500µL PBS containing a final concentration of 20µg/mL propidium iodide and 200µg/mL RNase A and left in the dark for 30 minutes at room temperature. DNA analysis was then performed using a Becton Dickinson FACsort flow cytometer with a 488 nm laser line and analyzed using BD CellQuest Pro™ Software (BD Biosciences).

Peptide Competition Assay

To confirm the specificity of antibodies used, we performed peptide competition assays using peptides obtained from Abcam. Immunoblot analyses were performed as described above. The antibody incubation step was performed in tandem for three experimental groups per antibody tested. The first group was the antibody to be tested alone while the second group was the same antibody after incubation with peptides specific to the antibody's target. The third group was the same antibody after incubation with a non-specific peptide. Analysis of the resulting immunoblots was performed as above. The peptides used were obtained from Abcam and were as follows: H3K9me3 ab1773, H3K9me1 ab1771, H4K20me3 ab17567 and H4K20me1 ab17043. Each peptide was used at a final concentration of 2 µg/mL and incubated with the antibodies for 1 hour at room temperature.

siRNA Knockdown

The knockdown of SUV420h1 and SUV420h2 was performed using the Lipofectamine RNAiMAX kit (Invitrogen) as per manufacturer's

instructions on cells grown on coverslips in a 6 well dish. siRNAs against both SUV420h1 and SUV420h2 were obtained from Qiagen (catalogue numbers of SI00235914 and SI01438367 respectively). One siRNA construct was generously donated by Dr. Alan Underhill. Cells were then re-transfected 2 days following the initial transfection to enhance the knockdown. Cells were subsequently fixed in 4% paraformaldehyde four days after the initial transfection. Indirect immunofluorescence microscopy was then performed on the coverslips as described above.

Section 3

Results

3.1 Mitotic defects found in HeLa cells treated with Adenosine Dialdehyde

In order to test whether or not protein methylation events that occur during entry into mitosis, such as the trimethylation of histone H3 lysine 9, are functionally important, we examined the effects of AdOx on asynchronous HeLa cell cultures by indirect immunofluorescence (IIF). AdOx is known to be a general methylation inhibitor that inhibits S-adenosylhomocysteine hydrolase (Keller and Borchardt, 1987). This leads to inhibition of S-adenosylmethionine-dependent methylation events in the cell (Bartel and Borchardt, 1984). If a protein methylation event, such as the G2 trimethylation of lysine 9, were crucial for proper chromosome alignment, we would expect that short treatments with AdOx would lead to mitotic defects. To test this, cells were treated with 250 μ M AdOx for two hours and then analyzed. This resulted in a prominent cell defect in mitosis, but non-mitotic cell viability was unaffected as shown by DAPI staining and no change in methylation intensity. Fig. 5 shows representative cells with mitotic defects after AdOx treatment. The defect is characterized by chromosomes that fail to align properly on the metaphase plate.

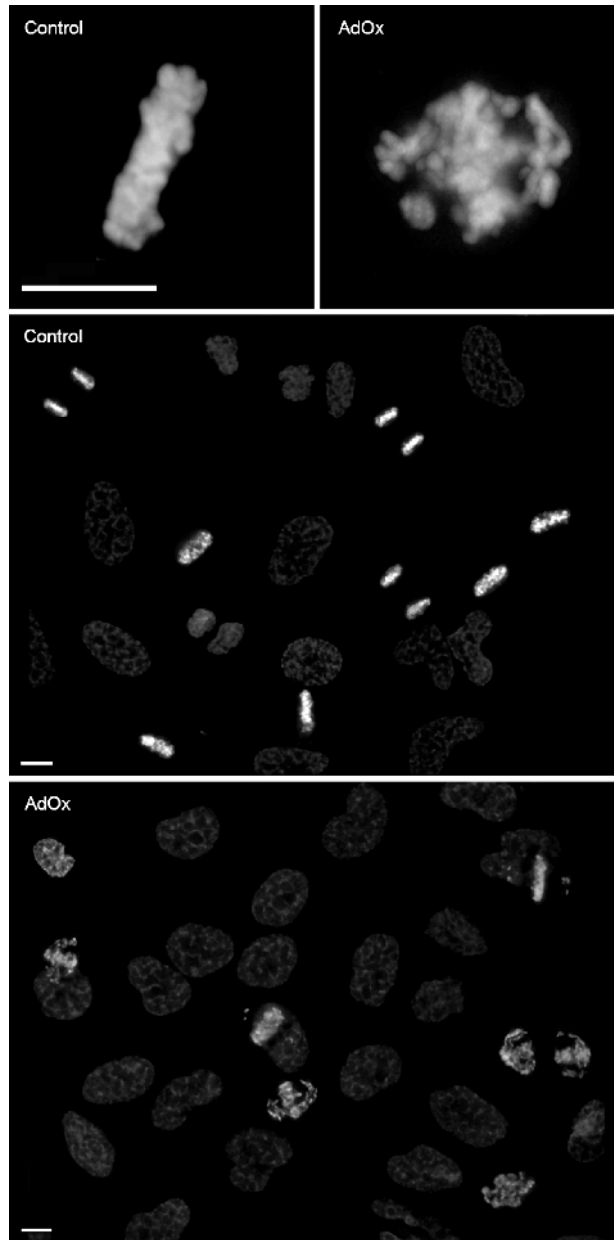


Figure 5 – DNA staining shows evidence of mitotic defects in HeLa cells with AdOx treatment

Representative digital images of metaphase HeLa cells immunofluorescently labeled with the DNA binding dye, DAPI. A representative high-resolution image of a cell treated for 2 hours with AdOx (right image) is compared to a control (left image). Depicted in the AdOx-treated cell are chromosomes that are misaligned at metaphase. Lower magnification images are shown in the bottom two panels (40X). Scale bars: 15 μ m

Evidence for chromosome alignment and segregation defects was found in prometaphase, metaphase, anaphase, telophase and early G1 cells (Fig. 6). Additionally, we observed widened metaphase plates (defined as having a metaphase plate width greater than 0.4 times the length of the metaphase plate) and an accumulation of mitotic cells. Overall, we found two subclasses of defective cells: cells with a well-defined and narrow metaphase plate containing several misaligned chromosomes and cells that have a loosely arranged metaphase plate and, generally, a larger number of misaligned chromosomes (Fig. 7). These subclasses typically comprise 65% and 35%, respectively, of the mitotic population in AdOx treatment groups. These groups will be referred to simply as “well-defined” and “poorly defined”. Visual scoring of over 300 mitotic cells per experiment showed a 6.7-fold increase in the number of mitotic cells with these defects upon exposure to AdOx. No obvious changes in interphase cells were observed during this brief treatment indicating that the entry into mitosis was particularly sensitive to inhibition of protein methylation.

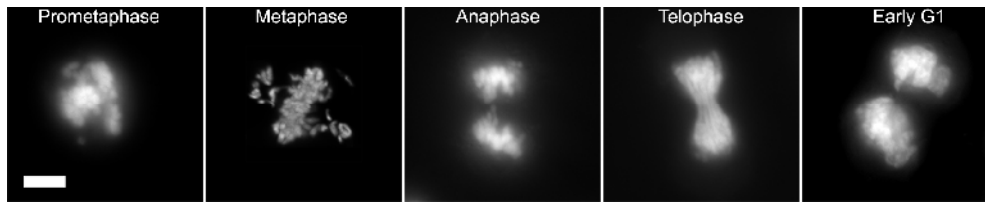


Figure 6 – Adenosine Dialdehyde defects in mitosis

Indirect immunofluorescent images of DAPI staining. Shown are the typical defects seen throughout the various stages of mitosis. Scale bar is 5 μm .

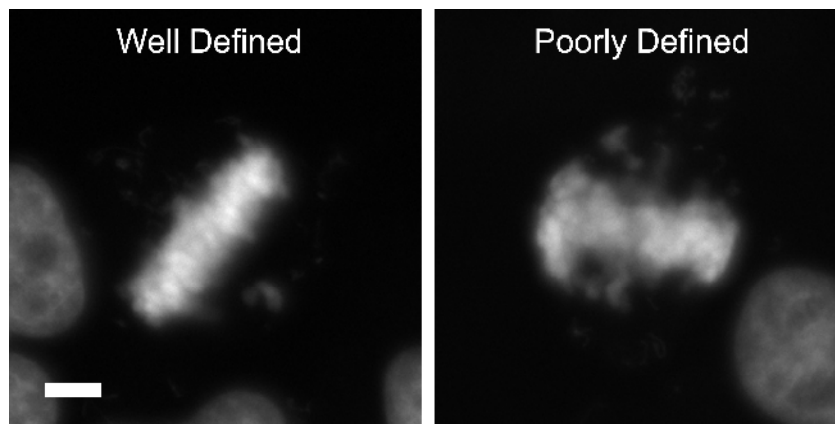


Figure 7 – High resolution images of the range of severity of AdOx mediated defects

Indirect immunofluorescent images of DAPI staining. The most common defect found with AdOx treatment is misaligned chromosomes during metaphase. Shown are the two subclasses of this metaphase defect: cells with a narrower and well defined metaphase plate (Well Defined) and cells with a wider, poorly defined metaphase plate (Poorly Defined). Scale bar is 10 μm .

3.2 AdOx treatment decreases the apparent abundance of H3K9me3 and H4K20me3

IIF and immunoblotting of several histone methylation residues (H3K9me1, H3K9me2, H3K9me3, H3K4me3, H4K20me1 and H3K9me3) were performed to establish which methylation moieties are affected. These experiments were performed on both asynchronous and mitotic cell populations to determine if there are any decreases in methylation of the tested sites and, if so, at what points in the cell cycle they occur. Interestingly, after 2 hours of exposure to AdOx, none of the methylated species tested were seen to decrease in an asynchronous cell population. It was only when mitotic populations were tested that a decrease of any methylated species became apparent (Fig. 8). Several methylated isoforms of histones, including H3K9me1, H3K9me2 and H3K4me3, remained stable in both asynchronous and mitotic populations (images of H3K4me3 are shown in Fig 9). By contrast H3K9me3 and H4K20me3 showed a marked decrease in intensity in the mitotic portion. As measured by IIF, H3K9me3 intensity in treated cells was 0.64 ± 0.03 times the intensity of control cells and in the case of H4K20me3, 0.62 ± 0.08 times the intensity of control cells. These results were averaged over three trials measuring 30 cells per trial. Antibody specificity was verified by doing a peptide competition assay (Fig. 10). The decrease measured by immunoblotting was similar (0.61 ± 0.05 times the intensity of control cells for H3K9me3 and 0.54 ± 0.04 for H4K20me3). A less prominent but still quantifiable decrease in methylation

intensity was also found for H4K20me1: 0.80 +/- 0.04 times the intensity of control cells when measured by IIF. The decrease of H4K20me1 is important to note as a positive control for our study as this modification is known to increase in late G2 (Pesavento et al., 2008b; Rice et al., 2002; Xiao et al., 2005). Of the modified histone groups measured, it would seem that the mitotic defects resulting from loss of methylation are most closely correlated with H3K9me3 and H4K20me3 (Table 1). Our results show that specific methylated histones undergoing methylation in G2 correspond to methylated histones that are enriched in pericentromeric heterochromatin (Peters et al., 2003; Schotta et al., 2004; Sullivan and Karpen, 2004).

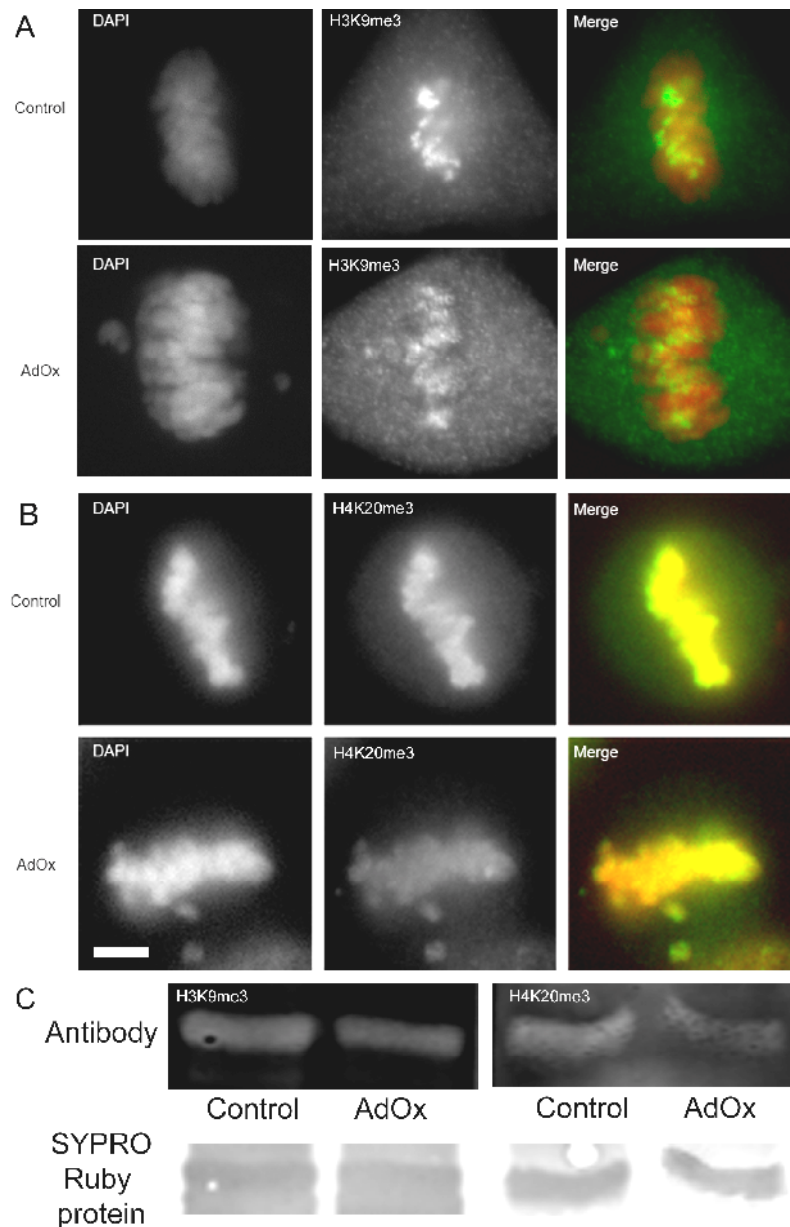


Figure 8 – Altered methylation levels in AdOx treated HeLa cells

Asynchronous HeLa cells were grown overnight, paraformaldehyde fixed and stained with DAPI and anti-H3K9me3 (A) or DAPI and anti-H4K20me3 antibodies (B). (A) Depicted here are representative metaphase cells of both control cells (top row in both A and B) and cells treated with AdOx for 2 hours (bottom row of both A and B). The final column of both A and B is a merged image of both wavelengths, the methylation antibodies are shown in green and DAPI is shown in red. C depicts western blots of mitotic cells treated with the same antibodies as in 2A and 2B. SYPRO Ruby protein blot stain confirms protein loading. Scale bar is 7 μ m.

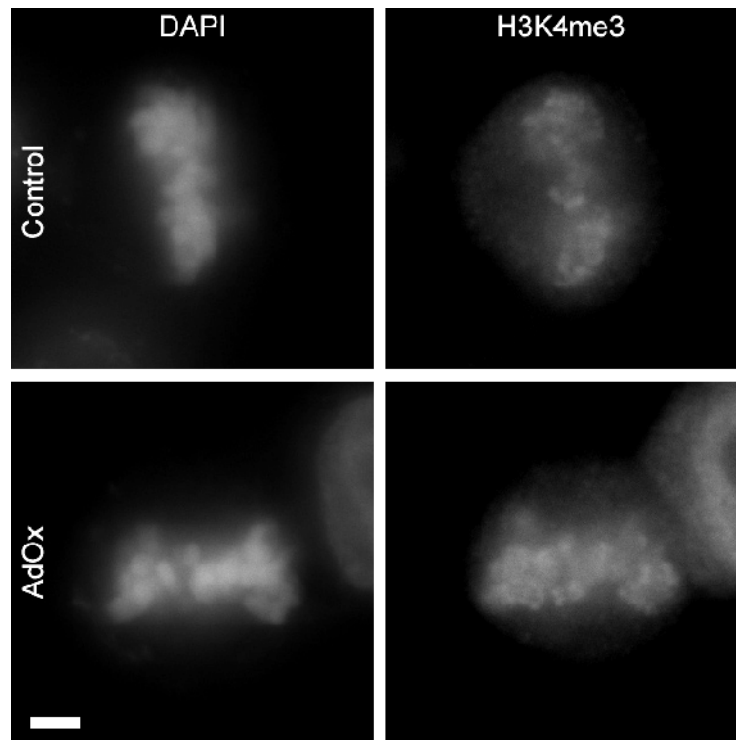


Figure 9 – H3K4me3 unaffected in mitotic AdOx treated cells

Indirect immunofluorescent images of DAPI and H3K4me3. Several histone methyl residues show no decrease in intensity in mitosis with a 2 hour treatment of AdOx, depicted here is one such residue, H3K4me3. Scale bar is 5 μ m.

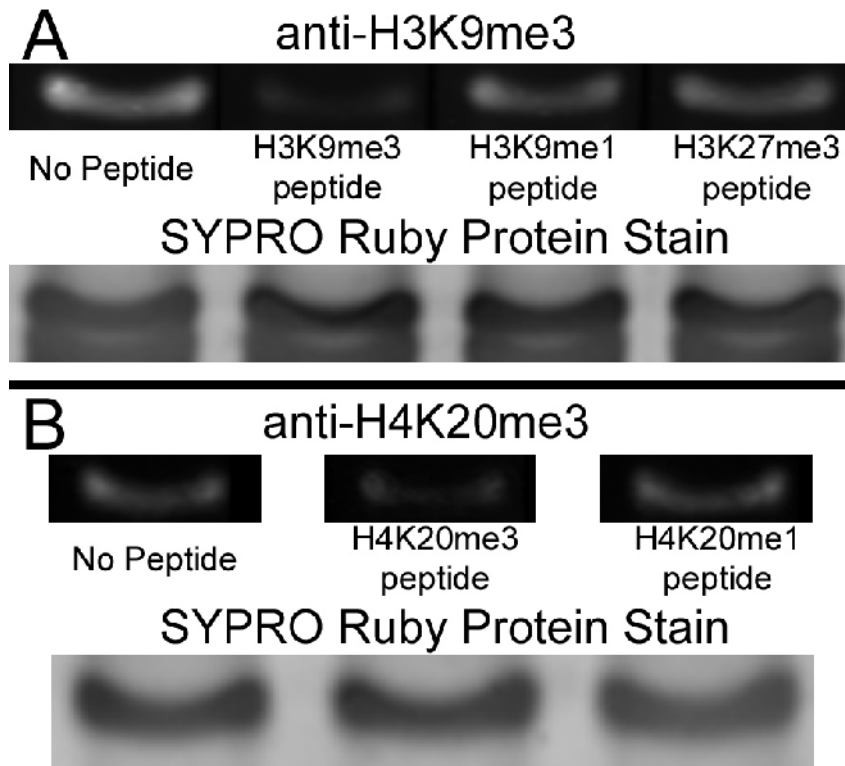


Figure 10 Peptide competition assay

Peptide competition assay. Images shown are western blots of (A) anti-H3K9me3 and (B) anti-H4K20me3 with peptide competition. The leftmost lane depicts the respective antibodies alone, the second lane is the respective antibodies incubated with the specific peptide (H3K9me3 and H4K20me3) and the rightmost lane is the respective antibodies incubated with the monomethyl containing peptide (H3K9me1 and H4K20me1). The anti-H3K9me3 was also incubated with H3K27me3 peptide as this methylation site contains the same peptide sequence (RKS) as H3K9me3. This figure shows the specificity of the antibodies used in the paper.

Histone Modification Studied	Intensity difference in unsynchronized cells	Intensity difference in mitotic cells	Intensity drop in AdOx treated mitotic cells (AdOx intensity/Control intensity)	
			IIF	WB
H3K9me1	No	No	-----	-----
H3K9me2	No	No	-----	-----
H3K9me3	No	Yes	0.64+/-0.03	0.61+/-0.05
H4K20me1	No	Yes	0.80+/-0.04	
H4K20me3	No	Yes	0.62+/-0.08	0.54+/-0.04
H3K4me3	No	No	-----	-----

Table 1 – Histone modifications affected by methylation inhibition

Integrated intensities of several modified histone residues are measured and compared between a control group and an AdOx treated group. Differences in intensity were noted and quantified when present. This experiment was performed on both unsynchronized cell populations and mitotic cell populations. Mitotic cells were isolated by mitotic shakeoff. Differences in intensity were determined by quantitative measurements of both indirect immunofluorescence (IIF) images and western blotting (WB) of nuclear extracts.

3.3 Loss of H3K9me3 does not account for the full severity of the defect seen after inhibiting global methylation

H3K9me3 and H4K20me3 are species that we found to be most affected by an inhibition of methylation, however, this does not address the issue of whether these moieties account for the full severity of the chromosome alignment defect seen with AdOx treatment. In order to determine the extent of the influence of these histone modifications in chromosome segregation, we compared the severity of the defect in two mouse epithelial fibroblast cell lines; SUV39h1/h2 ^{-/-} and the parental cell line. SUV39h1/h2 ^{-/-} cells lack the methyltransferases responsible for the trimethylation of H3K9 and, as a consequence, lack any H3K9me3 in pericentromeric heterochromatin (Peters et al., 2001). H4K20me3 is also decreased globally and lost from heterochromatin in these null cells (Schotta et al., 2004; Siddiqui et al., 2007). Wild type and SUV39h1/h2^{-/-} mouse embryonic fibroblast cell lines were synchronized using a double thymidine block and released. In order to test whether DNA methylation plays a role, 5-Azacytidine was added immediately following release from the double thymidine block in the applicable treatment groups. Further, AdOx was added 6 hours post double thymidine block in the applicable treatment groups. All treatment groups were fixed at 8 hours after double thymidine block to allow enrichment of mitotic cells (Fig 11). The percentage of cells containing lagging chromosomes and the standard deviations were calculated from the averages of three separate trials (Fig. 12).

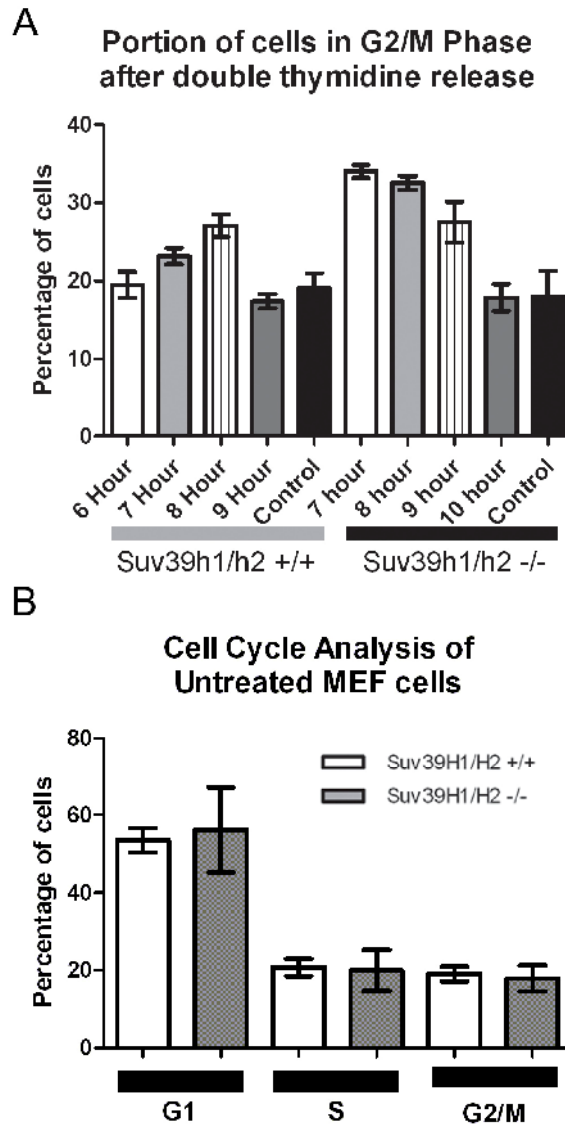


Figure 11 - Flow cytometry DNA profiles of SUV39h1/h2 $-/-$ and parental mouse epithelial fibroblast (WT) cells.

(A) The graph depicts the percentage of cells in G2/M phase of the cell cycle at varying time points after release from a double thymidine block. The parental cell line does not synchronize as readily as the knockout cell line, however the 8 hour time point (the time point used in Figure 3) is shown to be an appropriate point for mitotic enrichment for both cell lines. (B) DNA analysis of untreated WT and SUV39h1/h2 $-/-$ show similar cell cycle profiles between the two cell lines.

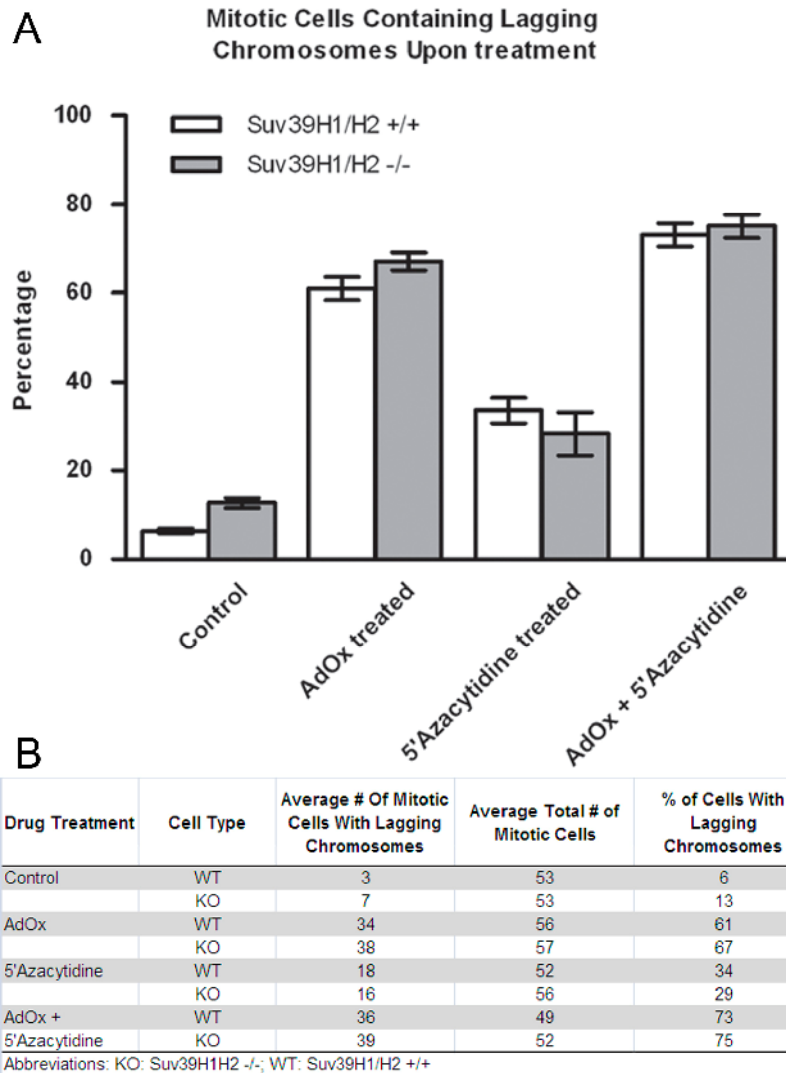


Figure 12 – H3K9me3, H4K20me3 and DNA methylation do not account for the full severity of the mitotic defect seen with AdOx treatment.

The severities of metaphase defects were compared between various treatment groups of both wild-type (*SUV39h1/h2*^{+/+}) and *SUV39h1/h2*^{-/-} mouse embryonic fibroblast cell lines. Cells were synchronized with a double thymidine block and released. All treatment groups were fixed 8 hours after double thymidine release to allow for mitotic enrichment. (A) The treatment groups were scored for metaphase cells containing misaligned chromosomes and the result expressed as the percentage of total metaphase cells that were scored as misaligned. Percentages and standard deviations were calculated from the averages of three separate trials, each with a minimum of 50 cells. (B) Data shown.

From these data we note several findings: The ~twofold increase in the number of defective metaphase cells between control *SUV39h1/h2^{-/-}* and the control parental cell line confirms that H3K9me3 plays a role in mitosis. The increase in the proportion of defective cells seen with AdOx treatment in H3K9me3-deficient cells, however, provides evidence that additional methylated residues play a role. This is supported by the additional finding that siRNA knockdown of SUV420h1 and SUV420h2 in *SUV39h1/h2^{-/-}* cells shows no significant increase in the proportion of mitotic cells that contain missegregated chromosomes (Fig 13). The same knockdown of SUV420h1 and SUV420h2 in the parental cell line, however, leads to an increase in chromosomal alignment defects such that the wild type and knockout cells, without AdOx, show the same level of defect. This suggests that H4K20me3 in pericentromeric heterochromatin plays an important role in mitotic chromosome alignment as *SUV39h1/h2^{-/-}* cells also lack pericentromeric H4K20me3 although they still contain H4K20me3 along the chromosome arms (Schotta et al., 2004). The fact that the knockout cells show no apparent increase in chromosomal alignment defects, whereas the parental cell line does, gives support to the importance of pericentromeric H4K20me3. Several papers have shown, however, that knockout of SUV420h1 and SUV420h2 leads to the near complete loss of both H4K20me3 and H4K20me2 (Sakaguchi et al., 2008; Schotta et al., 2008). It is possible that the loss of dimethylation of histone H4 at lysine 20 is responsible for the observed changes or contributes to the phenotype. However, *SUV39h1/h2^{-/-}* cells lack

proper localization of H4K20me3 but reportedly retain H4K20me2 (Schotta et al., 2004). Because H4K20me2 is retained in *SUV39h1/h2^{-/-}* cells, the similar proportion of mitotic defects observed with knockdown of SUV420h1 and SUV420h2 in wild-type cells and in the *SUV39h1/h2^{-/-}* cells means that the loss of H4K20me3 is the only known change in methylation that is common to both cell types.

We also find that a decrease in DNA methylation with 5-azacytidine treatment leads to an increased defective portion of metaphase cells in both cell lines (Fig. 12); however, there was an additive effect when cells were treated with both AdOx and 5-azacytidine concomitantly. This leads us to believe the mitotic alignment defects seen with AdOx treatment is affected by more than the loss of H3K9me3, H4K20me3 and DNA methylation. All comparisons made were statistically significant ($P < 0.05$, Student's *t*-test).

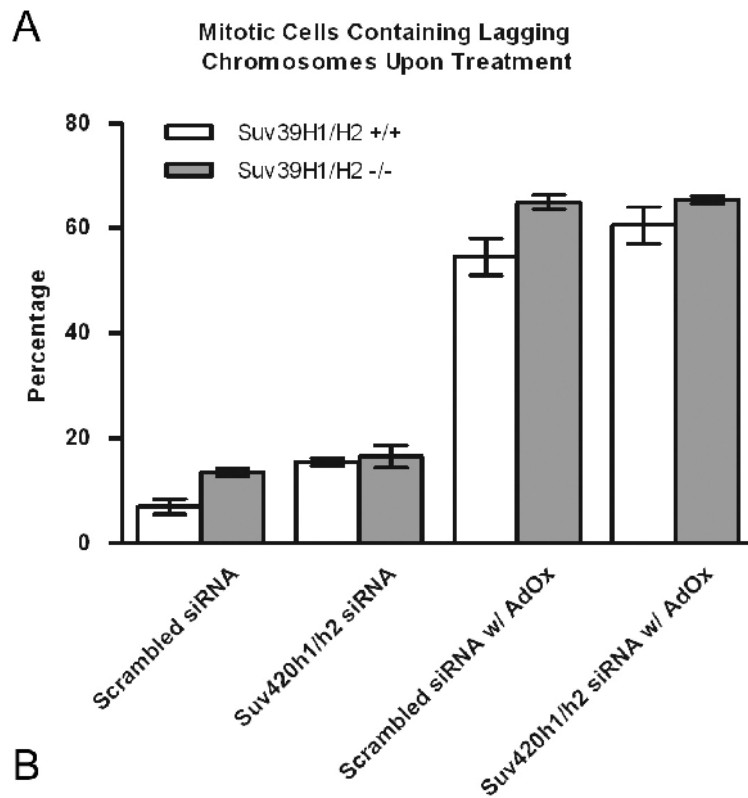
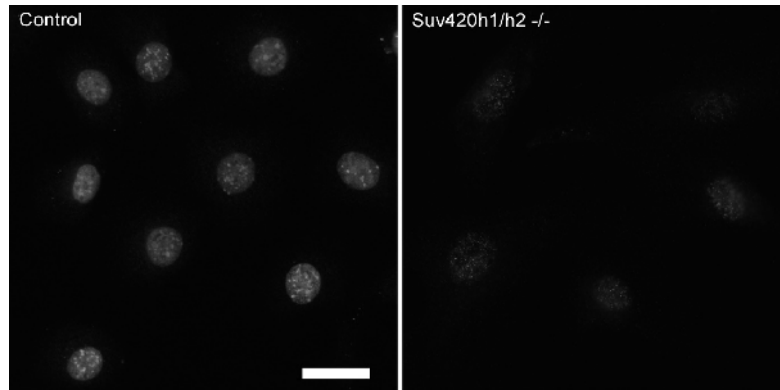


Figure 13 - SUV420h1 and SUV420h2 knockdown in MEF cells.

(A) shows indirect immunofluorescent images of H4K20me3 in the MEF cell line (parental to SUV39h1/h2^{-/-} cells) to confirm knockdown of SUV420h1/h2. Scale bar is 30 μ m. (B) depicts the proportion of mitotic cells in the varying treatment groups that contain misaligned chromosomes. The numbers seem to indicate that loss of both SUV420h1/h2 concurrently with SUV39h1/h2^{-/-} fails to account for the full severity of the defect shown in Figure 12.

3.4 Methylation is most critical for chromosome segregation 1-3 hours prior to mitosis

We were interested in further defining the timing of the methylation event(s) critical for proper progression through mitosis. Cells were synchronized in early S phase with a double thymidine block and then released. Upon release, cells proceed through S phase, G2 and mitosis with synchronized timing. Control cells were found to contain the largest proportion of mitotic cells 9-11 hours post-release. Experimental groups of cells were pulse-treated with AdOx for 2-hour windows, washed with phosphate buffered saline (PBS) and fresh media was then added. The AdOx pulse treatment began at 4, 5, 6, 7 and 8 hours after the release of the S-phase block. All groups were fixed at 10 hours, corresponding to the time period of the mitotic peak of the control cell population (Fig. 14A). Although all time points showed a significant increase in the proportion of defective cells observed in mitosis, the largest increase in defective cells occurred when AdOx was administered 3 hours prior to fixation (Fig. 14B). This crucial period corresponds to late G2 and overlaps with the pulse of H3K9 trimethylation described in our earlier manuscript (McManus et al., 2006).

Time Course of Drug Treatments

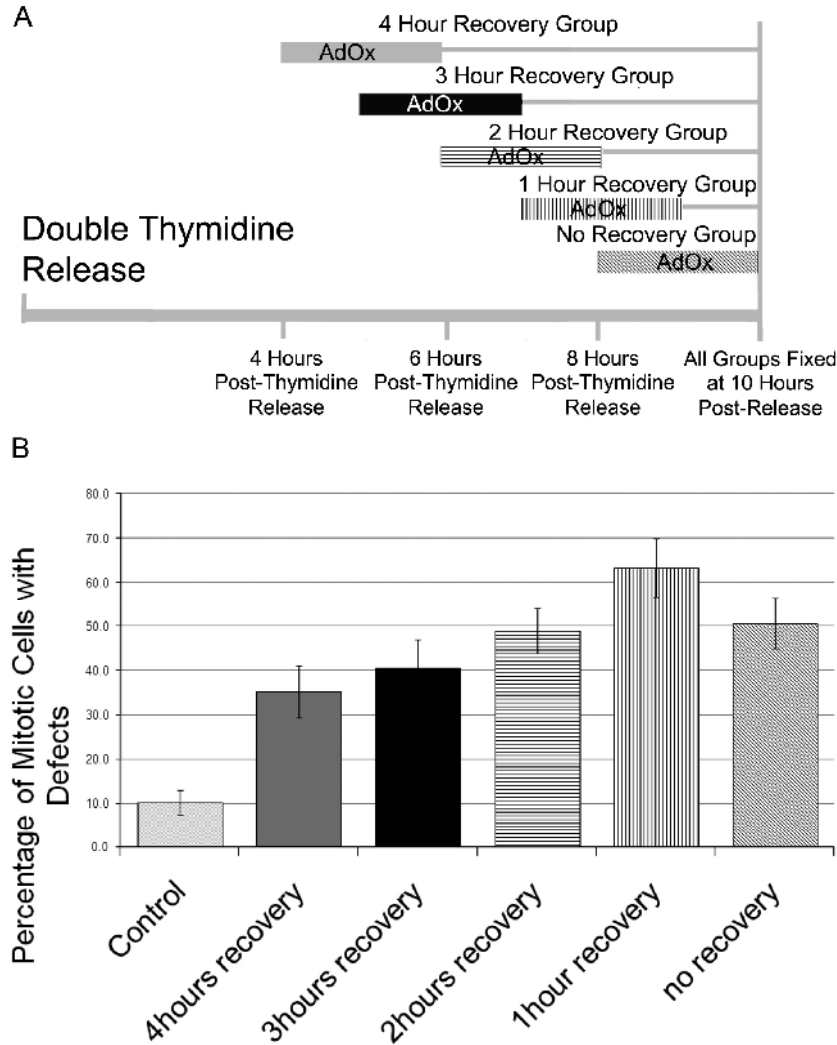


Figure 14 – Pulsed inhibition of methylation reveals an important window of ongoing methylation occurring 1-3 hours prior to mitosis.

A double thymidine block was used to synchronize cells in S-phase. At varying times after release from the S-phase block, treatment groups had 250 μ M AdOx added for 2 hours and then the media was replaced with fresh media without drug. All groups were allowed to progress for 10 hours after initial thymidine release and then fixed. A minimum of 50 cells were then scored to determine what percentage of mitotic cells showed the described defects. This experiment was repeated three times. (A) Graphical representation of the treatment window and experimental protocol. (B) Percentage of mitotic cells scored that showed defects in each treatment group. Error bars indicate standard deviations.

3.5 Mitotic checkpoint activation with AdOx treatment

We next determined whether these methylation events affected the mitotic checkpoint. This checkpoint inhibits the progression of a metaphase cell into anaphase until all kinetochores are correctly and stably connected by microtubules to the mitotic spindles (Chan et al., 2005). To test this, cells were synchronized with a double thymidine block and released for 8 hours into fresh medium. At 8 hours after the release from the S-phase block, AdOx was added with increasing length of treatment times ranging from 2 hours to 5 hours (Fig. 15A). Cells were then fixed and mitotic cells were counted and compared to control groups. As noted earlier, mitotic enrichment was highest between 9 and 11 hours after the release of the S-phase block in control cells. By contrast, the AdOx-treated cells show continued accumulation of metaphase cells from the 10 hour time point (2 hours treatment) to the 13 hour time point (5 hours treatment). Moreover, the proportion of anaphase and telophase cells decreased as compared with untreated cells (Fig. 15B). Both findings demonstrate an activated and functional mitotic checkpoint. It is important to note that some telophase cells still appear with AdOx treatment indicating either that this subset of cells progress through mitosis with proper chromosome alignment or that the checkpoint eventually fails. To distinguish between these two possibilities, we examined telophase cells and found that they commonly displayed chromosome bridges (Fig. 15C), a structure consistent with an eventual failure of the mitotic checkpoint.

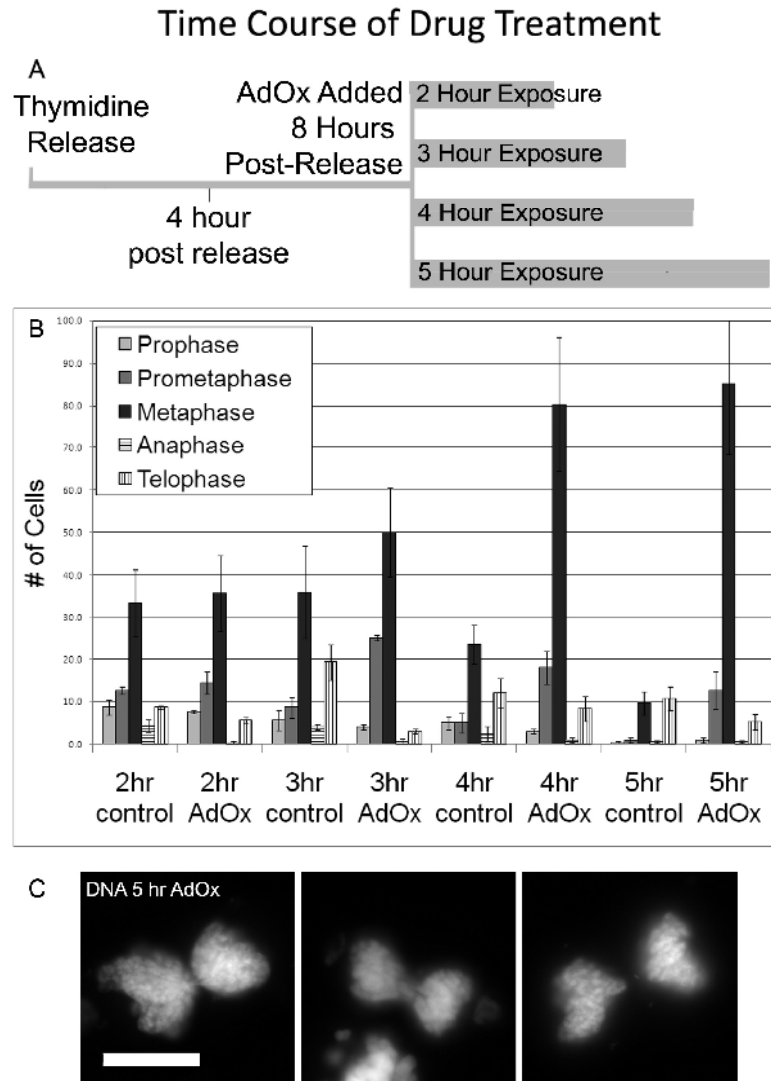


Figure 15 – Metaphase-Anaphase Checkpoint is active but checkpoint failure does occur in some cells.

A double thymidine block was used to synchronize HeLa cells at S phase. Cells were released from thymidine block and allowed to progress for 8 hours, at which point 250 μ M AdOx was added. Cells were then fixed at varying time points and counted in order to determine the number of cells in each phase of mitosis. (A) Graphical presentation of the experimental design. Time of the experiment progresses from left to right. At 8 hours, the cells were separated into 4 treatment groups in order to vary the length of treatment. (B) Number of cells in each phase of mitosis for each treatment group out of a total of 350 cells counted. Error bars indicate standard deviations. (C) An image of DAPI-stained chromatin in telophase-early G1 cells typical of cells counted in the telophase of the 5-hour AdOx group. Scale bar: 25 μ m.

To extend these results, we performed time-lapse microscopy on HeLa cells expressing histone H2B-GFP (histone H2B fused to green fluorescent protein). We found that mitotic cells treated with AdOx spent a considerable amount of time progressing through mitosis, due to the activation of the mitotic checkpoint (Fig. 16). A subset of chromosomes tended to become trapped at the spindle poles and this resulted in a failure to properly align chromosomes at metaphase. Interestingly, these chromosomes do not move from these positions, suggesting that they may fail to associate with microtubules. After a prolonged period without alignment of the chromosomes, the checkpoint eventually fails and the cells progress to the next interphase. The resulting post-mitotic cells are larger than normal, have irregular nuclear boundaries and are tetraploid. These findings show that although the mitotic checkpoint can fail after extended arrest, it is activated and, therefore, is largely unaffected by the loss of late G2 methylation events.

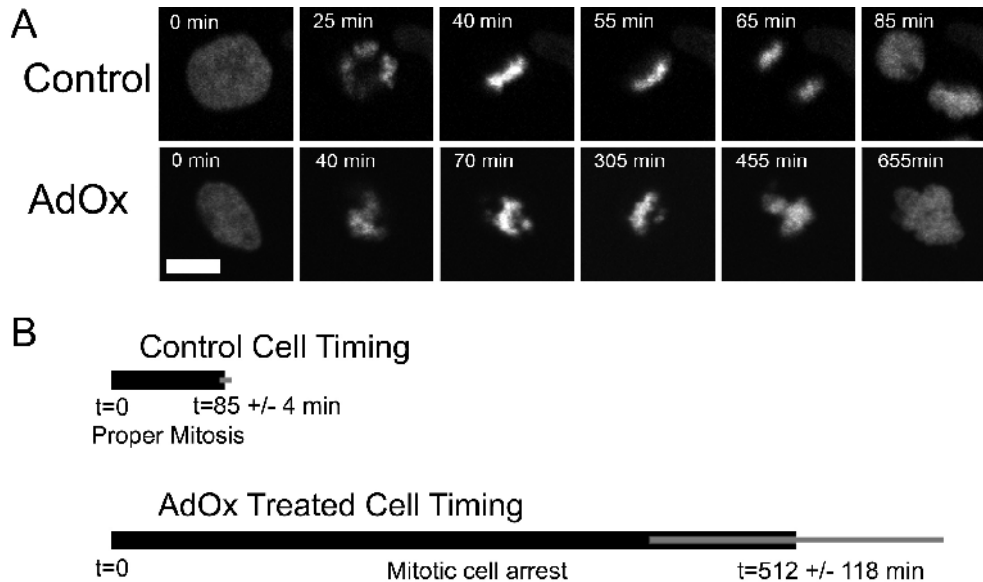


Figure 16 – Time lapse microscopy of stably transfected Histone H2B-GFP HeLa cells shows tetraploidy

(A) Representative digital images of two cells undergoing mitosis are shown to compare an untreated H2B-GFP cell (top) with an AdOx-treated cell (bottom). AdOx was added 3 hours prior to imaging. The first image in each series ($T=0$) was taken 25 minutes before the first indication of mitosis (prometaphase staining pattern). The proceeding images are then matched between treated and untreated according to the apparent stage in the cell cycle. The final image in each series was taken 10 minutes after DNA was full decondensed (as determined by the absence of significant further nuclei expansion). The time of each image relative to the first in both series is shown. Images were collected on a spinning disk confocal microscope at 20X and at 5-minute intervals to minimize phototoxicity. Scale bar: 25 μ m. (B) Mean duration of mitosis in both the control (85 ± 4 minutes, $N=5$) and the AdOx-treated (512 ± 118 minutes, $N=5$) groups diagrammatically represents the extent of cell-cycle arrest. Error bars represent s.e.m. The mean of AdOx-treated minus control groups equals 427 minutes, $P < 0.01$ (Student's t -test).

3.6 Kinetochore proteins are affected by loss of methylation

These results described above suggest that inhibition of the G2 methylation caused defects in the centromere, kinetochore and or microtubule structure and function. Consequently, we examined the assembly of microtubules and centromere and kinetochore proteins to determine whether or not the composition of either the centromere or kinetochore was altered. The most obvious candidate for study is tubulin which can indicate whether defective microtubules play a role in the observed disorganized metaphase plate. Microtubules that are not stably bound to kinetochores can be dissociated by adding ice-cold media (Brinkley and Cartwright, 1975) and so this technique (termed 'cold destabilization'), was used to observe only the kinetochore-bound subset of microtubules. In this experiment it is clear that microtubules fail to stably associate with the misaligned chromosomes (as denoted by the arrows in Fig. 17). This defect appears to be restricted to the misaligned kinetochores because the microtubules remain stable when associated with the chromosomes within the metaphase plate.

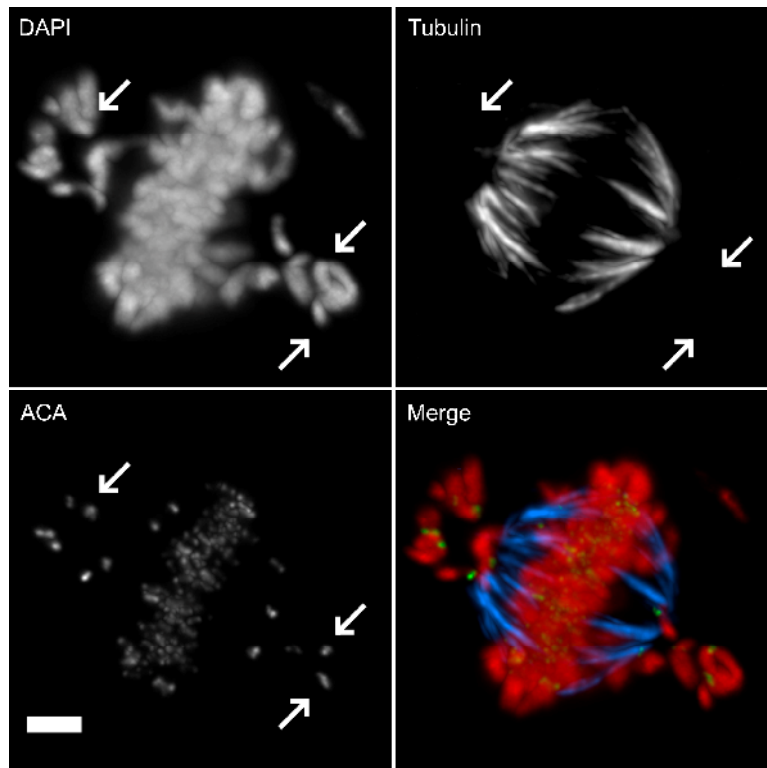


Figure 17 – CENH3, CENP-B and CENP-C localize properly in AdOx-treated cells but microtubules fail to stably attach to kinetochores.

Asynchronous HeLa cells were grown overnight on coverslips, paraformaldehyde fixed and stained with DAPI, anti-ACA and anti-tubulin. Prior to fixation, cells underwent cold destabilization of unattached microtubules so that only microtubules stably attached to kinetochores remained intact. Cells were then visualized and a representative cell is shown. All four images depict the same AdOx treated cell with different combinations of antibodies shown. Arrows show misaligned, unattached centromeres. Scale bar is 5 μm .

CENH3 is another centromeric protein that is crucial for proper mitotic division. CENH3 is a H3 homolog that replaces H3 in nucleosomes within the centromere (Palmer et al., 1991; Warburton et al., 1997). Anti-centromere antibody (ACA) stains the centromeres of cells by binding to CENH3, CENP-B and CENP-C (Earnshaw et al., 1986). We found no difference in ACA staining patterns following methylation inhibition. Misaligned chromosomes and aligned chromosomes both displayed proper ACA staining (Fig. 17).

The literature describes many mitotic segregation defects that are similar to those noted here and implicate certain kinetochore proteins in the defect (Bomont et al., 2005; Chan et al., 2000; Chan et al., 1999; Feng et al., 2006; Holt et al., 2005; Kallio et al., 2002; Liao et al., 1995; Maia et al., 2007; Mao et al., 2005; Morrow et al., 2005; Musio et al., 2004; Rattner et al., 1993; Tanudji et al., 2004; Yao et al., 2000; Yen et al., 1992). Kinetochore proteins that have been implicated include CENP-F, Aurora B/Aim-1, CENP-E, BUBR1 and ZW10. We have determined the effect of AdOx treatment on the localization of kinetochore proteins to determine if their improper localization plays a role. Several proteins that were studied showed no obvious change in abundance or in localization. Among these were CENP-F, a microtubule binding protein that is required for kinetochore attachment and the mitotic checkpoint (Bomont et al., 2005; Feng et al., 2006; Holt et al., 2005; Liao et al., 1995; Rattner et al., 1993), and Aurora B

(also known as Aim-1) a mitotic checkpoint protein kinase (Kallio et al., 2002; Morrow et al., 2005) (Fig 18).

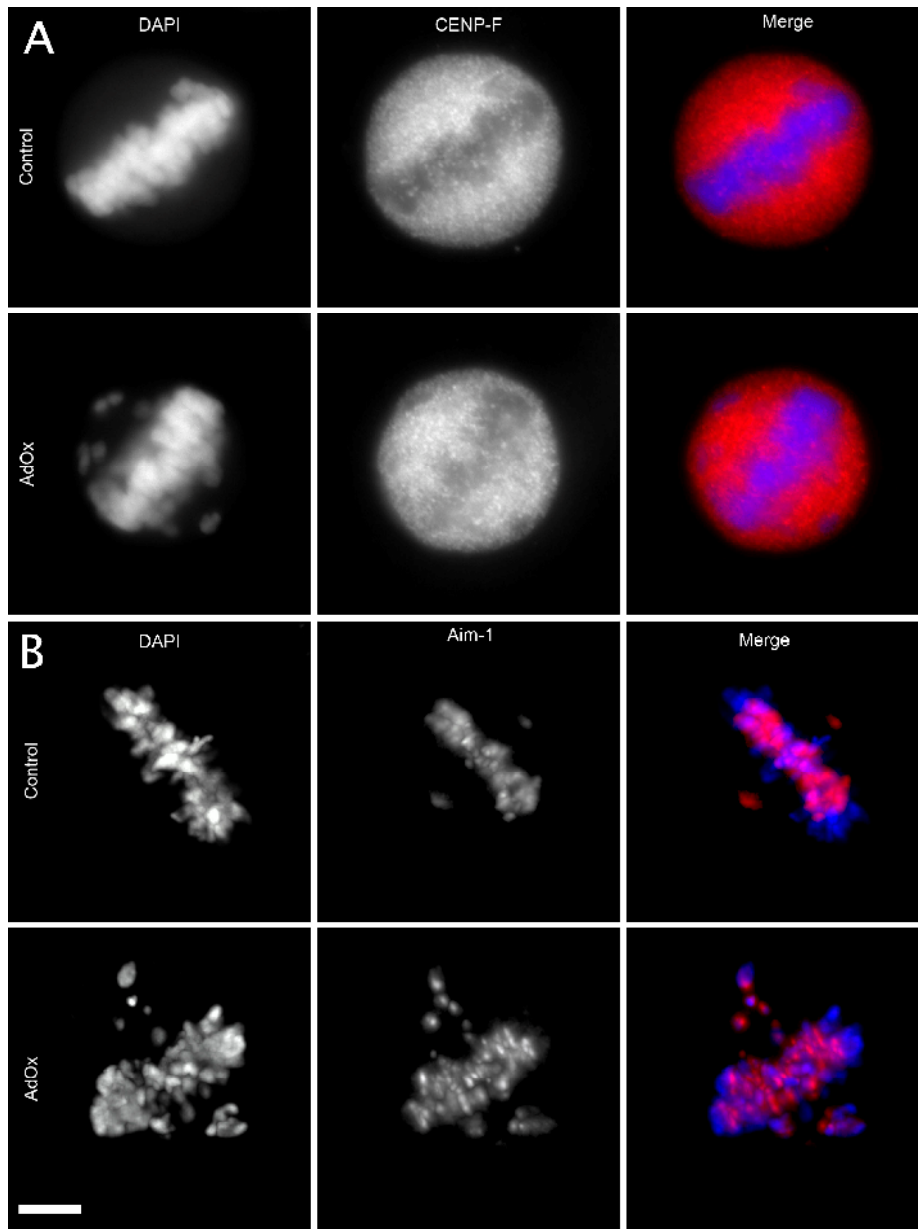


Figure 18 – CENP-F and Aim-1 localization remains unchanged with AdOx treatment

(A) Asynchronous HeLa cells were grown overnight, paraformaldehyde fixed and stained with DAPI and anti-CENP-F antibodies. (B) Asynchronous HeLa cells were transfected with Aim-1 GFP DNA, grown overnight, paraformaldehyde fixed and stained with DAPI. Depicted here are representative metaphase cells of both control and AdOx treated cells. The final column depicts a merge with CENP-F in red and DAPI in blue. Scale bar is 5 μ m.

Several proteins needed for proper chromosome segregation did show altered localization patterns when exposed to AdOx for two hours: CENP-E, BubR1 and ZW10 (Chan et al., 2000; Chan et al., 1999; Maia et al., 2007; Mao et al., 2005; Musio et al., 2004; Tanudji et al., 2004; Yao et al., 2000; Yen et al., 1992). These three proteins showed similar results. In control cells, all three proteins were found localized to the kinetochores in prophase and prometaphase. Upon stable binding of microtubules, CENP-E, ZW10 and BubR1 began to depart from the kinetochores and the staining pattern became cytoplasmic. At late metaphase, immediately prior to the beginning of anaphase, all three of these proteins were completely depleted from the metaphase plate. Their depletion is believed to occur once microtubules have stably bound to kinetochores. Depletion is indicative of satisfaction of the mitotic checkpoint (Musacchio and Salmon, 2007). In AdOx-treated metaphase cells with unaligned chromosomes, these three proteins were found to be depleted from the metaphase plate. This is correlated with microtubule attachment. However, the misaligned chromosomes were each found to have an increased kinetochore localization of all three proteins when compared to control cell chromosomes (CENP-E and BubR1 are shown in Fig. 19, ZW10 is shown in Fig.20). This is consistent with a mechanism whereby cells can relocate CENP-E, ZW10 and BubR1 to misaligned chromosomes to increase microtubule stabilization or chromosome alignment, a mechanism already described for some kinetochore proteins (Gorbisky and Ricketts, 1993; Skoufias et al., 2001; Waters et al., 1998).

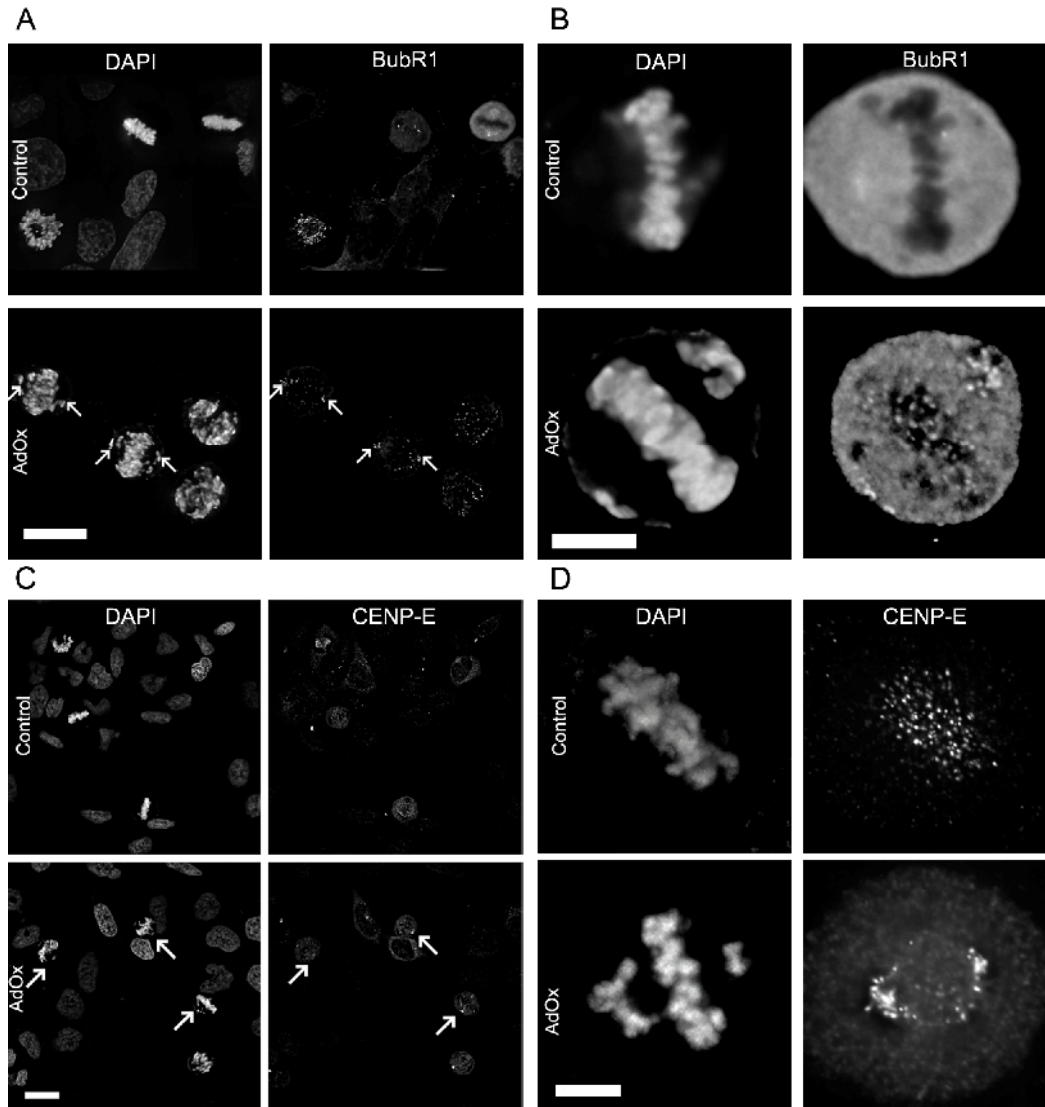


Figure 19 – Kinetochores proteins accumulate on chromosomes that are misaligned following AdOx treatment

HeLa cells were fixed with paraformaldehyde after growing overnight. (A,B) Cells were transfected with BUBR1-GFP and stained with DAPI. (C,D) Coverslips of cells were stained with anti-CENP-E antibody and DAPI. Control cells are compared to AdOx-treated cells. Arrows in low-resolution pictures (A,C) show the misaligned chromosomes. (B,D) Higher magnification images. Scale bars: 15 μm (A,C); 5 μm (B,D).

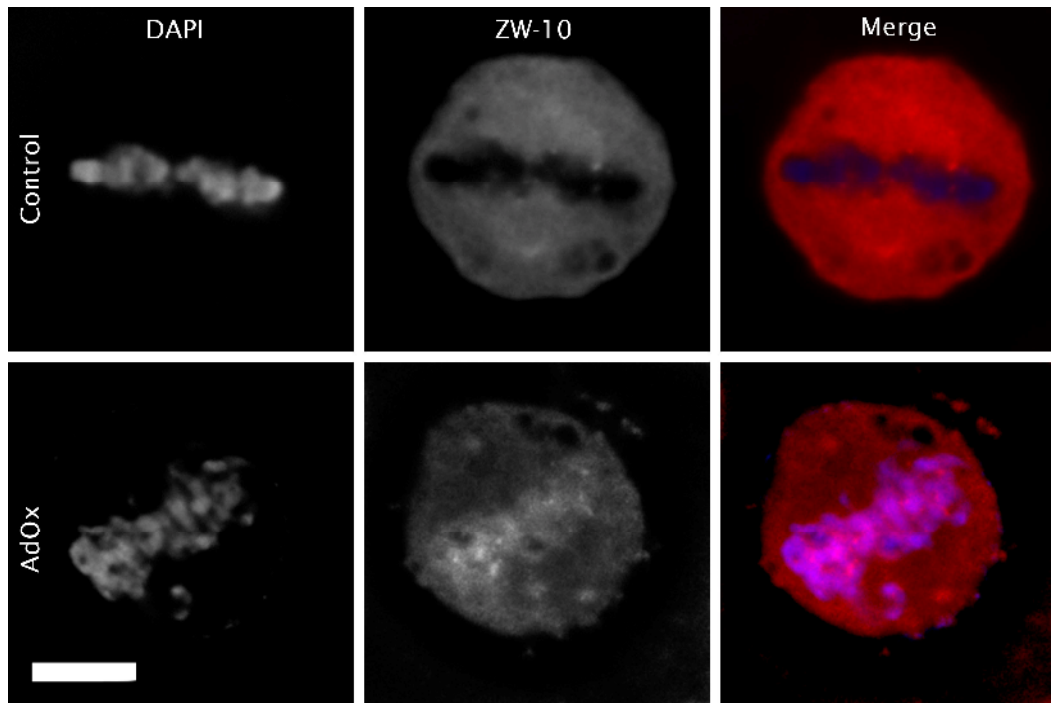


Figure 19 – ZW10 localization in control and AdOx treated cells

Asynchronous HeLa cells were transfected with ZW-10-GFP DNA, grown overnight, paraformaldehyde fixed and stained with DAPI. Depicted here are representative metaphase cells of both control cells treated with AdOx for 2 hours. The final column is a merged image of both wavelengths, ZW10-GFP in red and DAPI in blue. Scale bar is 5 μ m.

3.7 Interkinetochore distance in AdOx-treated cells indicates changes in tension or structural abnormalities

Both H3K9 and H4K20 trimethylation play major roles in heterochromatin formation and chromatin compaction and are found in pericentromeric heterochromatin (Melcher et al., 2000; Peters et al., 2001; Schotta et al., 2004; Sullivan and Karpen, 2004). These moieties are also found to decrease with AdOx treatment. We wished to determine whether the loss of methylation caused by AdOx treatment affected pericentromeric heterochromatin structure and whether a relaxed centromere could explain the widened metaphase plate. To address this possibility, HeLa cells were stained with anti-ACA, to identify the kinetochores. 3-D confocal images were obtained by deconvolution of a through-focus z-series and analyzed. In high resolution deconvolved images, it was possible to resolve both kinetochores found on each chromosome. The interkinetochore distance has been used as an indication of the amount of tension present on each individual chromosome (Waters et al., 1998).

Interkinetochore distance was measured in four experimental groups: control cells and AdOx-treated cells with and without cold destabilization of microtubules (Fig. 21A). A representative image of those used to obtain measurements is shown in Figure 21B and at higher magnification in Figure 21C. In HeLa cells without cold destabilization, interkinetochore distance decreased upon exposure to AdOx in both the well and poorly defined

subsets illustrating a decrease in tension. Interestingly, the interkinetochore distance decreases in control cells with cold destabilization but does not in AdOx-treated cells. All comparisons noted are statistically significant ($P < 0.05$ Student's *t*-test). As expected, misaligned chromosomes, regardless of cold destabilization, have a significantly smaller interkinetochore distance that is comparable to the distance of unattached kinetochores as shown by the nocodazole-treated, a microtubule depolymerization drug. These findings confirm that the misaligned chromosomes do not have any microtubule attachments that are able to generate tension and also demonstrate that aligned chromosomes may have structural defects that interfere with the transmission of tension through the centromere.

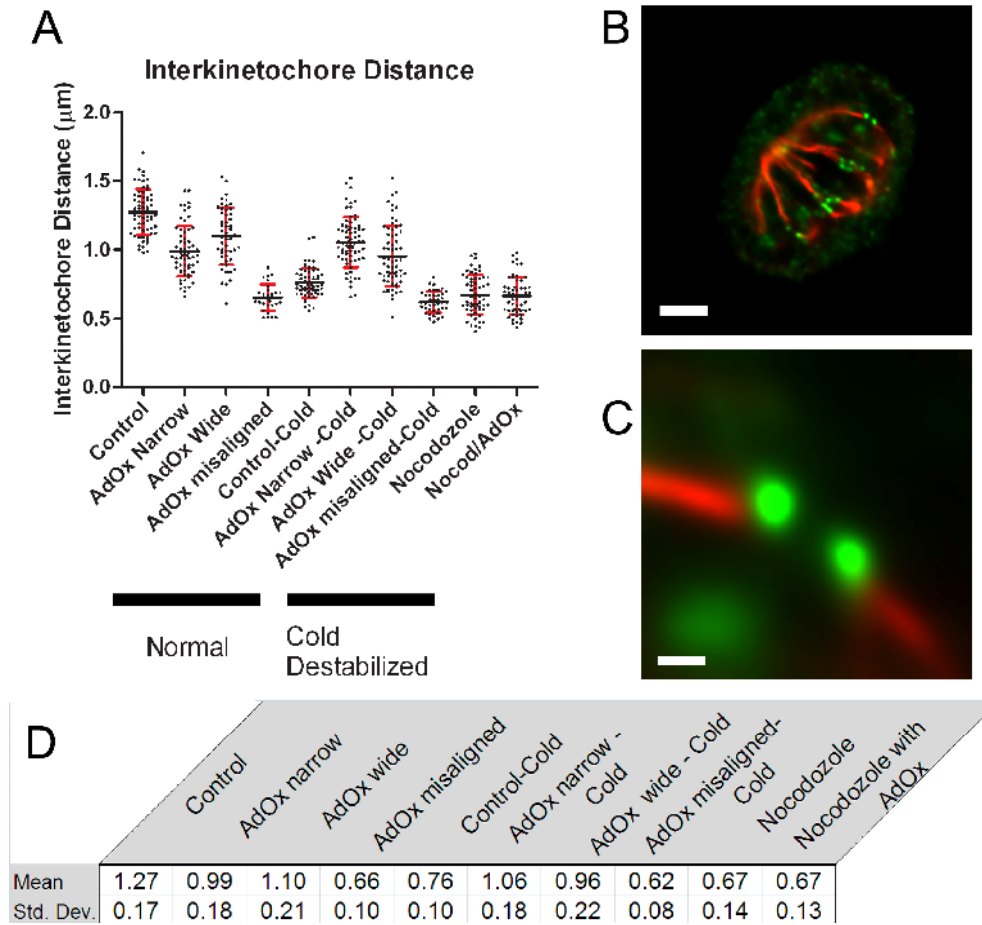


Figure 21 – Interkinetochores distance of four groups

Interkinetochores distance was measured and grouped according to experimental groups and phenotype. The four experimental groups are control and AdOx-treated groups with and without cold destabilization of microtubules. The AdOx-treated groups were further subdivided according to phenotype; cells with a well-defined metaphase plate (narrow) and cells with a poorly defined metaphase plate (wide). Also measured were misaligned chromosomes and, as a positive control for unattached kinetochores, nocodazole treated cells with and without AdOx. (A) Individual distances were marked on a dot plot with the mean shown. Error bars are standard deviation. (B) An example image of a cell used for measurement. Microtubules are shown in red and ACA staining is shown in green. Scale bar is 4 μm . (C) A higher magnification of one kinetochore set shown. Scale bar is 0.4 μm . (D) The mean and standard deviation of each experimental group is shown.

3.8 Transmission electron microscopy shows structural defects in AdOx-treated mitotic cells

The observed loss of tension at the metaphase plate in cells where methylation was inhibited implies that the centromeric structure may be affected. We therefore carried out a structural study with transmission electron microscopy (TEM) to determine whether or not there were any changes in the structure of the chromosomes and/or kinetochores. Figure 22A and 22B show examples of treated mitotic cells versus control cells. Unlike the control cell, where the centromere and kinetochore are well-defined, the drug-treated cells show several differences: centromeric chromatin was slightly expanded and the relationship between centromere and kinetochore was disrupted. Generally, there was a loosening of the kinetochore and centromere structure. It was also noted that some kinetochores of chromosomes within the metaphase plate in the poorly defined subset were also found with few or no microtubules attached (Fig. 22B). Counts of kinetochores within control and treated cells show that the percentage of aberrant kinetochores increases from 13% to 59% (Fig. 22C) when treated with AdOx. Findings from the TEM experiments confirm that there are major structural abnormalities when methylation is inhibited in late G2.

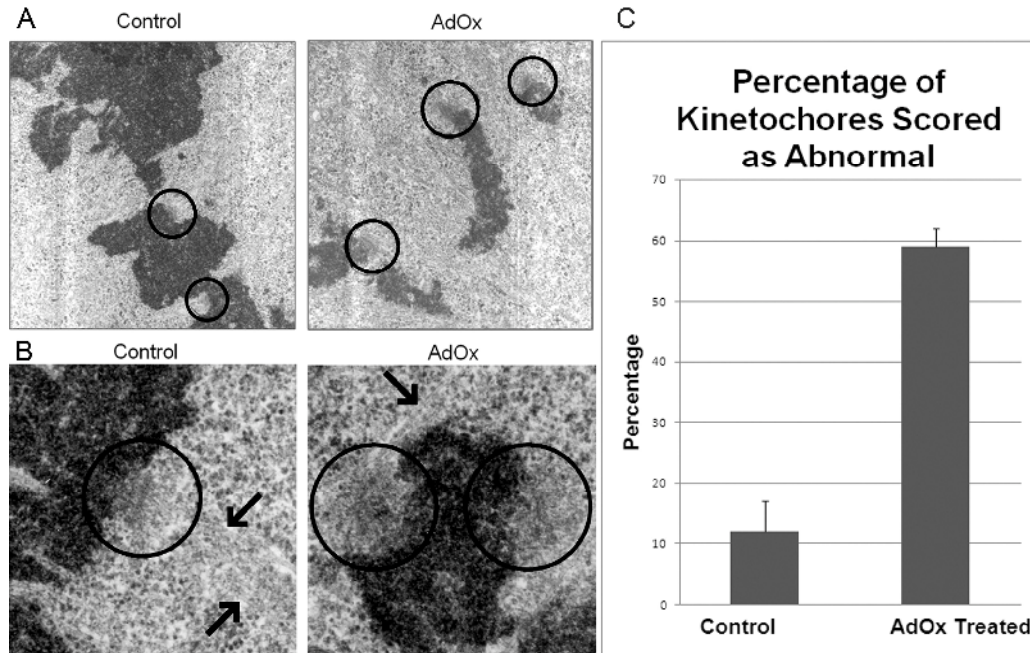


Figure 22 – TEM emphasizes structural defects in the centromere/kinetochore of the AdOx exposed cells

Transmission electron microscopy (TEM) of mitotic HeLa cells reveals structural defects in the centromere and/or kinetochore following AdOx-treatment. All images are of chromosomes that are aligned on the metaphase plate. (A) Kinetochores and underlying centromeric regions of chromatin are circled in black. (B) Higher magnification of kinetochores. Circles denote kinetochore and underlying centromere. Arrows highlight the microtubules. Note that there are no microtubules found on the rightmost kinetochore in the AdOx treatment. (C) Counts of normal vs. abnormal kinetochores show a large increase in abnormal kinetochores with exposure to AdOx: 12 +/- 5% in control cells, 59 +/- 3% in AdOx-treated cells. A total of 20 cells were counted, with an average 13 kinetochores counted per cell; over 250 kinetochores were counted in each experimental group. Error bars indicate standard deviations. TEM was done by Dr. J.B. Rattner.

Section 4

Discussion

The defect in mitotic alignment following inhibition of methylation that we have observed in this study is similar to a defect described in an earlier paper from this lab (McManus et al., 2006) wherein a stable mouse cell line deficient in SUV39h1 and SUV39h2 was found to have mitotic defects. This defect arose after a two hour treatment with the methylation inhibitor while knockout cell lines have been deficient for numerous cell divisions. These data confirm the presence and importance of cell cycle-regulated methylation occurring in G2. Recent findings have begun to disprove earlier notions regarding the permanence of histone methylation marks. These findings include the characterization of histone demethylases and the ability of histone methylation marks to spread laterally and replace competing modifications across the chromatin. Our results, however, are amongst the first to link a cell-cycle regulated histone methylation event to a specific role in cell cycle progression.

The defects arising from a brief treatment with AdOx were apparently limited to mitotic cells. None of the methyl residues tested decreased in interphase and no defects were found in interphase cells. As interphase accounts for the majority of the cell population in asynchronous cells, these findings explain negative results in earlier studies which concluded that

global histone methylation is stable. In mitotic cells, however, the defect was readily apparent and several residues were found to decrease with inhibition of methylation prior to mitosis. The defect, as defined with DAPI staining, shows both a widened metaphase plate, to varying degrees, as well as misaligned chromosomes. Both of these findings imply that microtubules are either unable to attach or unable to stabilize attachment to the kinetochore. The varying degrees of metaphase plate width may coincide with the length of methylation inhibition prior to mitosis. Because we have tested unsynchronized cells, the duration of exposure to drug can vary within the mitotic cell population that we have evaluated. Therefore, cells that have been treated with AdOx for a longer period of time prior to entering mitosis may be causing the most severe phenotypes.

The timing of the pulsed AdOx treatment that resulted in the most severe phenotype coincided with the timing of the mitotic increase in lysine 9 trimethylation that we described previously (McManus et al., 2006). In this study we have provided further evidence for the dynamic methylation of histones in late G2. We have confirmed both an increase of lysine 9 trimethylation as well as monomethylation of H4K20 (Pesavento et al., 2008b). Additionally, we provide evidence that H4K20me3 is dependent on late G2 methylation. However, findings in the literature do not suggest an increase in H4K20me3 in late G2 (Pesavento et al., 2008b). One possible explanation for this discrepancy is the dependence of SUV420h1/h2 on H3K9me3 (Schotta et al., 2004). The treatment with AdOx inhibits new

methylation within the cell and we see a drop in H4K20me3 in treated mitotic cells. There are at least two possible explanations: first, H4K20me3 increases dramatically upon entry into mitosis, a scenario that is not supported by the literature. Second, H4K20me3 is in a dynamic equilibrium, being both methylated and demethylated prior to mitosis. In this case, inhibiting active methylation will effectively decrease the amount of lysine 20 trimethylation. This second scenario would result in no increase in H4K20me3 in control cells, as seen in Pesavento *et al.*, 2008, but would show a decrease with methylation inhibition, as observed in our study. Additionally, SUV420h1/h2 is dependent on H3K9me3 for localization and activity and we confirm a large decrease in H3K9me3. H3K9me3 loss, then, could displace SUV420h1/h2 thereby exacerbating the loss of H4K20me3. Interestingly, the siRNA mediated knockdown of SUV420h1/h2 had no effect on the severity of mitotic defects in SUV39h1/h2 *-/-* cells, however this knockdown in the parental cell line cause mitotic defects similar to those seen in untreated SUV39h1/h2 *-/-* cells. This provides evidence that both H3K9me3 and H4K20me3 are required for proper chromosome segregation. Further study to confirm or disprove this second scenario is needed.

We postulate that the loss of H4K20me1 does not participate in the specific mitotic defect we have characterized. H4K20 monomethylation is catalyzed by PR-SET7 (also known as SET8) (Trojer and Reinberg, 2006) and is found enriched in facultative heterochromatin (Nishioka *et al.*, 2002; Rice *et al.*, 2002), a region of heterochromatin that can interconvert between transcriptionally

silent and transcriptionally active states (Trojer and Reinberg, 2007). H4K20me1 does not appear in constitutive heterochromatin. Loss of H4K20me1 upon PR-SET7 knockdown leads to G2 arrest (Houston et al., 2008; Sakaguchi and Steward, 2007). For these reasons, H4K20me1 may play a role in mitosis that differs from the roles of H3K9me3 and H4K20me3. It is likely that H4K20me1 is required for the general compaction of the chromosome but is not associated with pericentromeric heterochromatin compaction. For this reason, our focus lies predominantly with H3K9me3 and H4K20me3 in order to account for the effect on pericentromeric heterochromatin.

Our findings regarding the dynamics of histone methylation in mitosis are further strengthened by the negative results that we have observed with H3K4me3 and H3K9me1. Both are associated with euchromatin and so are not expected to increase with chromosome condensation. Our results do, however, imply that there are additional methylation events that occur during G2 and that are important in the regulation of mitotic processes. First, the mitotic defect seen with global loss of active methylation is more severe than that seen in SUV39h1/h2^{-/-} cells. This cell line is also deficient in H4K20me3 in pericentromeric heterochromatin (Schotta et al., 2004; Siddiqui et al., 2007). We also found that the siRNA mediated knockdown of SUV420h1/h2 in SUV39h1/h2^{-/-} cell line still does not replicate the severity of the defect seen with AdOx treatment. This implies that H3K9me3 and H4K20me3 are not the sole players in this defect. Second, the treatment with a DNA methylation inhibitor, 5-azacytidine, shows an increased proportion

of cells with mitotic defects in both SUV39h1/h2 $-/-$ and parental cell types and with or without AdOx treatment. This implies that DNA methylation also plays a role. Finally, the severity of mitotic defects with AdOx is not matched by the addition of 5-azacytidine to SUV39h1/h2 $-/-$ cells. This implies that additional methylated proteins play a role in the described defect.

Our initial hypothesis that these methylation sites are crucial for kinetochore protein localization is not supported by our data. First, using both live cell microscopy and synchronized cells we have determined that the mitotic checkpoint is active. Second, we have shown that many kinetochore proteins localize properly and only show an over-accumulation on misaligned chromosomes once the metaphase plate begins to form. This leads us to believe that the kinetochore assembly pathway is proceeding normally. The observed over-accumulation of a subset of kinetochore proteins can be explained by normal cell mechanisms. It is known that microtubule attachment results in the removal of several kinetochore proteins. It is also known that two kinetochore proteins, BubR1 and Bub1 (budding uninhibited by benzimidazoles 1), reassociate with kinetochores that have lost microtubule attachment (Gorbsky and Ricketts, 1993; Skoufias et al., 2001; Waters et al., 1998). This indicates that the over-accumulation of kinetochore proteins observed upon loss of methylation reflects the normal process that occurs in mitotic cells when chromosomes do not align properly.

If kinetochore formation seems not to be the major player, an additional role of methylation must be involved. H3K9me3 and H4K20me3 are enriched in pericentromeric heterochromatin and are required for the maintenance of heterochromatin integrity (Gonzalo et al., 2005; Schotta et al., 2004; Zinner et al., 2005). The finding that both of these modifications are dramatically and preferentially reduced by AdOx treatment suggests that disrupted heterochromatin formation and maintenance may lead to the defective mitotic phenotype. This is supported by our TEM results and interkinetochore distance measurements showing that AdOx treatment affects pericentromeric heterochromatin compaction and interkinetochore tension. One role that late G2 methylation may play is to facilitate the further compaction or enhance the stability of pericentromeric heterochromatin. This could provide the rigidity required to transmit tension applied by attached microtubules and/or to sense and stabilize these attachments. Our interkinetochore distance findings confirms that loss of methylation in late G2 affects the ability to properly transmit tension, as shown by the decreased distance in the chromosomes along the metaphase plate of the AdOx treatment group. Additionally, our data shows that loss of methylation also affects the elasticity of the chromatin. This is evident in the inability of chromosomes to decrease interkinetochore distance in AdOx-treated, cold-destabilized cells, which are no longer under microtubule-dependent tension.

Our results are consistent with a mechanism where the loss of H3K9me3 and H4K20me3 from pericentromeric heterochromatin diminishes

its structural integrity and leads to the mitotic defects we have described. Models of the chromatin structure in centromeres hold that CENH3 chromatin collects on one face of the chromatid, situated away from the sister chromatid while pericentromeric heterochromatin is grouped together underlying the CENH3 chromatin (Cleveland et al., 2003; Dalal et al., 2007b; Schueler and Sullivan, 2006; Sullivan and Karpen, 2004). The pulling force of microtubules is first transferred through the kinetochore, which is assembled on the CENH3 chromatin and then through the underlying pericentromeric heterochromatin. Microtubule attachment is stabilized by tension between sister kinetochores and is destabilized by a lack of tension (Nicklas, 1997; Nicklas et al., 2001). The stabilization of microtubule attachment is carried out, as mentioned above, by the tension-mediated hyperphosphorylation of BubR1 by polo-like kinase 1 (Plk1) (Elowe et al., 2007) and the physical separation of the Aurora B/Aim-1 kinase from its substrates, the phosphorylation of which destabilizes microtubules (Cheeseman and Desai, 2008; Liu et al., 2009).

Tension is also believed to be sensed by various tension-monitoring kinetochore proteins at the inner centromere, potentially via altering the inner centromere proteins conformation and subsequent loss of activity (Baumann et al., 2007; Gieni et al., 2008b). One protein likely involved in this mechanism is Sgo2, which relocalizes from the inner centromere to the kinetochore in the presence of tension (Lee et al., 2008a). While bound, Sgo2 plays a role in inhibiting separase in yeast (Clift et al., 2009). Once all

chromosomes have uniform tension, the mitotic checkpoint is satisfied and, ultimately, cohesin, which can properly localize independent of H3K9me3 (Koch et al., 2008), is cleaved and anaphase begins (Chan et al., 2005).

Understanding this pathway enables us to understand how the loss of methylation fits into mitotic segregation. We can see that tension is required in this model for two reasons: microtubule stabilization and satisfying the mitotic checkpoint. Our findings fit this model as we observe that misaligned chromosomes fail to stably bind to microtubules and that a robust mitotic checkpoint is present. In affected and visibly decondensed chromatin, the inability to transfer tension properly would lead to microtubule destabilization as seen by microscopy of cold-destabilized microtubules. Additionally, the inability to transfer tension through the pericentromeric heterochromatin to the inner centromere proteins would explain the persistence of an activated mitotic checkpoint observed in our cell cycle analysis and live cell imaging data. We postulate that although pericentromeric heterochromatin is present throughout the cell cycle, a large increase in methylation in late G2 and early mitosis is needed to stabilize or allow for the proper delineation of the pericentromeric and centromeric chromatin domains (Fig. 23). The loss of the well-defined chromatin domains may lead a poorly maintained localization of tension-sensing kinetochore proteins and a poorly-maintained separation between Aim-1 and its substrates. This would allow the phosphorylation of Aim-1 substrates despite

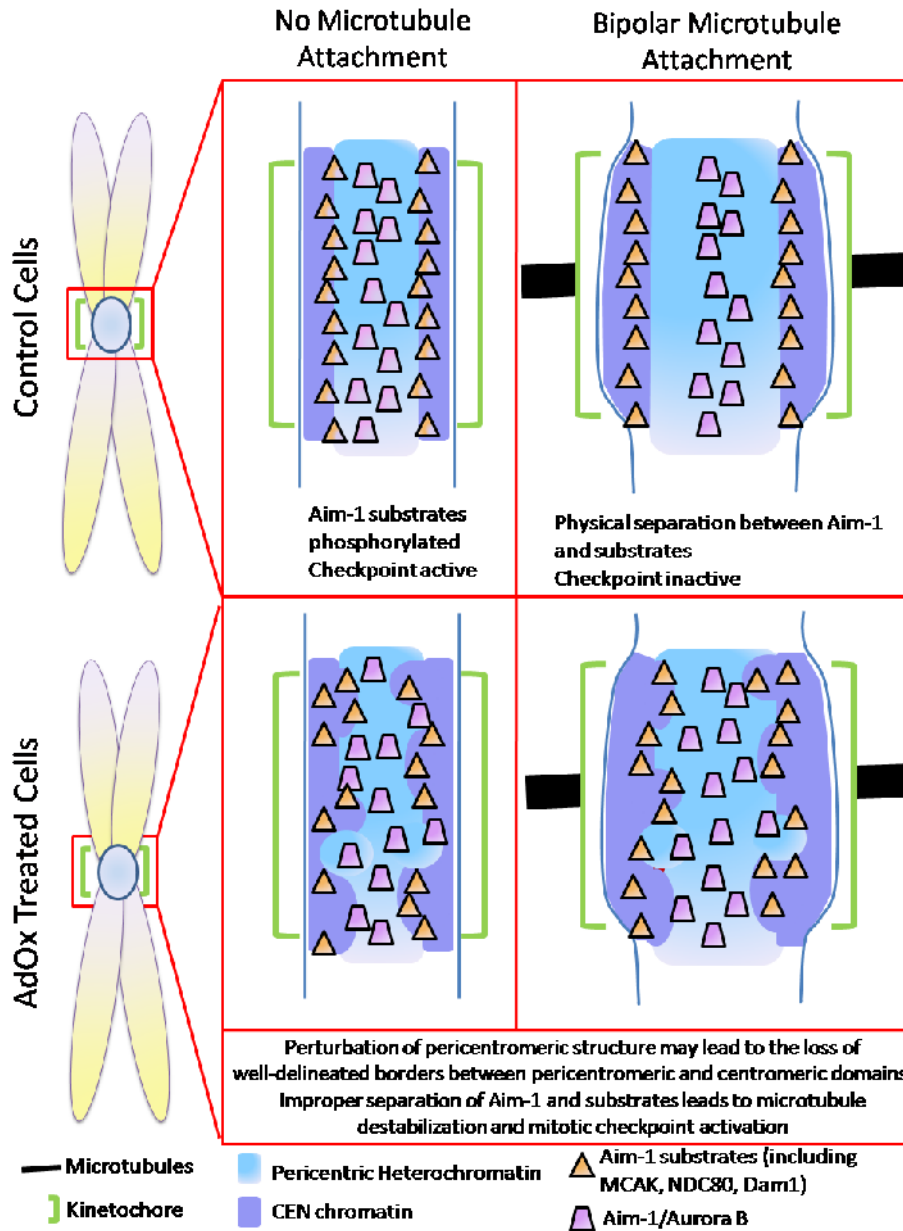


Figure 23 - Possible role for pericentromeric heterochromatin in chromosome segregation

Late G2 methylation may be crucial for chromosome segregation by maintaining proper centromeric and pericentromeric chromatin domains and separation of Aim-1 and its substrates. In the absence of late G2 methylation, improper separation of Aim-1 and its substrates would lead to the destabilization of microtubule attachments and the maintenance of the mitotic checkpoint.

bipolar microtubule attachment and tension and result in destabilization of microtubule attachments and the maintenance of the mitotic checkpoint.

The profound consequences of this defect are seen in cells that have overridden the mitotic checkpoint and progressed to interphase as tetraploid cells with irregular nuclear boundaries or aneuploid cells with bridged chromosomes. This drastic increase in chromosomal instability (CIN) is important to note as CIN is known to be a precursor to cancer. It appears that amplifying the levels of H3K9 and H4K20 during late G2 is critical to provide structural integrity to the heterochromatin for effective mitosis and chromosomal stability. A burst of these epigenetic modifications may ensure that alterations of heterochromatin structure that may have occurred over interphase (acetylation, demethylation, etc) are countered by fresh heterochromatin compaction-initiating modifications prior to the critical act of chromosome segregation during mitosis.

4.2 Future Directions

It is known that H3K9me3 and H4K20me3 are found in pericentromeric heterochromatin (Karachentsev et al., 2005; Kourmouli et al., 2004; Peters et al., 2003; Peters et al., 2001; Rice et al., 2003; Schotta et al., 2004) and are required for mitosis (Kourmouli et al., 2004; McManus et al., 2006; Peters et al., 2001; Schotta et al., 2004). It has also been shown that these modifications increase in late G2 (Heit et al., 2009; Houston et al., 2008; McManus et al., 2006; Rice et al., 2002; Schotta et al., 2004). What is lacking from the literature is the evidence that ties these findings together as we have tested a global methylation inhibitor which may have many effects not mediated by H3K9me3 and H4K20me3. In order to address this shortcoming, future experiments could make use of chaetocin, a newly characterized, more specific inhibitor of SET domain containing proteins (Greiner et al., 2005). This would allow the characterization of mitotic defects resulting from a more specific inhibition of SUV39h1/h2.

Additionally, the discrepancies found between our data and the literature involving H4K20me3 should be explored further. Possible explanations for this include a dynamic equilibrium or a lack of temporal resolution in prior studies. To confirm the active methylation of H4K20me3 in late G2 we can perform acid-urea triton (AUT) gel separation on nuclear extracts of cells incubated with tritiated-methyl groups. By measuring the intensity of tritium incorporation in control vs. AdOx-treated cells, we will be able to determine whether or not trimethylation of H4K20 increases in late G2 regardless of the presence of a dynamic equilibrium.

A limitation of this work is that we have restricted the analysis to the role of methylation in pericentromeric heterochromatin structure and function during entry into mitosis. We believe that the mitotic defect indicates a major role for pericentromeric heterochromatin in chromosome segregation. However, this seems to not fully account for the defect because mitotic defects following AdOx treatment are more severe than that seen in SUV39h1/h2 $-/-$ cells, which are deficient in pericentromeric H3K9me3 and H4K20me3. For this reason, it will be worthwhile for future studies to conduct a global screen of proteins methylated in mitosis in order to determine which, if any, non-histone proteins may be directly affected by the loss of methylation. This can be carried out by the initial identification of these proteins and further characterization of cell phenotype upon mutagenesis of the methylation sites. The identification can be carried out by characterizing protein spots in two-dimensional gels of proteins incorporating tritium into methyl groups during late G2. Additionally, global protein methylation can be characterized by mass spectrometry of fractionated samples of cells labeled with deuterated-methyl groups. In this experiment, the identification of methylated proteins would be accomplished by studying mass shifts between AdOx-treated and untreated cell populations. For the time being, the findings that heterochromatin stability is greatly decreased with the loss of methylation and the connection with histone methylation provides a strong basis to further characterize the structural roles of histone methylation as well as explore the novel roles of cell cycle methylation on a global scale.

Bibliography

Aagaard, L., Schmid, M., Warburton, P. and Jenuwein, T. (2000). Mitotic phosphorylation of SUV39H1, a novel component of active centromeres, coincides with transient accumulation at mammalian centromeres. *J Cell Sci* **113** (Pt 5), 817-29.

Adams, R. R., Eckley, D. M., Vagnarelli, P., Wheatley, S. P., Gerloff, D. L., Mackay, A. M., Svingen, P. A., Kaufmann, S. H. and Earnshaw, W. C. (2001a). Human INCENP colocalizes with the Aurora-B/AIRK2 kinase on chromosomes and is overexpressed in tumour cells. *Chromosoma* **110**, 65-74.

Adams, R. R., Maiato, H., Earnshaw, W. C. and Carmena, M. (2001b). Essential roles of Drosophila inner centromere protein (INCENP) and aurora B in histone H3 phosphorylation, metaphase chromosome alignment, kinetochore disjunction, and chromosome segregation. *J Cell Biol* **153**, 865-80.

Ahmad, K. and Henikoff, S. (2002). The histone variant H3.3 marks active chromatin by replication-independent nucleosome assembly. *Mol Cell* **9**, 1191-200.

Akhtar, A., Zink, D. and Becker, P. B. (2000). Chromodomains are protein-RNA interaction modules. *Nature* **407**, 405-9.

Alland, L., Muhle, R., Hou, H., Jr., Potes, J., Chin, L., Schreiber-Agus, N. and DePinho, R. A. (1997). Role for N-CoR and histone deacetylase in Sin3-mediated transcriptional repression. *Nature* **387**, 49-55.

Allshire, R. C., Javerzat, J. P., Redhead, N. J. and Cranston, G. (1994). Position effect variegation at fission yeast centromeres. *Cell* **76**, 157-69.

Annunziato, A. T., Eason, M. B. and Perry, C. A. (1995). Relationship between methylation and acetylation of arginine-rich histones in cycling and arrested HeLa cells. *Biochemistry* **34**, 2916-24.

Annunziato, A. T., Frado, L. L., Seale, R. L. and Woodcock, C. L. (1988). Treatment with sodium butyrate inhibits the complete condensation of interphase chromatin. *Chromosoma* **96**, 132-8.

Bannister, A. J., Zegerman, P., Partridge, J. F., Miska, E. A., Thomas, J. O., Allshire, R. C. and Kouzarides, T. (2001). Selective recognition of methylated lysine 9 on histone H3 by the HP1 chromo domain. *Nature* **410**, 120-4.

Barski, A., Cuddapah, S., Cui, K., Roh, T. Y., Schones, D. E., Wang, Z., Wei, G., Chepelev, I. and Zhao, K. (2007). High-resolution profiling of histone methylations in the human genome. *Cell* **129**, 823-37.

Bartel, R. L. and Borchardt, R. T. (1984). Effects of adenosine dialdehyde on S-adenosylhomocysteine hydrolase and S-adenosylmethionine-dependent transmethylation in mouse L929 cells. *Mol Pharmacol* **25**, 418-24.

Bartova, E., Pachernik, J., Harnicarova, A., Kovarik, A., Kovarikova, M., Hofmanova, J., Skalnikova, M., Kozubek, M. and Kozubek, S. (2005). Nuclear levels and patterns of histone H3 modification and HP1 proteins after inhibition of histone deacetylases. *J Cell Sci* **118**, 5035-46.

Bartsch, J., Truss, M., Bode, J. and Beato, M. (1996). Moderate increase in histone acetylation activates the mouse mammary tumor virus

promoter and remodels its nucleosome structure. *Proc Natl Acad Sci U S A* **93**, 10741-6.

Bassett, A., Cooper, S., Wu, C. and Travers, A. (2009). The folding and unfolding of eukaryotic chromatin. *Curr Opin Genet Dev*.

Baumann, C., Korner, R., Hofmann, K. and Nigg, E. A. (2007). PICH, a centromere-associated SNF2 family ATPase, is regulated by Plk1 and required for the spindle checkpoint. *Cell* **128**, 101-14.

Belmont, A. S., Sedat, J. W. and Agard, D. A. (1987). A three-dimensional approach to mitotic chromosome structure: evidence for a complex hierarchical organization. *J Cell Biol* **105**, 77-92.

Bernard, P. and Allshire, R. (2002). Centromeres become unstuck without heterochromatin. *Trends Cell Biol* **12**, 419-24.

Bernard, P., Maure, J. F., Partridge, J. F., Genier, S., Javerzat, J. P. and Allshire, R. C. (2001). Requirement of heterochromatin for cohesion at centromeres. *Science* **294**, 2539-42.

Berndsen, C. E., Selleck, W., McBryant, S. J., Hansen, J. C., Tan, S. and Denu, J. M. (2007). Nucleosome recognition by the Piccolo NuA4 histone acetyltransferase complex. *Biochemistry* **46**, 2091-9.

Biron, V. L., McManus, K. J., Hu, N., Hendzel, M. J. and Underhill, D. A. (2004). Distinct dynamics and distribution of histone methyl-lysine derivatives in mouse development. *Dev Biol* **276**, 337-51.

Black, B. E., Foltz, D. R., Chakravarthy, S., Luger, K., Woods, V. L., Jr. and Cleveland, D. W. (2004). Structural determinants for generating centromeric chromatin. *Nature* **430**, 578-82.

Blower, M. D., Sullivan, B. A. and Karpen, G. H. (2002). Conserved organization of centromeric chromatin in flies and humans. *Dev Cell* **2**, 319-30.

Bomont, P., Maddox, P., Shah, J. V., Desai, A. B. and Cleveland, D. W. (2005). Unstable microtubule capture at kinetochores depleted of the centromere-associated protein CENP-F. *Embo J* **24**, 3927-39.

Borun, T. W., Pearson, D. and Paik, W. K. (1972). Studies of histone methylation during the HeLa S-3 cell cycle. *J Biol Chem* **247**, 4288-98.

Botuyan, M. V., Lee, J., Ward, I. M., Kim, J. E., Thompson, J. R., Chen, J. and Mer, G. (2006). Structural basis for the methylation state-specific recognition of histone H4-K20 by 53BP1 and Crb2 in DNA repair. *Cell* **127**, 1361-73.

Bradbury, E. M. (1992). Reversible histone modifications and the chromosome cell cycle. *Bioessays* **14**, 9-16.

Braunstein, M., Rose, A. B., Holmes, S. G., Allis, C. D. and Broach, J. R. (1993). Transcriptional silencing in yeast is associated with reduced nucleosome acetylation. *Genes Dev* **7**, 592-604.

Brehm, A., Miska, E. A., McCance, D. J., Reid, J. L., Bannister, A. J. and Kouzarides, T. (1998). Retinoblastoma protein recruits histone deacetylase to repress transcription. *Nature* **391**, 597-601.

Brinkley, B. R. and Cartwright, J., Jr. (1975). Cold-labile and cold-stable microtubules in the mitotic spindle of mammalian cells. *Ann N Y Acad Sci* **253**, 428-39.

- Brownell, J. E., Zhou, J., Ranalli, T., Kobayashi, R., Edmondson, D. G., Roth, S. Y. and Allis, C. D.** (1996). Tetrahymena histone acetyltransferase A: a homolog to yeast Gcn5p linking histone acetylation to gene activation. *Cell* **84**, 843-51.
- Cam, H. P., Sugiyama, T., Chen, E. S., Chen, X., FitzGerald, P. C. and Grewal, S. I.** (2005). Comprehensive analysis of heterochromatin- and RNAi-mediated epigenetic control of the fission yeast genome. *Nat Genet* **37**, 809-19.
- Chadwick, B. P. and Willard, H. F.** (2004). Multiple spatially distinct types of facultative heterochromatin on the human inactive X chromosome. *Proc Natl Acad Sci U S A* **101**, 17450-5.
- Chan, G. K., Jablonski, S. A., Starr, D. A., Goldberg, M. L. and Yen, T. J.** (2000). Human Zw10 and ROD are mitotic checkpoint proteins that bind to kinetochores. *Nat Cell Biol* **2**, 944-7.
- Chan, G. K., Jablonski, S. A., Sudakin, V., Hittle, J. C. and Yen, T. J.** (1999). Human BUBR1 is a mitotic checkpoint kinase that monitors CENP-E functions at kinetochores and binds the cyclosome/APC. *J Cell Biol* **146**, 941-54.
- Chan, G. K., Liu, S. T. and Yen, T. J.** (2005). Kinetochores: structure and function. *Trends Cell Biol* **15**, 589-98.
- Cheeseman, I. M. and Desai, A.** (2008). Molecular architecture of the kinetochores-microtubule interface. *Nat Rev Mol Cell Biol* **9**, 33-46.
- Chen, T., Hevi, S., Gay, F., Tsujimoto, N., He, T., Zhang, B., Ueda, Y. and Li, E.** (2007). Complete inactivation of DNMT1 leads to mitotic catastrophe in human cancer cells. *Nat Genet* **39**, 391-6.
- Chen, Y., Baker, R. E., Keith, K. C., Harris, K., Stoler, S. and Fitzgerald-Hayes, M.** (2000). The N terminus of the centromere H3-like protein Cse4p performs an essential function distinct from that of the histone fold domain. *Mol Cell Biol* **20**, 7037-48.
- Cherry, L. M., Faulkner, A. J., Grossberg, L. A. and Balczon, R.** (1989). Kinetochores: size variation in mammalian chromosomes: an image analysis study with evolutionary implications. *J Cell Sci* **92** (Pt 2), 281-9.
- Cheutin, T., McNairn, A. J., Jenuwein, T., Gilbert, D. M., Singh, P. B. and Misteli, T.** (2003). Maintenance of stable heterochromatin domains by dynamic HP1 binding. *Science* **299**, 721-5.
- Christensen, M. O., Larsen, M. K., Barthelme, H. U., Hock, R., Andersen, C. L., Kjeldsen, E., Knudsen, B. R., Westergaard, O., Boege, F. and Mielke, C.** (2002). Dynamics of human DNA topoisomerases IIalpha and IIbeta in living cells. *J Cell Biol* **157**, 31-44.
- Cimini, D., Mattiuzzo, M., Torosantucci, L. and Degrossi, F.** (2003). Histone hyperacetylation in mitosis prevents sister chromatid separation and produces chromosome segregation defects. *Mol Biol Cell* **14**, 3821-33.
- Cleveland, D. W., Mao, Y. and Sullivan, K. F.** (2003). Centromeres and kinetochores: from epigenetics to mitotic checkpoint signaling. *Cell* **112**, 407-21.
- Clift, D., Bizzari, F. and Marston, A. L.** (2009). Shugoshin prevents cohesin cleavage by PP2A(Cdc55)-dependent inhibition of separase. *Genes Dev* **23**, 766-80.

- Cloos, P. A., Christensen, J., Agger, K., Maiolica, A., Rappsilber, J., Antal, T., Hansen, K. H. and Helin, K.** (2006). The putative oncogene GASC1 demethylates tri- and dimethylated lysine 9 on histone H3. *Nature* **442**, 307-11.
- Cowieson, N. P., Partridge, J. F., Allshire, R. C. and McLaughlin, P. J.** (2000). Dimerisation of a chromo shadow domain and distinctions from the chromodomain as revealed by structural analysis. *Curr Biol* **10**, 517-25.
- Czvitkovich, S., Sauer, S., Peters, A. H., Deiner, E., Wolf, A., Laible, G., Opravil, S., Beug, H. and Jenuwein, T.** (2001). Over-expression of the SUV39H1 histone methyltransferase induces altered proliferation and differentiation in transgenic mice. *Mech Dev* **107**, 141-53.
- Dalal, Y., Furuyama, T., Vermaak, D. and Henikoff, S.** (2007a). Structure, dynamics, and evolution of centromeric nucleosomes. *Proc Natl Acad Sci U S A* **104**, 15974-81.
- Dalal, Y., Wang, H., Lindsay, S. and Henikoff, S.** (2007b). Tetrameric structure of centromeric nucleosomes in interphase Drosophila cells. *PLoS Biol* **5**, e218.
- Davie, J. R.** (1996). Histone modifications, chromatin structure, and the nuclear matrix. *J Cell Biochem* **62**, 149-57.
- Dewar, H., Tanaka, K., Nasmyth, K. and Tanaka, T. U.** (2004). Tension between two kinetochores suffices for their bi-orientation on the mitotic spindle. *Nature* **428**, 93-7.
- Dhalluin, C., Carlson, J. E., Zeng, L., He, C., Aggarwal, A. K. and Zhou, M. M.** (1999). Structure and ligand of a histone acetyltransferase bromodomain. *Nature* **399**, 491-6.
- Dion, M. F., Altschuler, S. J., Wu, L. F. and Rando, O. J.** (2005). Genomic characterization reveals a simple histone H4 acetylation code. *Proc Natl Acad Sci U S A* **102**, 5501-6.
- Dorigo, B., Schalch, T., Kulangara, A., Duda, S., Schroeder, R. R. and Richmond, T. J.** (2004). Nucleosome arrays reveal the two-start organization of the chromatin fiber. *Science* **306**, 1571-3.
- Dunleavy, E. M., Roche, D., Tagami, H., Lacoste, N., Ray-Gallet, D., Nakamura, Y., Daigo, Y., Nakatani, Y. and Almouzni-Pettinotti, G.** (2009). HJURP is a cell-cycle-dependent maintenance and deposition factor of CENP-A at centromeres. *Cell* **137**, 485-97.
- Earnshaw, W., Bordwell, B., Marino, C. and Rothfield, N.** (1986). Three human chromosomal autoantigens are recognized by sera from patients with anti-centromere antibodies. *J Clin Invest* **77**, 426-30.
- Earnshaw, W. C., Halligan, B., Cooke, C. A., Heck, M. M. and Liu, L. F.** (1985). Topoisomerase II is a structural component of mitotic chromosome scaffolds. *J Cell Biol* **100**, 1706-15.
- Earnshaw, W. C. and Migeon, B. R.** (1985). Three related centromere proteins are absent from the inactive centromere of a stable isodicentric chromosome. *Chromosoma* **92**, 290-6.
- Elowe, S., Hummer, S., Uldschmid, A., Li, X. and Nigg, E. A.** (2007). Tension-sensitive Plk1 phosphorylation on BubR1 regulates the stability of kinetochore microtubule interactions. *Genes Dev* **21**, 2205-19.

Eltsov, M., Maclellan, K. M., Maeshima, K., Frangakis, A. S. and Dubochet, J. (2008). Analysis of cryo-electron microscopy images does not support the existence of 30-nm chromatin fibers in mitotic chromosomes in situ. *Proc Natl Acad Sci U S A* **105**, 19732-7.

Feng, J., Huang, H. and Yen, T. J. (2006). CENP-F is a novel microtubule-binding protein that is essential for kinetochore attachments and affects the duration of the mitotic checkpoint delay. *Chromosoma* **115**, 320-9.

Firestein, R., Cui, X., Huie, P. and Cleary, M. L. (2000). Set domain-dependent regulation of transcriptional silencing and growth control by SUV39H1, a mammalian ortholog of *Drosophila* Su(var)3-9. *Mol Cell Biol* **20**, 4900-9.

Fischle, W., Tseng, B. S., Dormann, H. L., Ueberheide, B. M., Garcia, B. A., Shabanowitz, J., Hunt, D. F., Funabiki, H. and Allis, C. D. (2005). Regulation of HP1-chromatin binding by histone H3 methylation and phosphorylation. *Nature*.

Fischle, W., Wang, Y., Jacobs, S. A., Kim, Y., Allis, C. D. and Khorasanizadeh, S. (2003). Molecular basis for the discrimination of repressive methyl-lysine marks in histone H3 by Polycomb and HP1 chromodomains. *Genes Dev* **17**, 1870-81.

Fodor, B. D., Kubicek, S., Yonezawa, M., O'Sullivan, R. J., Sengupta, R., Perez-Burgos, L., Opravil, S., Mechtler, K., Schotta, G. and Jenuwein, T. (2006). Jmjd2b antagonizes H3K9 trimethylation at pericentric heterochromatin in mammalian cells. *Genes Dev* **20**, 1557-62.

Folco, H. D., Pidoux, A. L., Urano, T. and Allshire, R. C. (2008). Heterochromatin and RNAi are required to establish CENP-A chromatin at centromeres. *Science* **319**, 94-7.

Foltz, D. R., Jansen, L. E., Bailey, A. O., Yates, J. R., 3rd, Bassett, E. A., Wood, S., Black, B. E. and Cleveland, D. W. (2009). Centromere-specific assembly of CENP-a nucleosomes is mediated by HJURP. *Cell* **137**, 472-84.

Fukagawa, T., Mikami, Y., Nishihashi, A., Regnier, V., Haraguchi, T., Hiraoka, Y., Sugata, N., Todokoro, K., Brown, W. and Ikemura, T. (2001). CENP-H, a constitutive centromere component, is required for centromere targeting of CENP-C in vertebrate cells. *Embo J* **20**, 4603-17.

Fukagawa, T., Nogami, M., Yoshikawa, M., Ikeno, M., Okazaki, T., Takami, Y., Nakayama, T. and Oshimura, M. (2004). Dicer is essential for formation of the heterochromatin structure in vertebrate cells. *Nat Cell Biol* **6**, 784-91.

Garcia-Ramirez, M., Dong, F. and Ausio, J. (1992). Role of the histone "tails" in the folding of oligonucleosomes depleted of histone H1. *J Biol Chem* **267**, 19587-95.

Garcia-Ramirez, M., Rocchini, C. and Ausio, J. (1995). Modulation of chromatin folding by histone acetylation. *J Biol Chem* **270**, 17923-8.

Gerchman, S. E. and Ramakrishnan, V. (1987). Chromatin higher-order structure studied by neutron scattering and scanning transmission electron microscopy. *Proc Natl Acad Sci U S A* **84**, 7802-6.

Ghirlando, R. and Felsenfeld, G. (2008). Hydrodynamic studies on defined heterochromatin fragments support a 30-nm fiber having six nucleosomes per turn. *J Mol Biol* **376**, 1417-25.

Gieni, R. S., Chan, G. K. and Hendzel, M. J. (2008a). Epigenetics regulate centromere formation and kinetochore function. *J Cell Biochem*.

Gieni, R. S., Chan, G. K. and Hendzel, M. J. (2008b). Epigenetics regulate centromere formation and kinetochore function. *J Cell Biochem* **104**, 2027-39.

Giet, R. and Glover, D. M. (2001). Drosophila aurora B kinase is required for histone H3 phosphorylation and condensin recruitment during chromosome condensation and to organize the central spindle during cytokinesis. *J Cell Biol* **152**, 669-82.

Gilbert, N. and Allan, J. (2001). Distinctive higher-order chromatin structure at mammalian centromeres. *Proc Natl Acad Sci U S A* **98**, 11949-54.

Gonzalo, S., Garcia-Cao, M., Fraga, M. F., Schotta, G., Peters, A. H., Cotter, S. E., Eguia, R., Dean, D. C., Esteller, M., Jenuwein, T. et al. (2005). Role of the RB1 family in stabilizing histone methylation at constitutive heterochromatin. *Nat Cell Biol* **7**, 420-8.

Govatsky, G. J. and Ricketts, W. A. (1993). Differential expression of a phosphoepitope at the kinetochores of moving chromosomes. *J Cell Biol* **122**, 1311-21.

Goshima, G., Kiyomitsu, T., Yoda, K. and Yanagida, M. (2003). Human centromere chromatin protein hMis12, essential for equal segregation, is independent of CENP-A loading pathway. *J Cell Biol* **160**, 25-39.

Govin, J., Lestrat, C., Caron, C., Pivot-Pajot, C., Rousseaux, S. and Khochbin, S. (2006). Histone acetylation-mediated chromatin compaction during mouse spermatogenesis. *Ernst Schering Res Found Workshop*, 155-72.

Grady, D. L., Ratliff, R. L., Robinson, D. L., McCanlies, E. C., Meyne, J. and Moyzis, R. K. (1992). Highly conserved repetitive DNA sequences are present at human centromeres. *Proc Natl Acad Sci U S A* **89**, 1695-9.

Greiner, D., Bonaldi, T., Eskeland, R., Roemer, E. and Imhof, A. (2005). Identification of a specific inhibitor of the histone methyltransferase SU(VAR)3-9. *Nat Chem Biol* **1**, 143-5.

Grewal, S. I. and Jia, S. (2007). Heterochromatin revisited. *Nat Rev Genet* **8**, 35-46.

Grunstein, M. (1997). Histone acetylation in chromatin structure and transcription. *Nature* **389**, 349-52.

Han, X., Jin, M., Breuker, K. and McLafferty, F. W. (2006). Extending top-down mass spectrometry to proteins with masses greater than 200 kilodaltons. *Science* **314**, 109-12.

Hansen, J. C., Lu, X., Ross, E. D. and Woody, R. W. (2006). Intrinsic protein disorder, amino acid composition, and histone terminal domains. *J Biol Chem* **281**, 1853-6.

Hayashi, T., Fujita, Y., Iwasaki, O., Adachi, Y., Takahashi, K. and Yanagida, M. (2004). Mis16 and Mis18 are required for CENP-A loading and histone deacetylation at centromeres. *Cell* **118**, 715-29.

- Hayes, J. J., Clark, D. J. and Wolffe, A. P.** (1991). Histone contributions to the structure of DNA in the nucleosome. *Proc Natl Acad Sci U S A* **88**, 6829-33.
- Heit, R., Rattner, J. B., Chan, G. K. and Hendzel, M. J.** (2009). G2 histone methylation is required for the proper segregation of chromosomes. *J Cell Sci*.
- Heit, R., Underhill, D. A., Chan, G. and Hendzel, M. J.** (2006). Epigenetic regulation of centromere formation and kinetochore function. *Biochem Cell Biol* **84**, 605-18.
- Hendzel, M. J., Wei, Y., Mancini, M. A., Van Hooser, A., Ranalli, T., Brinkley, B. R., Bazett-Jones, D. P. and Allis, C. D.** (1997). Mitosis-specific phosphorylation of histone H3 initiates primarily within pericentromeric heterochromatin during G2 and spreads in an ordered fashion coincident with mitotic chromosome condensation. *Chromosoma* **106**, 348-60.
- Henikoff, S.** (2000). Heterochromatin function in complex genomes. *Biochim Biophys Acta* **1470**, O1-8.
- Hirota, T., Lipp, J. J., Toh, B. H. and Peters, J. M.** (2005). Histone H3 serine 10 phosphorylation by Aurora B causes HP1 dissociation from heterochromatin. *Nature*.
- Holt, S. V., Vergnolle, M. A., Hussein, D., Wozniak, M. J., Allan, V. J. and Taylor, S. S.** (2005). Silencing Cenp-F weakens centromeric cohesion, prevents chromosome alignment and activates the spindle checkpoint. *J Cell Sci* **118**, 4889-900.
- Houston, S. I., McManus, K. J., Adams, M. M., Sims, J. K., Carpenter, P. B., Hendzel, M. J. and Rice, J. C.** (2008). Catalytic Function of the PR-Set7 Histone H4 Lysine 20 Monomethyltransferase Is Essential for Mitotic Entry and Genomic Stability. *J Biol Chem* **283**, 19478-88.
- Huang, Y., Fang, J., Bedford, M. T., Zhang, Y. and Xu, R. M.** (2006). Recognition of histone H3 lysine-4 methylation by the double tudor domain of JMJD2A. *Science* **312**, 748-51.
- Hudson, D. F., Vagnarelli, P., Gassmann, R. and Earnshaw, W. C.** (2003). Condensin is required for nonhistone protein assembly and structural integrity of vertebrate mitotic chromosomes. *Dev Cell* **5**, 323-36.
- Inoue, A., Hyle, J., Lechner, M. S. and Lahti, J. M.** (2008). Perturbation of HP1 localization and chromatin binding ability causes defects in sister-chromatid cohesion. *Mutat Res* **657**, 48-55.
- Iovcheva, C., Mladenova, I. and Dessev, G.** (1984). Removal of histone H1 exposes linker DNA in chromatin to DNase I. *Mol Biol Rep* **10**, 9-12.
- Jackson, J. D., Falciano, V. T. and Gorovsky, M. A.** (1996). A likely histone H2A.F/Z variant in *Saccharomyces cerevisiae*. *Trends Biochem Sci* **21**, 466-7.
- Jacobs, S. A. and Khorasanizadeh, S.** (2002). Structure of HP1 chromodomain bound to a lysine 9-methylated histone H3 tail. *Science* **295**, 2080-3.
- Johnson, C. A., O'Neill, L. P., Mitchell, A. and Turner, B. M.** (1998). Distinctive patterns of histone H4 acetylation are associated with defined

sequence elements within both heterochromatic and euchromatic regions of the human genome. *Nucleic Acids Res* **26**, 994-1001.

Kallio, M. J., McClelland, M. L., Stukenberg, P. T. and Gorbsky, G. J. (2002). Inhibition of aurora B kinase blocks chromosome segregation, overrides the spindle checkpoint, and perturbs microtubule dynamics in mitosis. *Curr Biol* **12**, 900-5.

Kamakaka, R. T. and Biggins, S. (2005). Histone variants: deviants? *Genes Dev* **19**, 295-310.

Kanellopoulou, C., Muljo, S. A., Kung, A. L., Ganesan, S., Drapkin, R., Jenuwein, T., Livingston, D. M. and Rajewsky, K. (2005). Dicer-deficient mouse embryonic stem cells are defective in differentiation and centromeric silencing. *Genes Dev* **19**, 489-501.

Karachentsev, D., Sarma, K., Reinberg, D. and Steward, R. (2005). PR-Set7-dependent methylation of histone H4 Lys 20 functions in repression of gene expression and is essential for mitosis. *Genes Dev* **19**, 431-5.

Keene, M. A., Corces, V., Lowenhaupt, K. and Elgin, S. C. (1981). DNase I hypersensitive sites in Drosophila chromatin occur at the 5' ends of regions of transcription. *Proc Natl Acad Sci U S A* **78**, 143-6.

Keller, B. T. and Borchardt, R. T. (1987). Adenosine dialdehyde: a potent inhibitor of vaccinia virus multiplication in mouse L929 cells. *Mol Pharmacol* **31**, 485-92.

Kimura, H. and Cook, P. R. (2001). Kinetics of core histones in living human cells: little exchange of H3 and H4 and some rapid exchange of H2B. *J Cell Biol* **153**, 1341-53.

Kireeva, N., Lakonishok, M., Kireev, I., Hirano, T. and Belmont, A. S. (2004). Visualization of early chromosome condensation: a hierarchical folding, axial glue model of chromosome structure. *J Cell Biol* **166**, 775-85.

Klose, R. J., Yamane, K., Bae, Y., Zhang, D., Erdjument-Bromage, H., Tempst, P., Wong, J. and Zhang, Y. (2006). The transcriptional repressor JHDM3A demethylates trimethyl histone H3 lysine 9 and lysine 36. *Nature* **442**, 312-6.

Klose, R. J. and Zhang, Y. (2007). Regulation of histone methylation by demethyliminination and demethylation. *Nat Rev Mol Cell Biol* **8**, 307-18.

Koch, B., Kueng, S., Ruckenbauer, C., Wendt, K. S. and Peters, J. M. (2008). The Suv39h-HP1 histone methylation pathway is dispensable for enrichment and protection of cohesin at centromeres in mammalian cells. *Chromosoma* **117**, 199-210.

Kornberg, R. D. (1974). Chromatin structure: a repeating unit of histones and DNA. *Science* **184**, 868-71.

Kourmouli, N., Jeppesen, P., Mahadevhaiah, S., Burgoyne, P., Wu, R., Gilbert, D. M., Bongiorno, S., Prantera, G., Fanti, L., Pimpinelli, S. et al. (2004). Heterochromatin and tri-methylated lysine 20 of histone H4 in animals. *J Cell Sci* **117**, 2491-501.

Kouzarides, T. (2007). Chromatin modifications and their function. *Cell* **128**, 693-705.

- Krajewski, W. A. and Becker, P. B.** (1998). Reconstitution of hyperacetylated, DNase I-sensitive chromatin characterized by high conformational flexibility of nucleosomal DNA. *Proc Natl Acad Sci U S A* **95**, 1540-5.
- Kristjuhan, A., Wittschieben, B. O., Walker, J., Roberts, D., Cairns, B. R. and Svejstrup, J. Q.** (2003). Spreading of Sir3 protein in cells with severe histone H3 hypoacetylation. *Proc Natl Acad Sci U S A* **100**, 7551-6.
- Krouwels, I. M., Wiesmeijer, K., Abraham, T. E., Molenaar, C., Verwoerd, N. P., Tanke, H. J. and Dirks, R. W.** (2005). A glue for heterochromatin maintenance: stable SUV39H1 binding to heterochromatin is reinforced by the SET domain. *J Cell Biol* **170**, 537-49.
- Kubicek, S., Schotta, G., Lachner, M., Sengupta, R., Kohlmaier, A., Perez-Burgos, L., Linderson, Y., Martens, J. H., O'Sullivan, R. J., Fodor, B. D. et al.** (2006). The role of histone modifications in epigenetic transitions during normal and perturbed development. *Ernst Schering Res Found Workshop*, 1-27.
- Kuo, M. H. and Allis, C. D.** (1998). Roles of histone acetyltransferases and deacetylases in gene regulation. *Bioessays* **20**, 615-26.
- Kuo, M. H., Zhou, J., Jambeck, P., Churchill, M. E. and Allis, C. D.** (1998). Histone acetyltransferase activity of yeast Gcn5p is required for the activation of target genes in vivo. *Genes Dev* **12**, 627-39.
- Lachner, M., O'Carroll, D., Rea, S., Mechtler, K. and Jenuwein, T.** (2001). Methylation of histone H3 lysine 9 creates a binding site for HP1 proteins. *Nature* **410**, 116-20.
- Lam, A. L., Boivin, C. D., Bonney, C. F., Rudd, M. K. and Sullivan, B. A.** (2006). Human centromeric chromatin is a dynamic chromosomal domain that can spread over noncentromeric DNA. *Proc Natl Acad Sci U S A* **103**, 4186-91.
- Lechner, M. S., Schultz, D. C., Negorev, D., Maul, G. G. and Rauscher, F. J., 3rd.** (2005). The mammalian heterochromatin protein 1 binds diverse nuclear proteins through a common motif that targets the chromoshadow domain. *Biochem Biophys Res Commun* **331**, 929-37.
- Lee, J., Kitajima, T. S., Tanno, Y., Yoshida, K., Morita, T., Miyano, T., Miyake, M. and Watanabe, Y.** (2008a). Unified mode of centromeric protection by shugoshin in mammalian oocytes and somatic cells. *Nat Cell Biol* **10**, 42-52.
- Lee, J., Thompson, J. R., Botuyan, M. V. and Mer, G.** (2008b). Distinct binding modes specify the recognition of methylated histones H3K4 and H4K20 by JMJD2A-tudor. *Nat Struct Mol Biol* **15**, 109-11.
- Lehnertz, B., Ueda, Y., Derijck, A. A., Braunschweig, U., Perez-Burgos, L., Kubicek, S., Chen, T., Li, E., Jenuwein, T. and Peters, A. H.** (2003). Suv39h-mediated histone H3 lysine 9 methylation directs DNA methylation to major satellite repeats at pericentric heterochromatin. *Curr Biol* **13**, 1192-200.
- Li, Z., Chen, L., Kabra, N., Wang, C., Fang, J. and Chen, J.** (2009). Inhibition of SUV39H1 Methyltransferase Activity by DBC1. *J Biol Chem* **284**, 10361-6.

- Liao, H., Winkfein, R. J., Mack, G., Rattner, J. B. and Yen, T. J.** (1995). CENP-F is a protein of the nuclear matrix that assembles onto kinetochores at late G2 and is rapidly degraded after mitosis. *J Cell Biol* **130**, 507-18.
- Liu, D., Vader, G., Vromans, M. J., Lampson, M. A. and Lens, S. M.** (2009). Sensing chromosome bi-orientation by spatial separation of aurora B kinase from kinetochore substrates. *Science* **323**, 1350-3.
- Liu, S. T., Hittle, J. C., Jablonski, S. A., Campbell, M. S., Yoda, K. and Yen, T. J.** (2003). Human CENP-I specifies localization of CENP-F, MAD1 and MAD2 to kinetochores and is essential for mitosis. *Nat Cell Biol* **5**, 341-5.
- Loenen, W. A.** (2006). S-adenosylmethionine: jack of all trades and master of everything? *Biochem Soc Trans* **34**, 330-3.
- Loyola, A. and Almouzni, G.** (2004). Histone chaperones, a supporting role in the limelight. *Biochim Biophys Acta* **1677**, 3-11.
- Lu, Q. and Richardson, B.** (2004). DNaseI hypersensitivity analysis of chromatin structure. *Methods Mol Biol* **287**, 77-86.
- Luger, K., Mader, A. W., Richmond, R. K., Sargent, D. F. and Richmond, T. J.** (1997). Crystal structure of the nucleosome core particle at 2.8 Å resolution. *Nature* **389**, 251-60.
- Luo, R. X., Postigo, A. A. and Dean, D. C.** (1998). Rb interacts with histone deacetylase to repress transcription. *Cell* **92**, 463-73.
- Maeshima, K. and Laemmli, U. K.** (2003). A two-step scaffolding model for mitotic chromosome assembly. *Dev Cell* **4**, 467-80.
- Magnaghi-Jaulin, L., Groisman, R., Naguibneva, I., Robin, P., Lorain, S., Le Villain, J. P., Troalen, F., Trouche, D. and Harel-Bellan, A.** (1998). Retinoblastoma protein represses transcription by recruiting a histone deacetylase. *Nature* **391**, 601-5.
- Maia, A. F., Lopes, C. S. and Sunkel, C. E.** (2007). BubR1 and CENP-E have antagonistic effects upon the stability of microtubule-kinetochore attachments in *Drosophila* S2 cell mitosis. *Cell Cycle* **6**, 1367-78.
- Maison, C. and Almouzni, G.** (2004). HP1 and the dynamics of heterochromatin maintenance. *Nat Rev Mol Cell Biol* **5**, 296-304.
- Maison, C., Bailly, D., Peters, A. H., Quivy, J. P., Roche, D., Taddei, A., Lachner, M., Jenuwein, T. and Almouzni, G.** (2002). Higher-order structure in pericentric heterochromatin involves a distinct pattern of histone modification and an RNA component. *Nat Genet* **30**, 329-34.
- Malik, H. S. and Henikoff, S.** (2003). Phylogenomics of the nucleosome. *Nat Struct Biol* **10**, 882-91.
- Malik, H. S., Vermaak, D. and Henikoff, S.** (2002). Recurrent evolution of DNA-binding motifs in the *Drosophila* centromeric histone. *Proc Natl Acad Sci U S A* **99**, 1449-54.
- Mangenot, S., Leforestier, A., Durand, D. and Livolant, F.** (2003). X-ray diffraction characterization of the dense phases formed by nucleosome core particles. *Biophys J* **84**, 2570-84.

- Mao, Y., Desai, A. and Cleveland, D. W.** (2005). Microtubule capture by CENP-E silences BubR1-dependent mitotic checkpoint signaling. *J Cell Biol* **170**, 873-80.
- Marsden, M. P. and Laemmli, U. K.** (1979). Metaphase chromosome structure: evidence for a radial loop model. *Cell* **17**, 849-58.
- Marshall, O. J., Marshall, A. T. and Choo, K. H.** (2008). Three-dimensional localization of CENP-A suggests a complex higher order structure of centromeric chromatin. *J Cell Biol* **183**, 1193-202.
- Mateos-Langerak, J., Bohn, M., de Leeuw, W., Giromus, O., Manders, E. M., Verschure, P. J., Indemans, M. H., Gierman, H. J., Heermann, D. W., van Driel, R. et al.** (2009). Spatially confined folding of chromatin in the interphase nucleus. *Proc Natl Acad Sci U S A* **106**, 3812-7.
- McEwen, B. F., Chan, G. K., Zubrowski, B., Savoian, M. S., Sauer, M. T. and Yen, T. J.** (2001). CENP-E is essential for reliable bioriented spindle attachment, but chromosome alignment can be achieved via redundant mechanisms in mammalian cells. *Mol Biol Cell* **12**, 2776-89.
- McGhee, J. D., Nickol, J. M., Felsenfeld, G. and Rau, D. C.** (1983). Higher order structure of chromatin: orientation of nucleosomes within the 30 nm chromatin solenoid is independent of species and spacer length. *Cell* **33**, 831-41.
- McManus, K. J., Biron, V. L., Heit, R., Underhill, D. A. and Hendzel, M. J.** (2006). Dynamic changes in histone H3 lysine 9 methylations: identification of a mitosis-specific function for dynamic methylation in chromosome congression and segregation. *J Biol Chem* **281**, 8888-97.
- McManus, K. J. and Hendzel, M. J.** (2003). Quantitative analysis of CBP- and P300-induced histone acetylations in vivo using native chromatin. *Mol Cell Biol* **23**, 7611-27.
- Melcher, M., Schmid, M., Aagaard, L., Selenko, P., Laible, G. and Jenuwein, T.** (2000). Structure-function analysis of SUV39H1 reveals a dominant role in heterochromatin organization, chromosome segregation, and mitotic progression. *Mol Cell Biol* **20**, 3728-41.
- Mellone, B. G., Ball, L., Suka, N., Grunstein, M. R., Partridge, J. F. and Allshire, R. C.** (2003). Centromere silencing and function in fission yeast is governed by the amino terminus of histone H3. *Curr Biol* **13**, 1748-57.
- Mikkelsen, T. S., Ku, M., Jaffe, D. B., Issac, B., Lieberman, E., Giannoukos, G., Alvarez, P., Brockman, W., Kim, T. K., Koche, R. P. et al.** (2007). Genome-wide maps of chromatin state in pluripotent and lineage-committed cells. *Nature* **448**, 553-60.
- Minc, E., Allory, Y., Worman, H. J., Courvalin, J. C. and Buendia, B.** (1999). Localization and phosphorylation of HP1 proteins during the cell cycle in mammalian cells. *Chromosoma* **108**, 220-34.
- Morrow, C. J., Tighe, A., Johnson, V. L., Scott, M. I., Ditchfield, C. and Taylor, S. S.** (2005). Bub1 and aurora B cooperate to maintain BubR1-mediated inhibition of APC/CCdc20. *J Cell Sci* **118**, 3639-52.
- Muchardt, C., Guilleme, M., Seeler, J. S., Trouche, D., Dejean, A. and Yaniv, M.** (2002). Coordinated methyl and RNA binding is required for heterochromatin localization of mammalian HP1alpha. *EMBO Rep* **3**, 975-81.

- Musacchio, A. and Salmon, E. D.** (2007). The spindle-assembly checkpoint in space and time. *Nat Rev Mol Cell Biol* **8**, 379-93.
- Musio, A., Mariani, T., Montagna, C., Zambroni, D., Ascoli, C., Ried, T. and Vezzi, P.** (2004). Recapitulation of the Roberts syndrome cellular phenotype by inhibition of INCENP, ZWINT-1 and ZW10 genes. *Gene* **331**, 33-40.
- Nakano, M., Okamoto, Y., Ohzeki, J. and Masumoto, H.** (2003). Epigenetic assembly of centromeric chromatin at ectopic alpha-satellite sites on human chromosomes. *J Cell Sci* **116**, 4021-34.
- Nakayama, J., Rice, J. C., Strahl, B. D., Allis, C. D. and Grewal, S. I.** (2001). Role of histone H3 lysine 9 methylation in epigenetic control of heterochromatin assembly. *Science* **292**, 110-3.
- Nicklas, R. B.** (1997). How cells get the right chromosomes. *Science* **275**, 632-7.
- Nicklas, R. B., Waters, J. C., Salmon, E. D. and Ward, S. C.** (2001). Checkpoint signals in grasshopper meiosis are sensitive to microtubule attachment, but tension is still essential. *J Cell Sci* **114**, 4173-83.
- Nishihashi, A., Haraguchi, T., Hiraoka, Y., Ikemura, T., Regnier, V., Dodson, H., Earnshaw, W. C. and Fukagawa, T.** (2002). CENP-I is essential for centromere function in vertebrate cells. *Dev Cell* **2**, 463-76.
- Nishioka, K., Rice, J. C., Sarma, K., Erdjument-Bromage, H., Werner, J., Wang, Y., Chuikov, S., Valenzuela, P., Tempst, P., Steward, R. et al.** (2002). PR-Set7 is a nucleosome-specific methyltransferase that modifies lysine 20 of histone H4 and is associated with silent chromatin. *Mol Cell* **9**, 1201-13.
- Nonaka, N., Kitajima, T., Yokobayashi, S., Xiao, G., Yamamoto, M., Grewal, S. I. and Watanabe, Y.** (2002). Recruitment of cohesin to heterochromatic regions by Swi6/HP1 in fission yeast. *Nat Cell Biol* **4**, 89-93.
- Ogryzko, V. V., Schiltz, R. L., Russanova, V., Howard, B. H. and Nakatani, Y.** (1996). The transcriptional coactivators p300 and CBP are histone acetyltransferases. *Cell* **87**, 953-9.
- Pal-Bhadra, M., Leibovitch, B. A., Gandhi, S. G., Rao, M., Bhadra, U., Birchler, J. A. and Elgin, S. C.** (2004). Heterochromatic silencing and HP1 localization in *Drosophila* are dependent on the RNAi machinery. *Science* **303**, 669-72.
- Palmer, D. K., O'Day, K. and Margolis, R. L.** (1989). Biochemical analysis of CENP-A, a centromeric protein with histone-like properties. *Prog Clin Biol Res* **318**, 61-72.
- Palmer, D. K., O'Day, K., Trong, H. L., Charbonneau, H. and Margolis, R. L.** (1991). Purification of the centromere-specific protein CENP-A and demonstration that it is a distinctive histone. *Proc Natl Acad Sci U S A* **88**, 3734-8.
- Palmer, D. K., O'Day, K., Wener, M. H., Andrews, B. S. and Margolis, R. L.** (1987). A 17-kD centromere protein (CENP-A) copurifies with nucleosome core particles and with histones. *J Cell Biol* **104**, 805-15.

Paull, T. T., Rogakou, E. P., Yamazaki, V., Kirchgessner, C. U., Gellert, M. and Bonner, W. M. (2000). A critical role for histone H2AX in recruitment of repair factors to nuclear foci after DNA damage. *Curr Biol* **10**, 886-95.

Perez-Castro, A. V., Shamanski, F. L., Meneses, J. J., Lovato, T. L., Vogel, K. G., Moyzis, R. K. and Pedersen, R. (1998). Centromeric protein B null mice are viable with no apparent abnormalities. *Dev Biol* **201**, 135-43.

Perry, C. A. and Annunziato, A. T. (1989). Influence of histone acetylation on the solubility, H1 content and DNase I sensitivity of newly assembled chromatin. *Nucleic Acids Res* **17**, 4275-91.

Pesavento, J. J., Bullock, C. R., LeDuc, R. D., Mizzen, C. A. and Kelleher, N. L. (2008a). Combinatorial modification of human histone H4 quantitated by two-dimensional liquid chromatography coupled with top down mass spectrometry. *J Biol Chem* **283**, 14927-37.

Pesavento, J. J., Yang, H., Kelleher, N. L. and Mizzen, C. A. (2008b). Certain and progressive methylation of histone H4 at lysine 20 during the cell cycle. *Mol Cell Biol* **28**, 468-86.

Peters, A. H., Kubicek, S., Mechtler, K., O'Sullivan, R. J., Derijck, A. A., Perez-Burgos, L., Kohlmaier, A., Opravil, S., Tachibana, M., Shinkai, Y. et al. (2003). Partitioning and plasticity of repressive histone methylation states in mammalian chromatin. *Mol Cell* **12**, 1577-89.

Peters, A. H., O'Carroll, D., Scherthan, H., Mechtler, K., Sauer, S., Schofer, C., Weipoltshammer, K., Pagani, M., Lachner, M., Kohlmaier, A. et al. (2001). Loss of the Suv39h histone methyltransferases impairs mammalian heterochromatin and genome stability. *Cell* **107**, 323-37.

Pidoux, A. L. and Allshire, R. C. (2004). Kinetochores and heterochromatin domains of the fission yeast centromere. *Chromosome Res* **12**, 521-34.

Pidoux, A. L., Choi, E. S., Abbott, J. K., Liu, X., Kagansky, A., Castillo, A. G., Hamilton, G. L., Richardson, W., Rappsilber, J., He, X. et al. (2009). Fission yeast Scm3: A CENP-A receptor required for integrity of subkinetochore chromatin. *Mol Cell* **33**, 299-311.

Poirier, M. G. and Marko, J. F. (2002). Mitotic chromosomes are chromatin networks without a mechanically contiguous protein scaffold. *Proc Natl Acad Sci U S A* **99**, 15393-7.

Pradhan, S. and Kim, G. D. (2002). The retinoblastoma gene product interacts with maintenance human DNA (cytosine-5) methyltransferase and modulates its activity. *Embo J* **21**, 779-88.

Pray-Grant, M. G., Daniel, J. A., Schieltz, D., Yates, J. R., 3rd and Grant, P. A. (2005). Chd1 chromodomain links histone H3 methylation with SAGA- and SLIK-dependent acetylation. *Nature* **433**, 434-8.

Rattner, J. B., Rao, A., Fritzler, M. J., Valencia, D. W. and Yen, T. J. (1993). CENP-F is a .ca 400 kDa kinetochore protein that exhibits a cell-cycle dependent localization. *Cell Motil Cytoskeleton* **26**, 214-26.

Rea, S., Eisenhaber, F., O'Carroll, D., Strahl, B. D., Sun, Z. W., Schmid, M., Opravil, S., Mechtler, K., Ponting, C. P., Allis, C. D. et al. (2000).

Regulation of chromatin structure by site-specific histone H3 methyltransferases. *Nature* **406**, 593-9.

Rice, J. C., Briggs, S. D., Ueberheide, B., Barber, C. M., Shabanowitz, J., Hunt, D. F., Shinkai, Y. and Allis, C. D. (2003). Histone methyltransferases direct different degrees of methylation to define distinct chromatin domains. *Mol Cell* **12**, 1591-8.

Rice, J. C., Nishioka, K., Sarma, K., Steward, R., Reinberg, D. and Allis, C. D. (2002). Mitotic-specific methylation of histone H4 Lys 20 follows increased PR-Set7 expression and its localization to mitotic chromosomes. *Genes Dev* **16**, 2225-30.

Richards, E. J. and Elgin, S. C. (2002). Epigenetic codes for heterochromatin formation and silencing: rounding up the usual suspects. *Cell* **108**, 489-500.

Ridsdale, J. A., Rattner, J. B. and Davie, J. R. (1988). Erythroid-specific gene chromatin has an altered association with linker histones. *Nucleic Acids Res* **16**, 5915-26.

Robbins, A. R., Jablonski, S. A., Yen, T. J., Yoda, K., Robey, R., Bates, S. E. and Sackett, D. L. (2005). Inhibitors of histone deacetylases alter kinetochore assembly by disrupting pericentromeric heterochromatin. *Cell Cycle* **4**, 717-26.

Robertson, K. D., Ait-Si-Ali, S., Yokochi, T., Wade, P. A., Jones, P. L. and Wolffe, A. P. (2000). DNMT1 forms a complex with Rb, E2F1 and HDAC1 and represses transcription from E2F-responsive promoters. *Nat Genet* **25**, 338-42.

Robinson, P. J., An, W., Routh, A., Martino, F., Chapman, L., Roeder, R. G. and Rhodes, D. (2008). 30 nm chromatin fibre decompaction requires both H4-K16 acetylation and linker histone eviction. *J Mol Biol* **381**, 816-25.

Robinson, P. J., Fairall, L., Huynh, V. A. and Rhodes, D. (2006). EM measurements define the dimensions of the "30-nm" chromatin fiber: evidence for a compact, interdigitated structure. *Proc Natl Acad Sci U S A* **103**, 6506-11.

Rogakou, E. P., Pilch, D. R., Orr, A. H., Ivanova, V. S. and Bonner, W. M. (1998). DNA double-stranded breaks induce histone H2AX phosphorylation on serine 139. *J Biol Chem* **273**, 5858-68.

Rougeulle, C. and Avner, P. (2003). Controlling X-inactivation in mammals: what does the centre hold? *Semin Cell Dev Biol* **14**, 331-40.

Rougeulle, C., Navarro, P. and Avner, P. (2003). Promoter-restricted H3 Lys 4 di-methylation is an epigenetic mark for monoallelic expression. *Hum Mol Genet* **12**, 3343-8.

Ruthenburg, A. J., Li, H., Patel, D. J. and Allis, C. D. (2007). Multivalent engagement of chromatin modifications by linked binding modules. *Nat Rev Mol Cell Biol* **8**, 983-94.

Sakaguchi, A. and Steward, R. (2007). Aberrant monomethylation of histone H4 lysine 20 activates the DNA damage checkpoint in *Drosophila melanogaster*. *J Cell Biol* **176**, 155-62.

Sakuno, T., Tada, K. and Watanabe, Y. (2009). Kinetochores geometry defined by cohesion within the centromere. *Nature* **458**, 852-8.

Sanders, S. L., Portoso, M., Mata, J., Bahler, J., Allshire, R. C. and Kouzarides, T. (2004). Methylation of histone H4 lysine 20 controls recruitment of Crb2 to sites of DNA damage. *Cell* **119**, 603-14.

Sarma, K. and Reinberg, D. (2005). Histone variants meet their match. *Nat Rev Mol Cell Biol* **6**, 139-49.

Schalch, T., Duda, S., Sargent, D. F. and Richmond, T. J. (2005). X-ray structure of a tetranucleosome and its implications for the chromatin fibre. *Nature* **436**, 138-41.

Schneider, R., Bannister, A. J., Myers, F. A., Thorne, A. W., Crane-Robinson, C. and Kouzarides, T. (2004). Histone H3 lysine 4 methylation patterns in higher eukaryotic genes. *Nat Cell Biol* **6**, 73-7.

Schotta, G., Lachner, M., Sarma, K., Ebert, A., Sengupta, R., Reuter, G., Reinberg, D. and Jenuwein, T. (2004). A silencing pathway to induce H3-K9 and H4-K20 trimethylation at constitutive heterochromatin. *Genes Dev* **18**, 1251-62.

Schotta, G., Sengupta, R., Kubicek, S., Malin, S., Kauer, M., Callen, E., Celeste, A., Pagani, M., Opravil, S., De La Rosa-Velazquez, I. A. et al. (2008). A chromatin-wide transition to H4K20 monomethylation impairs genome integrity and programmed DNA rearrangements in the mouse. *Genes Dev* **22**, 2048-61.

Schueler, M. G. and Sullivan, B. A. (2006). Structural and functional dynamics of human centromeric chromatin. *Annu Rev Genomics Hum Genet* **7**, 301-13.

Serrano, A., Rodriguez-Corsino, M. and Losada, A. (2009). Heterochromatin protein 1 (HP1) proteins do not drive pericentromeric cohesin enrichment in human cells. *PLoS ONE* **4**, e5118.

Shahbazian, M. D. and Grunstein, M. (2007). Functions of site-specific histone acetylation and deacetylation. *Annu Rev Biochem* **76**, 75-100.

Shi, Y., Lan, F., Matson, C., Mulligan, P., Whetstone, J. R., Cole, P. A., Casero, R. A. and Shi, Y. (2004). Histone demethylation mediated by the nuclear amine oxidase homolog LSD1. *Cell* **119**, 941-53.

Shilatifard, A. (2006). Chromatin Modifications by Methylation and Ubiquitination: Implications in the Regulation of Gene Expression. *Annu Rev Biochem*.

Shogren-Knaak, M., Ishii, H., Sun, J. M., Pazin, M. J., Davie, J. R. and Peterson, C. L. (2006). Histone H4-K16 acetylation controls chromatin structure and protein interactions. *Science* **311**, 844-7.

Siddiqui, H., Fox, S. R., Gunawardena, R. W. and Knudsen, E. S. (2007). Loss of RB compromises specific heterochromatin modifications and modulates HP1alpha dynamics. *J Cell Physiol* **211**, 131-7.

Sims, R. J., 3rd, Chen, C. F., Santos-Rosa, H., Kouzarides, T., Patel, S. S. and Reinberg, D. (2005). Human but not yeast CHD1 binds directly and selectively to histone H3 methylated at lysine 4 via its tandem chromodomains. *J Biol Chem* **280**, 41789-92.

Skoufias, D. A., Andreassen, P. R., Lacroix, F. B., Wilson, L. and Margolis, R. L. (2001). Mammalian mad2 and bub1/bubR1 recognize distinct spindle-attachment and kinetochore-tension checkpoints. *Proc Natl Acad Sci U S A* **98**, 4492-7.

Smallwood, A., Esteve, P. O., Pradhan, S. and Carey, M. (2007). Functional cooperation between HP1 and DNMT1 mediates gene silencing. *Genes Dev* **21**, 1169-78.

Smothers, J. F. and Henikoff, S. (2000). The HP1 chromo shadow domain binds a consensus peptide pentamer. *Curr Biol* **10**, 27-30.

Staynov, D. Z. (2008). The controversial 30 nm chromatin fibre. *Bioessays* **30**, 1003-9.

Stevens, F. E., Beamish, H., Warrener, R. and Gabrielli, B. (2008). Histone deacetylase inhibitors induce mitotic slippage. *Oncogene* **27**, 1345-54.

Stewart, M. D., Li, J. and Wong, J. (2005). Relationship between histone H3 lysine 9 methylation, transcription repression, and heterochromatin protein 1 recruitment. *Mol Cell Biol* **25**, 2525-38.

Strahl, B. D. and Allis, C. D. (2000). The language of covalent histone modifications. *Nature* **403**, 41-5.

Strauss, F. and Prunell, A. (1983). Organization of internucleosomal DNA in rat liver chromatin. *Embo J* **2**, 51-6.

Strukov, Y. G. and Belmont, A. S. (2009). Mitotic chromosome structure: reproducibility of folding and symmetry between sister chromatids. *Biophys J* **96**, 1617-28.

Sullivan, B. A. and Karpen, G. H. (2004). Centromeric chromatin exhibits a histone modification pattern that is distinct from both euchromatin and heterochromatin. *Nat Struct Mol Biol* **11**, 1076-83.

Sullivan, B. A. and Schwartz, S. (1995). Identification of centromeric antigens in dicentric Robertsonian translocations: CENP-C and CENP-E are necessary components of functional centromeres. *Hum Mol Genet* **4**, 2189-97.

Sural, T. H., Peng, S., Li, B., Workman, J. L., Park, P. J. and Kuroda, M. I. (2008). The MSL3 chromodomain directs a key targeting step for dosage compensation of the *Drosophila melanogaster* X chromosome. *Nat Struct Mol Biol* **15**, 1318-25.

Taddei, A., Maison, C., Roche, D. and Almouzni, G. (2001). Reversible disruption of pericentric heterochromatin and centromere function by inhibiting deacetylases. *Nat Cell Biol* **3**, 114-20.

Takahashi, K., Chen, E. S. and Yanagida, M. (2000). Requirement of Mis6 centromere connector for localizing a CENP-A-like protein in fission yeast. *Science* **288**, 2215-9.

Takahashi, K., Takayama, Y., Masuda, F., Kobayashi, Y. and Saitoh, S. (2005). Two distinct pathways responsible for the loading of CENP-A to centromeres in the fission yeast cell cycle. *Philos Trans R Soc Lond B Biol Sci* **360**, 595-606; discussion 606-7.

Tanudji, M., Shoemaker, J., L'Italien, L., Russell, L., Chin, G. and Schebye, X. M. (2004). Gene silencing of CENP-E by small interfering RNA in

HeLa cells leads to missegregation of chromosomes after a mitotic delay. *Mol Biol Cell* **15**, 3771-81.

Taunton, J., Hassig, C. A. and Schreiber, S. L. (1996). A mammalian histone deacetylase related to the yeast transcriptional regulator Rpd3p. *Science* **272**, 408-11.

Taverna, S. D., Li, H., Ruthenburg, A. J., Allis, C. D. and Patel, D. J. (2007). How chromatin-binding modules interpret histone modifications: lessons from professional pocket pickers. *Nat Struct Mol Biol* **14**, 1025-40.

Tavormina, P. A., Come, M. G., Hudson, J. R., Mo, Y. Y., Beck, W. T. and Gorbsky, G. J. (2002). Rapid exchange of mammalian topoisomerase II alpha at kinetochores and chromosome arms in mitosis. *J Cell Biol* **158**, 23-9.

Thomas, J. O. (1999). Histone H1: location and role. *Curr Opin Cell Biol* **11**, 312-7.

Ting, A. H., Suzuki, H., Cope, L., Schuebel, K. E., Lee, B. H., Toyota, M., Imai, K., Shinomura, Y., Tokino, T. and Baylin, S. B. (2008). A requirement for DICER to maintain full promoter CpG island hypermethylation in human cancer cells. *Cancer Res* **68**, 2570-5.

Toth, K., Brun, N. and Langowski, J. (2006). Chromatin compaction at the mononucleosome level. *Biochemistry* **45**, 1591-8.

Trojer, P. and Reinberg, D. (2006). Histone lysine demethylases and their impact on epigenetics. *Cell* **125**, 213-7.

Trojer, P. and Reinberg, D. (2007). Facultative heterochromatin: is there a distinctive molecular signature? *Mol Cell* **28**, 1-13.

Tryndyak, V. P., Kovalchuk, O. and Pogribny, I. P. (2006). Loss of DNA methylation and histone H4 lysine 20 trimethylation in human breast cancer cells is associated with aberrant expression of DNA methyltransferase 1, Suv4-20h2 histone methyltransferase and methyl-binding proteins. *Cancer Biol Ther* **5**, 65-70.

Tsukada, Y., Fang, J., Erdjument-Bromage, H., Warren, M. E., Borchers, C. H., Tempst, P. and Zhang, Y. (2006). Histone demethylation by a family of JmjC domain-containing proteins. *Nature* **439**, 811-6.

Utlely, R. T., Ikeda, K., Grant, P. A., Cote, J., Steger, D. J., Eberharter, A., John, S. and Workman, J. L. (1998). Transcriptional activators direct histone acetyltransferase complexes to nucleosomes. *Nature* **394**, 498-502.

Vakoc, C. R., Mandat, S. A., Olenchock, B. A. and Blobel, G. A. (2005). Histone H3 lysine 9 methylation and HP1gamma are associated with transcription elongation through mammalian chromatin. *Mol Cell* **19**, 381-91.

Van Hooser, A. A., Ouspenski, II, Gregson, H. C., Starr, D. A., Yen, T. J., Goldberg, M. L., Yokomori, K., Earnshaw, W. C., Sullivan, K. F. and Brinkley, B. R. (2001). Specification of kinetochore-forming chromatin by the histone H3 variant CENP-A. *J Cell Sci* **114**, 3529-42.

Vaquero, A., Scher, M., Erdjument-Bromage, H., Tempst, P., Serrano, L. and Reinberg, D. (2007). SIRT1 regulates the histone methyltransferase SUV39H1 during heterochromatin formation. *Nature* **450**, 440-4.

Vaute, O., Nicolas, E., Vandell, L. and Trouche, D. (2002). Functional and physical interaction between the histone methyl transferase Suv39H1 and histone deacetylases. *Nucleic Acids Res* **30**, 475-81.

Verdel, A., Jia, S., Gerber, S., Sugiyama, T., Gygi, S., Grewal, S. I. and Moazed, D. (2004). RNAi-mediated targeting of heterochromatin by the RITS complex. *Science* **303**, 672-6.

Volpe, T. A., Kidner, C., Hall, I. M., Teng, G., Grewal, S. I. and Martienssen, R. A. (2002). Regulation of heterochromatic silencing and histone H3 lysine-9 methylation by RNAi. *Science* **297**, 1833-7.

Walia, H., Chen, H. Y., Sun, J. M., Holth, L. T. and Davie, J. R. (1998). Histone acetylation is required to maintain the unfolded nucleosome structure associated with transcribing DNA. *J Biol Chem* **273**, 14516-22.

Wang, F., Koyama, N., Nishida, H., Haraguchi, T., Reith, W. and Tsukamoto, T. (2006). The assembly and maintenance of heterochromatin initiated by transgene repeats are independent of the RNA interference pathway in mammalian cells. *Mol Cell Biol* **26**, 4028-40.

Warburton, P. E. (2001). Epigenetic analysis of kinetochore assembly on variant human centromeres. *Trends Genet* **17**, 243-7.

Warburton, P. E., Cooke, C. A., Bourassa, S., Vafa, O., Sullivan, B. A., Stetten, G., Gimelli, G., Warburton, D., Tyler-Smith, C., Sullivan, K. F. et al. (1997). Immunolocalization of CENP-A suggests a distinct nucleosome structure at the inner kinetochore plate of active centromeres. *Curr Biol* **7**, 901-4.

Waters, J. C., Chen, R. H., Murray, A. W. and Salmon, E. D. (1998). Localization of Mad2 to kinetochores depends on microtubule attachment, not tension. *J Cell Biol* **141**, 1181-91.

Weintraub, H. and Groudine, M. (1976). Chromosomal subunits in active genes have an altered conformation. *Science* **193**, 848-56.

Whetstine, J. R., Nottke, A., Lan, F., Huarte, M., Smolikov, S., Chen, Z., Spooner, E., Li, E., Zhang, G., Colaiacovo, M. et al. (2006). Reversal of histone lysine trimethylation by the JMJD2 family of histone demethylases. *Cell* **125**, 467-81.

Widom, J. (1992). A relationship between the helical twist of DNA and the ordered positioning of nucleosomes in all eukaryotic cells. *Proc Natl Acad Sci U S A* **89**, 1095-9.

Widom, J. and Klug, A. (1985). Structure of the 300A chromatin filament: X-ray diffraction from oriented samples. *Cell* **43**, 207-13.

Williams, J. S., Hayashi, T., Yanagida, M. and Russell, P. (2009). Fission yeast Scm3 mediates stable assembly of Cnp1/CENP-A into centromeric chromatin. *Mol Cell* **33**, 287-98.

Wolffe, A. P. and Hayes, J. J. (1999). Chromatin disruption and modification. *Nucleic Acids Res* **27**, 711-20.

Wong, L. H., Brettingham-Moore, K. H., Chan, L., Quach, J. M., Anderson, M. A., Northrop, E. L., Hannan, R., Saffery, R., Shaw, M. L., Williams, E. et al. (2007). Centromere RNA is a key component for the assembly of nucleoproteins at the nucleolus and centromere. *Genome Res* **17**, 1146-60.

Wysocka, J., Swigut, T., Xiao, H., Milne, T. A., Kwon, S. Y., Landry, J., Kauer, M., Tackett, A. J., Chait, B. T., Badenhorst, P. et al. (2006). A PHD finger of NURF couples histone H3 lysine 4 trimethylation with chromatin remodelling. *Nature* **442**, 86-90.

Xiao, B., Jing, C., Kelly, G., Walker, P. A., Muskett, F. W., Frenkiel, T. A., Martin, S. R., Sarma, K., Reinberg, D., Gambelin, S. J. et al. (2005). Specificity and mechanism of the histone methyltransferase Pr-Set7. *Genes Dev* **19**, 1444-54.

Xin, H., Yoon, H. G., Singh, P. B., Wong, J. and Qin, J. (2004). Components of a pathway maintaining histone modification and heterochromatin protein 1 binding at the pericentric heterochromatin in Mammalian cells. *J Biol Chem* **279**, 9539-46.

Yamada, T., Fischle, W., Sugiyama, T., Allis, C. D. and Grewal, S. I. (2005). The nucleation and maintenance of heterochromatin by a histone deacetylase in fission yeast. *Mol Cell* **20**, 173-85.

Yang, H., Pesavento, J. J., Starnes, T. W., Cryderman, D. E., Wallrath, L. L., Kelleher, N. L. and Mizzen, C. A. (2008). Preferential dimethylation of histone H4 lysine 20 by Suv4-20. *J Biol Chem* **283**, 12085-92.

Yang, M., Gocke, C. B., Luo, X., Borek, D., Tomchick, D. R., Machius, M., Otwinowski, Z. and Yu, H. (2006). Structural basis for CoREST-dependent demethylation of nucleosomes by the human LSD1 histone demethylase. *Mol Cell* **23**, 377-87.

Yao, X., Abrieu, A., Zheng, Y., Sullivan, K. F. and Cleveland, D. W. (2000). CENP-E forms a link between attachment of spindle microtubules to kinetochores and the mitotic checkpoint. *Nat Cell Biol* **2**, 484-91.

Yen, T. J., Li, G., Schaar, B. T., Szilak, I. and Cleveland, D. W. (1992). CENP-E is a putative kinetochore motor that accumulates just before mitosis. *Nature* **359**, 536-9.

Zeitlin, S. G., Shelby, R. D. and Sullivan, K. F. (2001). CENP-A is phosphorylated by Aurora B kinase and plays an unexpected role in completion of cytokinesis. *J Cell Biol* **155**, 1147-57.

Zhang, C. L., McKinsey, T. A. and Olson, E. N. (2002). Association of class II histone deacetylases with heterochromatin protein 1: potential role for histone methylation in control of muscle differentiation. *Mol Cell Biol* **22**, 7302-12.

Zhang, H. S., Gavin, M., Dahiya, A., Postigo, A. A., Ma, D., Luo, R. X., Harbour, J. W. and Dean, D. C. (2000). Exit from G1 and S phase of the cell cycle is regulated by repressor complexes containing HDAC-Rb-hSWI/SNF and Rb-hSWI/SNF. *Cell* **101**, 79-89.

Zhang, Y., Ng, H. H., Erdjument-Bromage, H., Tempst, P., Bird, A. and Reinberg, D. (1999). Analysis of the NuRD subunits reveals a histone deacetylase core complex and a connection with DNA methylation. *Genes Dev* **13**, 1924-35.

Zhou, J., Fan, J. Y., Rangasamy, D. and Tremethick, D. J. (2007). The nucleosome surface regulates chromatin compaction and couples it with transcriptional repression. *Nat Struct Mol Biol* **14**, 1070-6.

Zinner, R., Albiez, H., Walter, J., Peters, A. H., Cremer, T. and Cremer, M. (2005). Histone lysine methylation patterns in human cell types are arranged in distinct three-dimensional nuclear zones. *Histochem Cell Biol*, 1-17.